



# VCU

Virginia Commonwealth University  
VCU Scholars Compass

---

Theses and Dissertations

Graduate School

---

2016

## Allosteric Effects of G-Protein Coupled Receptor Heteromerization: Relevance to Psychosis

Jason W. Younkin  
*Virginia Commonwealth University*

Follow this and additional works at: <https://scholarscompass.vcu.edu/etd>



Part of the [Other Neuroscience and Neurobiology Commons](#)

© The Author

---

Downloaded from

<https://scholarscompass.vcu.edu/etd/4457>

This Dissertation is brought to you for free and open access by the Graduate School at VCU Scholars Compass. It has been accepted for inclusion in Theses and Dissertations by an authorized administrator of VCU Scholars Compass. For more information, please contact [libcompass@vcu.edu](mailto:libcompass@vcu.edu).

**Allosteric Effects of G-Protein Coupled Receptor Heteromerization:  
Relevance to Psychosis**

A dissertation submitted in partial fulfillment of the requirements for the degree of  
Doctor of Philosophy at Virginia Commonwealth University

by

**Jason Younkin**

B.S., Neuroscience, College of William and Mary, 2010

**Director: DIOMEDES E. LOGOTHETIS, PH.D.**  
Professor and Chair  
Department of Physiology and Biophysics

Virginia Commonwealth University  
Richmond, Virginia  
April, 2016

## ACKNOWLEDGEMENTS

I would like to thank my advisor, Dr. Diomedes E. Logothetis, for his support and wealth of ideas in pursuing this project. I would also like to thank the members of my committee and neuroscience program director, Dr. John Bigbee, for their insight and helpful suggestions regarding several aspects throughout my Ph.D. training. A special thanks to Drs. Logothetis and Bigbee for allowing me the chance to survive a rough first year in the program. This work would not have been possible without the assistance of all members past and present of the Logothetis Lab, but especially: Dr. Carlitos Villalba-Galea for always stopping whatever he was doing to help or answer questions, Dr. Lia Baki for her patience and teaching, Heikki Vaananen for his comraderie, and Dr. Edgar Leal-Pinto for early morning conversation and venting knowing nobody else would arrive anytime soon. Finally, I would like to thank my perfect wife Christine Elaine Younkin, who is under the impression that I think she doesn't support me. Unbeknownst to her, I am well aware of her unwavering 100% support throughout my almost 10 years of college, not to mention 9 years of US Navy service.

## TABLE OF CONTENTS

Acknowledgements	ii
List of Figures	vi
List of Abbreviations	ix
List of Tables	xiii
Abstract	xiv
Chapter 1: BACKGROUND	1
1.1: Introduction	1
1.2: Schizophrenia hypotheses	1
1.3: GPCRs and APDs	5
1.4: D2R, 5HT2AR, and mGlu2R localization	8
1.5: D2R-5HT2AR and mGlu2R-5HT2AR co-localization and heteromers	12

1.6. Allosteric effects upon heteromerization	21
1.7. <i>In vivo</i> and <i>ex vivo</i> studies	26
1.8. Trafficking and expression effects on mGlu2R-5HT2AR formation	28
1.9. Hypothesis	30
<b>Chapter 2: MATERIALS AND METHODS</b>	<b>41</b>
2.1: Molecular biology	41
2.2: Drugs and chemicals	41
2.3: Cells and transfections	42
2.4: Oocyte preparation and injection	42
2.5: Two-electrode voltage clamp and analysis	42
2.6: Whole-cell patch clamp recordings	43
2.7: Statistics	44
<b>Chapter 3: MGLU2R-5HT2AR SIGNALING IN MAMMALIAN CELLS</b>	<b>45</b>
3.1: Introduction	45
3.2: Results	48
3.2.1: Effects of 5HT2AR ligands on G <sub>i</sub> signaling of mGlu2R	49
3.2.2: Effects of mGlu2R ligands on G <sub>q</sub> signaling of 5HT2AR	49

3.2.3: Combinatorial Effects of mGlu2R and 5HT2AR ligands on G <sub>i</sub> signaling of mGlu2R	50
3.3: Discussion	51
Chapter 4: D2R-5HT2AR SIGNALING IN <i>XENOPUS</i> OOCYTES	63
4.1: Introduction	63
4.2: Results	64
4.2.1: Lateral allosterism and effects of varying cRNA injection ratios	65
4.2.2: Endogenous ligand-induced allosterism and a 5HT2AR mutant	66
4.2.3: Synthetic agonist-induced allosterism	67
4.2.4: Anti-psychotic drug-induced allosterism	68
4.2.5: Effects of drug combinations	71
4.3: Discussion	72
Chapter 5: DISCUSSION AND CONCLUDING REMARKS	101
Literature Cited	109
Appendix 1: Control and Verification Experiments	119
VITA	123

## LIST OF FIGURES

Figure 1.1. Key dopamine pathways in the brain	31
Figure 1.2. Key glutamate pathways in the brain	32
Figure 1.3. GPCR signaling	33
Figure 1.4. Direct evidence for mGlu2R-5HT2AR heteromerization	35
Figure 1.5. Direct evidence for D2R-5HT2AR heteromerization	36
Figure 1.6. Ion channel reporters for G-protein activity	37
Figure 1.7. Allosteric effects upon mGlu2R-5HT2AR heteromerization	38
Figure 1.8. Allosteric effects upon D2R-5HT2AR heteromerization	39
Figure 1.9. Heteromer trafficking and expression effects	40
Figure 3.1. An atypical APD increases glutamate-induced mGlu2R signaling	54
Figure 3.2. The atypical APD paliperidone increases glutamate-induced mGlu2R signaling in positive but not negative cross-talk clones	55
Figure 3.3. An mGlu2R inverse agonist increases 5HT-induced 5HT2AR signaling	56
Figure 3.4. The mGlu2R inverse agonist LY34 increases 5HT-induced 5HT2AR signaling in positive but not negative cross-talk clones	57

Figure 3.5. An atypical APD increases LY37-induced mGlu2R signaling	58
Figure 3.6. The atypical APD paliperidone increases LY37-induced mGlu2R signaling in negative but not positive cross-talk clones	59
Figure 3.7. The location of the mGlu2R-5HT2AR heteromer determines neurotransmitter effects on brain regions	60
Figure 4.1. Upon D2R-5HT2AR heteromerization, $G_i$ -induced currents increase while $G_q$ - induced currents decrease	76
Figure 4.2. Lateral Allosterism upon D2R-5HT2AR heteromerization	77
Figure 4.3. Lateral Allosterism upon D2R-5HT2AR heteromerization at different cRNA injection ratios based on 1ng/oocyte	78
Figure 4.4. Verification of $G_i$ signal at lower cRNA injection levels	79
Figure 4.5. Verification of $G_q$ signal at lower cRNA injection levels	80
Figure 4.6. Lateral allosterism at lower cRNA amounts and corresponding cRNA ratios: $G_i$ activity	81
Figure 4.7. Lateral allosterism at lower cRNA amounts and corresponding cRNA ratios: $G_q$ activity	82
Figure 4.8. The endogenous neurotransmitter 5HT cross-signals and increases the activity of the non-target receptor while the 5HT2AR 2-alanine mutant abrogates lateral and drug-induced allosterism	83
Figure 4.9. The endogenous neurotransmitter dopamine cross-signals and increases the activity of the non-target receptor	84
Figure 4.10. Synthetic agonists cross-signal and decrease the activity of the non-target receptor	85

Figure 4.11. Concentration responses of Pimavanserin as dopamine or 5HT antagonists at the D2R or 5HT2AR	86
Figure 4.12. 5HT2AR-selective potential APD Pimavanserin cross-signaling to the D2R	87
Figure 4.13. Concentration responses of Amisulpride as dopamine or 5HT antagonists at the D2R or 5HT2AR	88
Figure 4.14. D2R-selective APD Amisulpride cross-signaling to the 5HT2AR	89
Figure 4.15. Concentration responses of Amperozide as dopamine or 5HT antagonists at the D2R or 5HT2AR	90
Figure 4.16. Non-selective APD Amperozide cross-signaling to the D2R	91
Figure 4.17. Concentration responses of Paliperidone as dopamine or 5HT antagonists at the D2R or 5HT2AR	92
Figure 4.18. Non-selective APD Paliperidone cross-signaling to the 5HT2AR	93
Figure 4.19. Effects of drug combinations	94
Figure 4.20. The location of the D2R-5HT2AR heteromer determines neurotransmitter effects on brain regions	95
Figure A1.1. Whole-cell patch clamp controls	113
Figure A1.2. 5HT2AR (2A) mutant G <sub>q</sub> activity	114
Figure A1.3. GIRK4* controls	115
Figure A1.4. D2R and 5HT2AR controls	116

## LIST OF ABBREVIATIONS

<u>Abbreviation</u>	<u>Full Name</u>
AMIS	Amisulpride
AMP	Amperozide
APD	Anti-Psychotic Drug
BaCl <sub>2</sub>	Barium Chloride
Ca <sup>2+</sup>	Calcium
cAMP	Cyclic Adenosine Monophosphate
CNS	Central Nervous System
cRNA	Complementary Ribonucleic Acid
DA	Dopamine

DAG	Di-Acyl Glycerol
D2R	Dopamine 2 Receptor
DMEM	Dulbecco's modified Eagle's medium
DOI	2,5-Dimethoxy-4-iodoamphetamine
EPS	Extra-Pyramidal Symptoms
5HT	Serotonin
5HT2AR	Serotonin 2A Receptor
GABA	Gamma-Amino Butyric Acid
GDP	Guanosine Diphosphate
GIRK	G-Protein Coupled Inwardly Rectifying potassium channels
GRK	G-Protein Coupled Receptor Kinase
GTP	Guanosine Triphosphate
GPCR	G-Protein Coupled Receptor
HEK-293	Human Embryonic Kidney cells
HEPES	4-(2-hydroxyethyl)-1-piperazineethanesulfonic acid
iGluR	Ionotropic Glutamate Receptor
IP <sub>3</sub>	Inositol trisphosphate

K <sup>+</sup> or K	Potassium
LY34	LY341495
LY37	LY379268
MgCl <sub>2</sub>	Magnesium Chloride
mGluR	Metabotropic Glutamate Receptor
mGlu2R	Metabotropic Glutamate 2 Receptor
Na <sup>+</sup> or Na	Sodium
NMDAR	N-Methyl-D-Aspartate Receptor
PAL	Paliperidone
PCP	Phencyclidine
PIMA	Pimavanserin
PIP <sub>2</sub>	Phosphatidylinositol 4,5 bisphosphate
PI <sub>3</sub> K	Phosphoinositide 3 Kinase
PKA	Protein Kinase A
PKC	Protein Kinase C
PLC-β	Phospholipase C-Beta
PNS	Peripheral Nervous System

PTX

Pertussis Toxin

QP

Quinpirole

VTA

Ventral Tegmental Area

## LIST OF TABLES

Table 1.1. GPCRs integral to schizophrenia	34
Table 3.1. Properties of mGlu2R and 5HT2AR ligands	54
Table 3.2. Results from mGlu2R and 5HT2AR ligand application in HEK-293 cells	61
Table 4.1. Properties of D2R and 5HT2AR ligands	76
Table 4.2. Results from D2R and 5HT2AR ligand application in <i>Xenopus</i> oocytes	96

## **ABSTRACT**

### **Allosteric Effects of G-Protein Coupled Receptor Heteromerization: Relevance to Psychosis**

By Jason Younkin, B.S.

A dissertation submitted in partial fulfillment of the requirements for the degree of Doctor of Philosophy at Virginia Commonwealth University.

Virginia Commonwealth University, 2016

Dissertation Director: Diomedes E. Logothetis, Ph.D.  
Professor and Chair, Department of Physiology and Biophysics

G-protein coupled receptors (GPCRs) implicated in disease are the predominant pharmaceutical targets. Growing evidence suggests that GPCRs form homo- and heteromeric complexes, resulting in allosteric functional changes. Ligands targeting one receptor can alter the function of

the other receptor or receptors. Knowledge of these functional changes will provide unique opportunities to treat diseases. We examined two GPCR heteromers implicated in psychosis, or schizophrenia: mGlu2R-5HT2AR and D2R-5HT2AR. Using whole-cell patch clamp, we extended our previous mGlu2R-5HT2AR studies in *Xenopus* oocytes to stably transfected HEK-293 cells, a necessary study due to controversy over relevance of the oocyte results in mammalian systems. Cells possessing maximal or sub-maximal heteromer formation display an inverse functional coupling similar to that seen in oocytes. Maximal heteromer formation allows inverse agonists to increase the G-protein activity of the opposite receptor, while sub-maximal heteromer formation does not. However, similar results are obtained even in sub-maximal heteromer cells by applying a combination of a mGlu2R synthetic agonist with a 5HT2AR anti-psychotic drug. These results confirm relevance of the oocyte results to a mammalian cell line. Using two-electrode voltage clamp, we also investigated the allosteric changes upon heteromerization of D2R-5HT2AR in oocytes injected with appropriate cRNAs. Heteromer formation in the presence of dopamine or serotonin results in an increase in G-protein activity of each receptor while the simultaneous presence of both neurotransmitters further increases the G-protein activity of each receptor. The addition of synthetic agonists or anti-psychotics decreases the G-protein activity of the opposite receptor while agonizing or antagonizing its target receptor, respectively. Maximal lateral and ligand-induced allosteric effects upon D2R-5HT2AR formation only occur at a specific cRNA injection ratio, but partial effects exist at other ratios. Our data suggest that allosteric functional changes upon heteromerization are physiologically relevant and are mostly different when comparing mGlu2R-5HT2AR to D2R-5HT2AR.

## **Chapter 1: BACKGROUND**

### **1.1. Introduction**

Over 80 years of research to design and implement anti-psychotic drugs (APDs) for the treatment of psychosis, or schizophrenia, has yielded imperfect drugs displaying debilitating side effects, alleviation of only certain symptoms, and desensitization over short periods of time. Schizophrenia affects approximately 1% of the population and accounts for the expenditure of multi-millions of dollars in health-care. In light of these results and statistics, new approaches must be explored. Schizophrenia research is based on multiple hypotheses, but three have been researched the most. New approaches can be found from within these three hypotheses, specifically centering on three integral G-protein coupled receptors (GPCRs) and their direct physical interactions as heteromers within the involved neurotransmitter pathways.

### **1.2. Schizophrenia Hypotheses**

All schizophrenia hypotheses attempt to explain the extensive inter-connected symptoms of the disease in terms of certain neuro-circuitry. Five categories of schizophrenic symptoms exist: delusions, hallucinations, disorganized thought, grossly disorganized or abnormal motor

behavior, and negative symptoms. Delusions are beliefs that cannot be changed even when proven wrong. Hallucinations are perceptions that occur without provocation. Delusions and hallucinations are commonly referred to as positive symptoms, due to a 'gain' of function. Disorganized thought is normally gleaned from a patient's lack of speech or abnormal speech patterns. Motor behavior issues can include deficits or gains in movement or lack of movement control. Negative symptoms involve 'loss' of function conditions such as anhedonia (lack of pleasurable experiences), diminished emotional expression, avolition (lack of motivation), and asociality (American Psychiatric Association, 2013). Many schizophrenia symptoms are thought to originate from specific brain regions, but the mechanisms involved are debatable. Various schizophrenia hypotheses are postulated, but three are prevalent. All three hypotheses concern specific neuro-circuitry, networks of electrically-excited neurons signaling chemically to each other across short distances called synapses.

The first major hypothesis of schizophrenia is the dopamine hypothesis. The neurotransmitter dopamine is versatile, acting as either excitatory or inhibitory depending on the neuro-circuitry and receptors involved. The dopaminergic neuro-circuitry involved in the hypothesis consists of five pathways (**Fig. 1.1**): the nigro-striatal, meso-limbic, meso-cortical, tuberoinfundular, and thalamic. The nigro-striatal pathway is part of the extra-pyramidal nervous system and includes neurons projecting from the substantia nigra to the basal ganglia or striatum. Hypoactivity in this region results in lack or slowing of movement, tremors, dystonia (face or neck twisting), and akathisia (restlessness). Hyperactivity results in movement disorders, or dyskinesias, like chorea (feet and hands) and tics. The meso-limbic pathway includes neurons projecting from the ventral tegmental area (VTA) to the nucleus accumbens. Hyperactivity in this area accounts for the positive symptoms of schizophrenia, like hallucinations and delusions.

The meso-limbic pathway is also involved in motivation, pleasure and reward. Drugs of abuse are commonly used by schizophrenics, implicating this system's involvement. The meso-cortical system includes neurons projecting from the VTA to the frontal cortex. In the ventromedial prefrontal cortex, these projections mediate affect and emotions, whereas the dorsolateral prefrontal cortex mediates cognitive and executive functions. Hypoactivity of these dopaminergic neurons results in the negative, cognitive, and affective symptoms of schizophrenia. The other two pathways are the tuberoinfundular and thalamic. Involving the hypothalamus, anterior pituitary gland, and thalamus, these pathways are important but are not part of our research (Stahl SM, 2013).

Although it was the first major schizophrenia theory and possessed clear limitations, the dopamine hypothesis is still preferred by many schizophrenia researchers. In general, this theory assumes an excess of dopamine release in most midbrain regions and a deficit of dopamine release in frontal cortical regions, which fits well and may be inter-connected with the next two major schizophrenia hypotheses.

The second major hypothesis of schizophrenia is the glutamate hypothesis. Glutamate is the predominant excitatory neurotransmitter in the brain and its decarboxylation yields gamma-amino butyric acid (GABA), the main inhibitory neurotransmitter of the central nervous system (CNS). The involved glutamatergic neurocircuitry includes several pathways (**Fig. 1.2**): the cortico-brainstem, cortico-striatal, cortico-thalamic, direct or indirect cortico-cortical, hippocampal-striatal, and thalamo-cortical. Cortico-brainstem pathway neurons project from the frontal cortex to brainstem neurotransmitter centers to mediate serotonin (5HT) release from the raphe nucleus and dopamine release from the VTA and substantia nigra. Cortico-striatal pathway neurons project from the frontal cortex to the striatum or nucleus accumbens, where a relay to

the globus pallidus is formed. Cortico-thalamic pathway neurons project from the frontal cortex to the thalamus and play a role in sensory reaction. Direct cortico-cortical pathway pyramidal neurons form a relay using glutamate while the indirect cortico-cortical pathway incorporates one or more GABAergic interneurons. Hippocampal-striatal pathway neurons form a circuit from the hippocampus to the striatum, specifically the nucleus accumbens, then to the globus pallidus, and finally to the VTA. This pathway incorporates GABAergic, glutamatergic, and dopaminergic neurons. Finally, the thalamo-cortical pathway neurons project from the thalamus to the frontal cortex and play a role in sensory processing (Stahl SM, 2013).

In schizophrenia, glutamate hypothesis pathways result in an abnormal glutamate drive, mostly from the frontal cortex to other regions, which may result in the effects of the dopamine hypothesis via direct or indirect synaptic connections.

The third major hypothesis of schizophrenia is the N-methyl-D-aspartate receptor (NMDAR) hypo-activity hypothesis. NMDARs are ligand-gated ion channels located on post-synaptic terminals that modulate excitatory neurotransmission, typically when bound by glutamate. When researchers noticed the effects of phencyclidine (PCP) and ketamine, antagonists of NMDARs, mimicked many schizophrenia symptoms, including positive, negative, cognitive and affective, while other drugs, like amphetamines, acted as competitive substrates at pre-synaptic dopamine transporters and mimicked only positive schizophrenia symptoms, NMDAR hypofunction arose as a third major schizophrenia hypothesis. Any condition that causes NMDAR hypoactivity can result in psychosis. Examples include abnormal neuronal development of glutamatergic synapses, abnormal NMDAR function on prefrontal cortex GABAergic neurons containing parvalbumin, and a malfunction in enzymes that synthesize GABA from glutamate (Stahl SM, 2013).

Since these three schizophrenia hypotheses are connected so intimately, we asked the question: What common elements do these pathways possess? There are many elements involved in schizophrenia-related neuro-circuitry. However, the most effective treatments, APDs, are antagonists targeting GPCRs. Agonists, like dopamine, glutamate, and 5HT, bind GPCRs and elicit a biological response, whereas antagonists, like the APDs haloperidol and risperidone, bind GPCRs and block, or dampen, the effects of an agonist. Therefore, in our search for new approaches to research schizophrenia, we wanted to focus our examination on GPCRs integral to all three schizophrenia hypotheses and neuro-circuits.

### **1.3. GPCRs and APDs**

In order to understand the complex effects of APDs in the treatment of psychosis, we must first understand GPCRs and their function. Every GPCR has a few features in common. GPCRs are transmembrane proteins, consisting of seven domains spanning the cell membrane in order to receive a signal external to the cell and transduce that signal to the cytosol. External signals can be wide-ranging: neurotransmitters, peptides, lipids, photons of light, odors, ions, and many more. Cytosolic signals include heterotrimeric G-proteins, arrestins, and GPCR kinases (GRKs). With an external N-terminus, cytosolic C-terminus, three external loops, and three internal loops, GPCRs link their seven transmembrane domains to accomplish signal transduction (Sieler S and Milligan G, 2011).

The cytosolic signal on which we are focused is the GPCR namesake, the heterotrimeric G-protein. When an agonistic ligand binds a GPCR, the receptor changes its conformation and couples with a G-protein. Heterotrimeric G-proteins consist of alpha, beta, and gamma subunits, with the inactive alpha bound to guanosine diphosphate (GDP). After coupling, the GDP unbinds

and a guanosine triphosphate (GTP) takes its place. The G-protein uncouples from the receptor and the alpha subunit separates from the beta and gamma subunits, which remain bound to each other. The two signals, G- $\alpha$  and G- $\beta\gamma$ , travel away from the receptor to act at various effectors inside the cell (Sieler S and Milligan G, 2011).

Several subtypes of the alpha subunit exist. We are concerned with two subtypes, G<sub>i</sub> and G<sub>q</sub>. GPCRs coupled to the G<sub>i</sub>- $\alpha$  subtype, such as the dopamine 2 receptor (D2R) and metabotropic glutamate 2 receptor (mGlu2R), inhibit adenylyl cyclase (AC), reducing the production of cyclic adenosine monophosphate (cAMP), which in turn activates less protein kinase A (PKA). At the same time, the G<sub>i</sub>-activated  $\beta\gamma$  subunits activate G-protein coupled inwardly rectifying potassium channels (GIRKs). Further downstream, the  $\beta\gamma$  subunits can also activate phosphoinositide 3 kinase (PI<sub>3</sub>K) and phospholipase C-beta (PLC- $\beta_{2/3}$ ). G<sub>i</sub>-proteins are pertussis toxin (PTX) sensitive, meaning PTX ADP-ribosylates the alpha subunit which disrupts the communication of the GPCR with the G- $\alpha$  subunits (Sieler S and Milligan G, 2011; Hatcher-Solis C et al., 2014). Pre-synaptically, G<sub>i</sub>-coupled GPCRs act as autoreceptors, forming a negative feedback loop to inhibit neurotransmission. Post-synaptically, G<sub>i</sub>-coupled GPCRs generally lower neuronal electrical excitability by activating GIRKs and inhibiting calcium channels. However, the complexity of G<sub>i</sub> signaling (**Fig. 1.3A**) is evident in cases of locomotion. Enhanced locomotion is associated with activated post-synaptic neurons, but has been shown to occur due to D2Rs. GPCRs coupled to the G<sub>q</sub>-alpha subtype, such as serotonin 2A receptors (5HT2AR), activate PLC- $\beta_1$ , resulting in the hydrolysis of phosphatidylinositol 4,5 bisphosphate (PIP<sub>2</sub>) into inositol trisphosphate (IP<sub>3</sub>) and di-acyl glycerol (DAG). IP<sub>3</sub> goes on to release calcium from internal stores, while DAG activates protein kinase C (PKC) (Sieler S and Milligan G, 2011; Hatcher-Solis C et al., 2014). Pre-synaptically, G<sub>q</sub>-coupled GPCRs increase cytosolic calcium and

generally enhance neurotransmission. Post-synaptically, like  $G_i$ -coupled GPCRs,  $G_q$ -coupled GPCRs are similarly complex (**Fig. 1.3B**), acting as inhibitory or excitatory neuronal modulators.

Agonists activate GPCRs, but as mentioned, antagonists block or dampen agonist effects. Clinically available APDs are D2R and /or 5HT2AR antagonists predominantly targeting two neurotransmitter systems. The first generation typical APDs target the dopamine system, primarily as antagonists for the D2R. Many typical APDs are also termed neuroleptics due to their side-effects. Neuroleptics tend to induce cognitive and negative symptoms through the meso-cortical neuro-circuitry, but can also result in extra-pyramidal symptoms (EPS) which are drug-induced movement disorders. Intended to limit EPS and other side-effects, the second generation atypical APDs still target the D2R as antagonists, but also have similar affinities and efficacies as antagonists for the 5HT2AR of the 5HT system (Stahl SM, 2013).

Receptor profiles of APDs allow for interpretation of similarities and differences. Atypical APDs act at many receptors, including a few not found in the dopamine or 5HT GPCR families. Balanced activity at multiple receptors is thought to be partly responsible for improved efficacy of atypical APDs, but unfortunately it may be responsible for the miserable side effects as well. Especially notable is the similarity in binding affinities for the D2R and 5HT2AR. Although functional outcomes vary in the use of atypical APDs, most bind to both receptors at low nanomolar concentrations. Typical APDs are still clinically used to avoid certain adverse side effects (weight gain, type II diabetes, sexual dysfunction, cataracts) associated with atypical APDs, even though atypical APDs are generally more successful, further highlighting the level of imperfection of available APDs.

As multiple new targets for the treatment of schizophrenia emerge, such as other dopamine and 5HT GPCRs, kynurenic acid, complement component 4, and glycine reuptake inhibitors, new clinical trials will ensue. Although not clinically approved at this time, a new generation of potential APDs is already in clinical trials. Metabotropic glutamate receptors (mGluRs), especially mGlu2R, are distributed heavily in brain regions involved in schizophrenia hypotheses. Synthetic agonists and positive allosteric modulators targeting mGlu2R show promise as effective APDs (Ellaithy A et al., 2015), especially when used in combination with atypical APDs.

#### **1.4. D2R, 5HT2AR, and mGlu2R Localization**

Evidence continues to grow in support of a further complication in the use of APDs. The D2R, 5HT2AR, and mGlu2R, three very different (**Table 1.1**) GPCRs integral to schizophrenia research and neuro-circuitry, directly interact as two separate heteromeric complexes: mGlu2R-5HT2AR and D2R-5HT2AR. Heteromerization leads to possible expression differences, less or more trafficking to the plasma membrane, and allosteric functional changes, all of which potentially affect the efficacy of APDs. But first, GPCRs must exist in the same brain regions if they are going to form a heteromer.

The D2R is a class 'A' GPCR that couples to G<sub>i</sub>-proteins and exists in two naturally occurring isoforms. The D2R long (D2R<sub>L</sub>) isoform is more abundant, expressing at approximately 90% of the total D2R expression, and predominantly post-synaptic. The D2R short (D2R<sub>S</sub>) isoform is less abundant, expressing at approximately 10% of the total D2R expression, and predominantly pre-synaptic (Dal Toso R et al., 1989; Chio CL et al., 1990). The mRNA of both receptors is found in rat and human brain and pituitary gland (Dal Toso R et al.,

1989). The existence of two isoforms of D2R suggests a differential function which is as of yet unknown.

Although the D2R is less abundant in the brain than the D1R, APD pharmacology and actions implicate the D2R in schizophrenia. The D2R is distributed widely throughout the nervous system. Outside of the schizophrenia hypothesis pathways, D2R mRNA is found in rat pituitary gland (Le Moine C et al., 1990) and rat olfactory tubercle (Le Moine C and Bloch B, 1995), while D2R protein is found in the rat peripheral nervous system (PNS), such as the kidney (Wang X et al., 2010). However, we are most concerned with localization affecting the schizophrenia hypotheses pathways. Neurons in the striatum possess high densities of D2R: mRNA in human tissue samples (Meador-Woodruff et al., 1996), mRNA in rat enkephalin-containing neurons (Le Moine C et al., 1990), receptor protein in rat medium spiny neurons (Hersch SM et al., 1995; Aizman O et al., 2000), and receptor protein in rat tissue samples (Levey AI et al., 1993; Aizman O et al., 2000; Borroto-Escuela et al., 2013). The D2R is found heavily throughout the VTA: mRNA in rat tissue samples (Le Moine C et al., 1990), receptor protein in mouse tissue samples (Garzon M et al., 2013), and mRNA in rat tissue samples (Sun H et al., 2015). The nucleus accumbens contains the D2R: mRNA in rat tissue samples (Le Moine C et al., 1990; Sun H et al., 2015), mRNA in human tissue samples (Meador-Woodruff et al., 1996), and receptor protein in rat tissue samples (Borroto-Escuela et al., 2013). The D2R is located in the substantia nigra: mRNA in rat tissue samples (Le Moine C et al., 1990), receptor protein in rat tissue samples (Levey AI et al., 1993) and receptor protein in rat dopaminergic neurons (Lukasiewicz S et al., 2010). Although more sparsely distributed than it is in the midbrain regions, the D2R is located in the prefrontal cortex (PFC), especially in layers V and VI: mRNA in human tissue samples (Meador-Woodruff et al., 1996), receptor protein in monkey

(Khan ZU et al., 2001), mRNA in rat pyramidal and GABAergic neurons (Santana N et al., 2009), and receptor protein in rat mPFC pyramidal neurons (Lukasiewicz S et al., 2010).

Like the D2R, the 5HT2AR is also a class 'A' GPCR widely distributed throughout the nervous system. Unlike the D2R, the 5HT2AR couples to G<sub>q</sub>-proteins. Outside of the schizophrenia hypotheses pathways, 5HT2AR protein is found in rat olfactory nuclei (Xu T et al., 2000) and the spinal cord (Cornea-Hebert et al., 1999). The 5HT2AR is distributed heavily in the PFC, but is also found in the striatum, VTA, substantia nigra, nucleus accumbens, and hippocampus. The PFC shows a high density of 5HT2AR: mRNA in human tissue samples of the dorsolateral PFC (Burnet PW et al., 1996), receptor protein in rat tissue samples, specifically layers IV-VI (Cornea-Hebert et al., 1999), and receptor protein in rat tissue samples (Xu T et al., 2000; Miner LAH et al., 2003). The striatum houses the 5HT2AR as receptor protein in rat tissue samples (Cornea-Hebert et al., 1999; Rodriguez JJ et al., 1999; Xu T et al., 2000). 5HT2AR distribution in the VTA is lighter than other areas, but still detectable as receptor protein in rat tissue samples (Cornea-Hebert et al., 1999; Doherty MD et al., 2000; Nocjar C et al., 2002). The substantia nigra contains the 5HT2AR as receptor protein in rat tissue samples (Cornea-Hebert et al., 1999) and receptor protein in rat dopaminergic neurons (Lukasiewicz S et al., 2010). 5HT2AR is also found in the nucleus accumbens as receptor protein in rat tissue samples (Cornea-Hebert et al., 1999; Rodriguez JJ et al., 1999). The 5HT2AR exists in regions of the hippocampus as mRNA in human and rat tissue samples (Burnet PW et al., 1996) and receptor protein in rat tissue samples (Cornea-Hebert et al., 1999; Xu T et al., 2000).

The mGlu2R is a class 'C' GPCR possessing a large extracellular 'venus flytrap' domain (VFTD) that serves as the orthosteric binding site. The mGlu2R also enjoys wide distribution throughout the brain. Outside of the schizophrenia hypotheses pathways, mGlu2R is found as:

mRNA and receptor protein in rat tissue samples from the spinal cord (Cao DY et al., 2015) and as receptor protein in human cerebellar tissue samples (Phillips T et al., 2000). The mGlu2R is particularly expressed in brain regions concerning schizophrenia hypotheses, such as the PFC, hippocampus, striatum, and substantia nigra. The PFC expresses mGlu2R densely: as mRNA and receptor protein in mice frontal cortex (Kurita M et al., 2013), as receptor protein in human tissue samples (Phillips T et al., 2000), as receptor protein in rat tissue samples (Ohishi H et al., 1998), and as receptor protein in human frontal cortical tissue samples and in mouse cortical neurons (Gonzalez-Maeso J et al., 2008). The mGlu2R is found in the hippocampus as receptor protein in human tissue samples (Phillips T et al., 2000) and receptor protein in rat tissue samples (Ohishi H et al., 1998). The mGlu2R is expressed in the striatum and substantia nigra as receptor protein in human tissue samples (Phillips T et al., 2000) and receptor protein in rat tissue samples (Ohishi H et al., 1998).

The D2R and mGlu2R are located on both pre- and post-synaptic structures throughout their distribution, but the 5HT2AR is predominantly found in the PFC on postsynaptic structures. However, low levels do exist on presynaptic structures, though most do not appear to connect to active synapses (Miner LAH et al., 2003). This lack of 5HT2AR expression levels limits the chances of presynaptic co-localization with D2R and mGlu2R in the PFC, but it is possible and further studies of pre-synaptic 5HT2AR viability are warranted.

All three receptors, D2R, 5HT2AR, and mGlu2R, are found in various glial cells. D2R protein is located in mouse (Duffy AM et al., 2011) and monkey (Khan ZU et al., 2001) PFC astrocytes. 5HT2AR protein is found in rat tissue sample glia (Miner LAH et al., 2003) and human tissue sample astrocytes (Fraser E et al., 2003). Rat microglial cell lines contain the

mGlu2R (Taylor DL et al., 2005). Co-localization data in glial cells are not yet available, but the possibility of direct interactions obviously exists.

Schizophrenia produces changes in associated receptor localization in the brain. In schizophrenic human cortical membranes, significantly less mGlu2R and more 5HT2AR protein densities exist as well as do significantly lower levels of mGlu2R mRNA (Gonzalez-Maeso J et al., 2008). Epigenetic studies may provide an explanation for these changes. The signaling of the 5HT2AR affects the transcription of the mGlu2R in mouse frontal cortex, possibly due to increased acetylation at the Glu2R promoter (Kurita M et al., 2013), suggesting a novel interaction between the mGlu2R and 5HT2AR that affects their localization.

There is such a wealth of information available about D2R, 5HT2AR, and mGlu2R localization in brain regions – only a small portion can be examined here. Huge amounts of data including many obvious overlaps of receptor and receptor mRNA expression suggest a high probability of co-localization, much of which may not have been explored yet. In contrast to glial studies, evidence for GPCR co-localization in neurons, native tissues, and heterologous systems continues to grow.

### **1.5. D2R-5HT2AR and mGlu2R-5HT2AR Co-localization and Heteromers**

When examining GPCR co-localization and heteromer formation, monomers and homomers of the constituent GPCRs must be taken into consideration as well. The possibility exists that the available total of each of two GPCRs could be involved in forming heteromers, but is unlikely. A mixture of GPCR heteromers, homomers, and monomers should be the resulting population in a representative plasma membrane. The D2R and 5HT2AR are shown to exist as both monomers and homomers, although functionality of both is debatable. The

exception to a mixture of monomers and homomers is GPCRs known to exist as constitutive homodimers, such as the mGlu2R.

Physiological expression levels of a series of D2R constructs in transfected HEK-293 cells allowed bio-luminescence resonance energy transfer (BRET), fluorescence resonance energy transfer (FRET), and bi-fluorescence complementation (BiFC) to determine multiple states of D2R existence. The results showed the D2R as having two, three, and four protomers, all exhibiting function. Computer modeling even suggested the possibility of a physiological homo-octamer (Guo W et al., 2008). As for D2R monomers, another series of D2R constructs was stably transfected in HEK-293 T-REX cells already stably transfected with aequorin. The aequorin cells provide a calcium-dependent luminescence assay sensitive to G<sub>q</sub>-coupled GPCR-induced PLC- $\beta_1$  activation. During this study, monomers and homodimers expressed and functioned normally, suggesting a mixture at the plasma membrane (Han Y et al., 2009).

Radio-labeled DOI preferentially binds to 5HT2AR in the human brain and was utilized in competition binding against multiple 5HT2AR-specific ligands, including ketanserin and MDL-100907, in human frontal cortex layer V tissue samples. Many of the results indicated were heterogeneous, including mono- and bi-phasic dose responses, which may represent monomers and homomers (Lopez-Gimenez JF et al., 2001). In a separate study, monomeric 5HT2AR was used as a comparison to mGlu2R-5HT2AR as a heterodimer in a molecular dynamics simulation. The authors were careful to not comment on function, but considering their results and the obvious function of the mGlu2R-5HT2AR heteromer we will discuss later, function of the 5HT2AR monomer is possible (Bruno A et al., 2009). However, in transfected HEK-293 cells, over-expression of 5HT2AR exhibited constitutive homodimerization when explored using co-immunoprecipitation (co-IP), photo-bleaching, and FRET (Brea J et al., 2009).

While class ‘A’ monomer and homodimer existence is not heavily researched, more is known about class ‘C’ GPCRs which exist in the plasma membrane as constitutive dimers. Time-resolved FRET (Tr-FRET) showed a nearly 100% homodimer result using SNAP/CLIP tagged mGlu2R protomers (Doumazane E et al., 2011). These results fit those from the use of co-IP and IP of mGlu5Rs in transfected HEK-293 cells. Upon reduction, the receptor protein levels were halved, reflecting an already-formed disulfide bond (Romano C et al., 1996).

While the evidence is limited for homomer co-localization and formation, mostly due to the inherent difficulties in teasing out the data between two or more identical protomers, the evidence supporting co-localization and heteromer formation between dissimilar GPCRs is growing. The best examples of co-localization are achieved in native tissues or neurons. But heterologous systems are effective as well, allowing for tighter control of the involved receptors and effectors in the system.

To establish mGlu2R and 5HT2AR co-localization, early methods used fluorescent *in situ* hybridization (FISH) with labeled DNA oligonucleotide probes to show overlapping distribution of the mGlu2R and 5HT2AR in mouse cortical neurons, using confocal microscopy (Gonzalez-Maeso et al., 2008). Co-IP in human frontal cortex tissue samples incubated with anti-5HT2AR antibodies pulled down the 5HT2AR protein and then subsequent western blotting for the mGlu2R was positive (Gonzalez-Maeso et al., 2008). Over the next few years, the mGlu2R and 5HT2AR were found to be co-localized in other cells. Overlapping co-localization was seen in epifluorescence micrographs of mouse frontal cortex and primary neurons stained with anti-5HT2AR and anti-mGlu2R antibodies conjugated to fluorophores (Fribourg M et al., 2011). In the same study, co-IP of mouse frontal cortex membrane preparations after staining with anti-5HT2AR antibodies and subsequent western blotting of mGlu2R displayed co-localization

(Fribourg M et al., 2011). In mouse frontal cortex samples, two different sizes of gold-particle immune-labeling allowed for viewing of the 5HT2AR and mGlu2R together at synaptic junctions (Moreno JL et al., 2012). Unfortunately, the electron microscopy resolution did not allow for discerning whether the receptors were on a pre- or post-synaptic terminal.

Heterologous systems are excellent tools for supplementing co-localization data in neurons and native tissues. BRET in HEK-293 cells transfected with Rluc-tagged mGlu2R and GFP-tagged 5HT2AR resulted in a definitive saturation curve reflecting co-localization (Gonzalez-Maeso et al., 2008). CFP-tagged 5HT2AR and YFP-tagged mGlu2R displayed robust FRET in HEK-293 cells (Gonzalez-Maeso et al., 2008). Homogenous time-resolved fluorescence or FRET (HTRF) resolves a signal to only include receptors at the plasma membrane. Using HTRF, SNAP/CLIP-tagged mGlu2R and 5HT2AR displayed close proximity and interaction (Delille HK, 2012). BRET between flow cytometry and FRET in HEK-293 cells showed co-localization of mGlu2R and 5HT2AR (Moreno JL et al., 2012). Single-cell FRET in HEK-293 cells transfected with 5HT2AR and mGlu2R displayed co-localization at the plasma membrane (Moreno JL et al., 2012). Co-IP of HEK-293 cells expressing HA-tagged mGlu2R (HA-mGlu2R) and c-myc-tagged 5HT2AR (c-myc-5HT2AR) displayed mGlu2R protein by western blot after IP for the HA tag (Gonzalez-Maeso et al., 2008; Moreno JL et al., 2012; Moreno JL et al., 2016). HEK-293 cells stably transfected with HA-mGlu2R and c-myc-5HT2AR cDNA were stained with anti-HA and anti-c-myc antibodies conjugated to fluorophores, allowing for visualization of co-localization (Baki L et al., 2016).

A relationship had already been established between the 5HT2AR and group II mGluRs as having effects on each other's actions, but knowledge of the mechanism was lacking (Marek GJ et al., 2000). Group II mGluRs include both mGlu2R and mGlu3R, but while establishing co-

localization of 5HT2AR and mGlu2R, mGlu3R was shown to not be co-localized with the 5HT2AR (Gonzalez-Maeso et al., 2008). Using the same process, 5HT2CR, part of the same GPCR sub-family as the 5HT2AR, was shown to not co-localize with mGlu2R (Moreno JL et al., 2016). The mGlu3R not co-localizing with the 5HT2AR and the mGlu2R not co-localizing with the 5HT2CR proved to be an excellent negative control, especially for experiments establishing direct interaction between mGlu2R and 5HT2AR.

Co-localization assays establish the existence of close proximity between two molecules, but can only be said to provide suggestive evidence of direct physical interaction. The evidence of direct interaction between mGlu2R and 5HT2AR as a heteromer is sparse. Perhaps the best evidence is found in the following series of experiments. Since the mGlu3R was shown to not co-localize with the 5HT2AR, chimeric constructs of mGlu2R and mGlu3R were utilized to pinpoint the potential interaction site of the 5HT2AR-mGlu2R heteromer. Co-IP of HEK-293 cells expressing HA-mGlu2R and c-myc-5HT2AR displayed mGlu2R protein by western blot after IP for the HA tag. A chimera constructed of the mGlu3 VFTD and TM6-7 with mGlu2R TM1-5 tagged with HA (HA-mGlu3R $\Delta$ TM1-5) was tested in place of HA-mGlu2R and again co-IP of the HA tag pulled down the second receptor. This result suggested the mGlu2R TM1-5 was a key interaction. Next, two chimeras were constructed: one combining the mGlu2R VFTD and TM1-3, 6-7 along with mGlu3R TM4-5 (HA-mGlu2R $\Delta$ TM4-5) and another combining the mGlu3R VFTD and TM1-3, 6-7 along with mGlu2R TM4-5 (HA-mGlu3R $\Delta$ TM4-5). Tested in the same manner as before, HA-mGlu2R $\Delta$ TM4-5 did not pull down both receptors, but HA-mGlu3R $\Delta$ TM4-5 did, suggesting mGlu2R TM4-5 as a key interacting site (Gonzalez-Maeso et al., 2008).

The next step in chimeric experiments constructed four more chimeras: one combining the mGlu2R VFTD and TM1-3, 5-7 along with mGlu3R TM4 (HA-mGlu2R $\Delta$ TM4), one combining the mGlu2R VFTD and TM1-4, 6-7 along with mGlu3R TM5 (HA-mGlu2R $\Delta$ TM5), one combining the mGlu3R VFTD and TM1-3, 5-7 along with mGlu2R TM4 (HA-mGlu3R $\Delta$ TM4), and one combining the mGlu3R VFTD and TM1-4, 6-7 along with mGlu2R TM5 (HA-mGlu3R $\Delta$ TM5). Tested in the same manner as before, HA-mGlu2R $\Delta$ TM4 and HA-mGlu3R $\Delta$ TM5 did not pull down both receptors, but HA-mGlu2R $\Delta$ TM5 and HA-mGlu3R $\Delta$ TM4 did, suggesting mGlu2R TM4 as a key interacting site (Moreno JL et al., 2012).

A comparison between mGlu2R and mGlu3R TM4 sequence homologies led to three residues at the intracellular end of TM4: constructs in similar fashion as before replaced mGlu2R residues Ala-677<sup>4.40</sup>, Ala-681<sup>4.44</sup>, and Ala-685<sup>4.48</sup> with mGlu3R Ser-686<sup>4.40</sup>, Phe-690<sup>4.44</sup>, and Gly-694<sup>4.48</sup>, respectively (superscripts represent a GPCR residue numbering system, Ballesteros JA and Weinstein H, 1995). Keeping the three alanines (HA-mGlu2R $\Delta$ TM4C) allowed pulling both receptors down significantly more than does the loss of the three alanine residues (HA-mGlu2R $\Delta$ TM4N). (**Fig 1.4A**) (Moreno JL et al., 2012). Further experiments with mGlu2R mutants containing one or two point mutations of the involved alanines in a different assay (DOI binding competition with radio-labeled ketanserin in transfected HEK-293 cells) led to the conclusion that any two of the three alanines at the intracellular end of mGlu2R TM4 mediate mGlu2R-5HT2AR heteromerization (Moreno JL et al., 2012).

Now that the key residues of the mGlu2R for heteromerization were known, the 5HT2AR could be examined in a similar fashion. Since the 5HT2CR does not co-IP and pull down the mGlu2R (Moreno JL et al., 2016) and previous data suggested TM1 and 4 as potential class 'A' homodimer interaction sites, two chimeras between 5HT2AR and 5HT2CR were constructed:

one combining 5HT2AR TM2-7 along with 5HT2CR TM1 (c-myc-5HT2AR $\Delta$ 1) and one combining 5HT2AR TM1-3, 5-7 along with 5HT2CR TM4 (c-myc-5HT2AR $\Delta$ 4). IP of c-myc-5HT2AR $\Delta$ 4 did not pull down HA-mGlu2R, but IP of c-myc-5HT2AR $\Delta$ 1 did, leading to the conclusion that TM4 of 5HT2AR mediates heteromerization with mGlu2R (**Fig 1.4B**) (Moreno JL et al., 2016).

A final conclusion to be gleaned from these experiments is that any two out of three alanines at the intracellular end of mGlu2R TM4 and TM4 of 5HT2AR mediate the heteromerization of the two receptors. Computer modeling and molecular dynamics simulations can provide support for heteromerization of the mGlu2R and 5HT2AR. Early modeling of the potential mGlu2R-5HT2AR heteromer used the available crystal structures of the  $\beta$ 2-adrenergic receptor and rhodopsin, respectively, as templates and resulted in a TM4,5-TM4,5 configuration (Gonzalez-Maeso et al., 2008). At the time, this fit well with the known data. The same configuration was modeled using the same crystal structures as templates, this time inserting the three alanines at the intracellular end of mGlu2R TM4. The comparison was the same model with the three alanines mutated and inserted, resulting in the Ser-6774.40 and Gly-6854.48 pointing outward and Phe-6814.44 jutting inward towards 5HT2AR TM5, possibly disrupting the ability of the heteromer to form (Moreno JL et al., 2012). Again, this fit well with previous data. The latest model used the crystallized structure of the  $\beta$ 2-adrenergic receptor for both receptors. The structure included a G<sub>s</sub>-protein which allowed for a more accurate model of the active conformation. Two protomers of each receptor allowed for homo-dimer interfaces of TM1-TM1 in both cases and TM4-TM4 in the heteromer, reflecting the newest data (Moreno JL et al., 2016).

A molecular dynamics simulation based around a TM4-TM5 interface between mGlu2R and 5HT2AR showed interaction, more specifically a change in the binding pocket conformation of the 5HT2AR. The crystal structures of the rhodopsin receptor and  $\beta$ 2-adrenergic receptor were used as templates for the mGlu2R and 5HT2AR, respectively (Bruno A et al., 2009). Later, a metadynamics simulation was performed using the crystal structures of the rhodopsin receptor and  $\beta$ 2-adrenergic receptor as templates for the mGlu2R and 5HT2AR, respectively (Fribourg M et al., 2011). The 5HT2AR was simulated with ligands docked: agonist, antagonist, and inverse agonist. Each conformation initiated by one of the ligands reached its most stable state at its lowest free energy difference along a range from most active to most inactive. Upon the addition of the mGlu2R to the simulation, conformational changes in the 5HT2AR were represented by distinct changes in the ligand positions along the activity range. These results suggest a direct interaction as a heteromer between mGlu2R and 5HT2AR.

Evidence for co-localization and heteromerization of the D2R-5HT2AR is less studied than the mGlu2R-5HT2AR, but does exist. BRET in HEK-293T cells transfected with Rluc-tagged D2R<sub>L</sub> and increasing amounts of GFP-tagged 5HT2AR suggests co-localization (Borroto-Escuela DO et al., 2010). Overlaid confocal microscopy images display D2R-5HT2AR co-localization in rat mPFC and substantia nigra (Lukasiewicz S et al., 2010) as well as HEK-293 cells transfected with CFP-tagged 5HT2AR and YFP-tagged D2R (Lukasiewicz S et al., 2010; Lukasiewicz S et al., 2011). Single-cell FRET in HEK-293 cells using the same constructs also displayed co-localization (Lukasiewicz S et al., 2010; Lukasiewicz S et al., 2011). Co-IP in HEK-293 cells transfected with Rluc-tagged D2R and GFP-tagged 5HT2AR was performed. IP for the Rluc pulled down the GFP and IP for the GFP pulled down the Rluc, suggesting a direct interaction between the D2R and 5HT2AR (Albizu L et al., 2011). Photonics-based GPCR co-

localization studies in native tissues are lacking, but recently, proximity ligation assays (PLA) are being utilized to show *ex vivo* proximity. PLA in rat striatum and nucleus accumbens tissue samples showed D2R and 5HT2AR co-localization (Borrito-Escuela DO et al., 2013; Borrito-Escuela DO et al., 2014).

Point mutations at specific interaction sites were shown to disrupt the D2R and 5HT2AR co-localization. Electrostatic interactions between two-or-more-residue epitopes were shown in the heteromerization of D1R with D2R. Two negatively charged residues in the C-terminal tail of the D1R interacted with six positively charged residues in the IC3 of the D2R. The more positive residues that were mutated to alanines, the less strong the electrostatic interaction became (Lukasiewicz S et al., 2009). Since the 5HT2AR possesses the same epitope as the D1R, similar experiments were performed to look at the effects on D2R-5HT2AR heteromerization. As seen in HEK-293 cells transfected with the appropriate constructs, using confocal microscopy overlays and single-cell FRET, again, the more positive residues in the D2R IC3 that were mutated to alanines or when the two negative residues in the 5HT2AR C-terminus tail were mutated to alanines, the significantly less strong the interactions became (**Fig. 1.5**) (Lukasiewicz S et al., 2010).

A final conclusion to be gleaned from these experiments is that the six positively charged residues in the IC3 of the D2R and the two negatively charged residues in the C-terminus tail of the 5HT2AR mediate D2R-5HT2AR heteromer formation. Computer models and molecular dynamics simulations are not yet available for the D2R-5HT2AR to support this conclusion. However, a system of predicting heteromer formation and interacting sites was developed that could be considered a type of modeling. Using a mathematical method, homology triplets were determined that could predict whether or not a heteromer could form between two GPCRs, as

well as the triplet being in or near the interacting site. A ‘pro-triplet’ is a homology in at least one heterodimer but is not a homology in any non-heterodimer. Just the reverse, a ‘contra-triplet’ is in at least one non-heterodimer but does not appear in any heterodimer (Tarakanov AO and Fuxe K, 2010). With this system, the D2R-5HT2AR was shown to possess five pro-triplets that appear in both receptors and may mediate formation and one pro-triplet that appears in both receptors but does not mediate formation. One of the pro-triplets was very near the area of the D2R IC3 involved in the heteromer mediation. The mGlu2R-5HT2AR was also shown to contain pro-triplets: two pro-triplets that appear in both receptors and may mediate formation and one pro-triplet that appears in both receptors but does not mediate formation (Fuxe K et al., 2014).

### **1.6. Allosteric Effects Upon Heteromerization**

Proximity and interaction, be it indirect or direct, is now established between the 5HT2AR and either the mGlu2R or D2R. Allosteric functional changes upon heteromerization must next be examined. Allosterism is defined as “the process by which the interaction of a chemical or protein at one location on a protein or macromolecular complex (the allosteric site) influences the binding or function of the same or another chemical or protein at a topographically distinct site” (Ferre S et al., 2014). An example of this definition is a positive allosteric modulator of mGlu2R, such as biphenylindanone (BINA), which binds at a distinct site from the orthosteric site and enhances the function of the orthosteric ligand (Ellaithy A et al., 2015). In the context of GPCR heteromers, more specific terminology is helpful. ‘Lateral’ allosterism is the binding of one or more GPCRs to an activated GPCR along the plane of the membrane changing its conformation which subsequently changes its functional signaling and /or ligand affinity.

‘Classical,’ or ‘drug-induced,’ allosterism is the binding of a ligand on the newly-bound GPCR, changing the original GPCR’s conformation and subsequently changing its functional signaling and /or ligand affinity (Ferre S et al., 2014).

To examine allosteric changes in affinity and functional signaling upon GPCR heteromerization, we look at binding studies and functional assays. Many binding studies exist for the mGlu2R-5HT2AR, but one stands out from the rest because it establishes a bio-fingerprint for heteromerization. Using HEK-293 cells transfected with cDNA of mGlu2R, 5HT2AR, mGlu3R and the mGlu2R/mGlu3R receptor constructs with two or three alanines mutated at the intracellular end of TM4, competition binding assays between DOI and radio-labeled ketanserin were performed. Any combination of previously described transfected cDNAs that resulted in mGlu2R and 5HT2AR heteromerization showed a switch from a homomeric 5HT2AR two-site model to a heteromeric one-site model (Moreno JL et al., 2012). The use of this assay provides an efficient means to identify mGlu2R-5HT2AR heteromerization.

Studies involving functional signaling of the mGlu2R-5HT2AR are also plentiful, but again one such study stands out from the rest because of its thoroughness in using one assay to look at one signal. The assay employs ion channels as reporters for G-protein activity: the GIRK4\* for  $G_i$  activity and the IRK3 for  $G_q$  activity. GIRK1 and 4 homomers produce little to no channel activity, whereas the hetero-tetramer of GIRK 1/4 is the native configuration in the heart and acts as a normal inwardly-rectifying  $K^+$  channel with robust currents. A point mutation in the pore region of GIRK4 from Serine to Threonine (S143T) results in a homomeric channel (GIRK4\*) with robust currents and expression in heterologous systems similar to GIRK1/4 (Vivaudou M et al., 1997).  $G_i\beta\gamma$  directly enhances the current through GIRK4\*, making it an accurate reporter for  $G_i$ -coupled GPCR activity. PTX can then block the activity of the  $G_i$  protein

(**Fig. 1.6A**). IRK3, or Kir2.3, is an inwardly-rectifying  $K^+$  channel that is activated by  $PIP_2$ . GIRK4\* is also activated by  $PIP_2$ . Since activated  $G_q$ -coupled GPCRs result in  $PIP_2$  hydrolysis, IRK3 and GIRK4\* currents are inhibited, making both ion channels sensitive reporters of  $G_q$ -coupled GPCR activity. RGS2 can then be used to block the activity of the  $G_q$  protein (**Fig. 1.6B**) (Hatcher-Solis C et al., 2014).

*Xenopus* oocytes were injected with cRNAs for mGlu2R and/or 5HT2AR plus the appropriate ion channel and blocker (PTX or RGS2), depending on whether  $G_i$  or  $G_q$  activity was to be measured. After approximately two days of expression, the oocytes were stimulated with a high  $K^+$  solution containing combinations of ligands and the ion channel current was then blocked with high- $K^+$  containing barium. The difference between the basal current in high- $K^+$  solution and the G-protein induced current was then normalized to the barium sensitive current, resulting in a normalized G-protein activity. The mGlu2R was perfused with glutamate or the 5HT2AR with 5HT. In the presence of both receptors, the glutamate-induced  $G_i$  activity increased by ~100% and the 5HT-induced  $G_q$  activity decreased by ~50% when compared to the G-protein activities of the homomeric receptors (lateral allosterism). These results prompted the development of a metric, the balance index (BI), that can be used to predict the pro- or anti-psychotic nature of a drug (**Fig. 1.7A**). When 5HT and glutamate were applied concurrently in the presence of both receptors, the G-protein activities did not change further. Glutamate and methysergide (5HT2AR antagonist) or 5HT and e-glu (mGlu2R antagonist) applied concurrently in the presence of both receptors also did not change the G-protein activities any further. However, glutamate and DOI (5HT2AR agonist) or 5HT and LY37 (mGlu2R agonist) applied concurrently in the presence of both receptors decreases the endogenous ligand-induced G-protein activity (drug-induced allosterism). Furthermore, glutamate and clozapine (5HT2AR

inverse agonist) or 5HT and LY34 (mGlu2R inverse agonist) applied concurrently in the presence of both receptors increases the endogenous ligand-induced G-protein activity (**Fig. 1.7B-C**) (Fribourg M et al., 2011). This study provides a straightforward examination of one functional signal with a wide range of ligands applied to a GPCR heteromer.

A second bio-fingerprint of the mGlu2R-5HT2AR is the ability to apply a synthetic agonist (LY37 or DOI) to one receptor and with no endogenous agonist present, a G-protein signal increase is seen from the other receptor. First seen in *Xenopus* oocytes using TEVC (Fribourg M et al., 2011), this result was replicated by calcium-measurement and GTP $\gamma$ S assays in HEK-293 cells transfected with cDNAs for both receptors and mouse tissue samples (Moreno JL et al., 2016).

As with co-localization and interaction studies of the D2R-5HT2AR heteromer, allosteric studies are also limited. Using a CRE-luciferase assay in HEK-293T cells transfected with the cDNAs of both receptors to examine cAMP levels (a cAMP decrease reflects a G<sub>i</sub> activity increase), a right-shift in the QP (D2R agonist) concentration response curve was observed in D2R-5HT2AR cells treated with 5HT, reflecting a decreased potency of QP to elicit G<sub>i</sub> activity. In the same assay, 5HT and TCB2 (5HT2AR agonist) decreased the QP-induced G<sub>i</sub> activity (TCB2 was not significant), while ketanserin (5HT2AR antagonist) blocked the effects of 5HT and TCB2 (Borroto-Escuela DO et al., 2010). In a separate study by the same group, this assay was used again. This time, TCB2 elicited no change, but DOI and LSD (5HT2AR antagonist) significantly decreased the QP-induced G<sub>i</sub> activity (Borroto-Escuela DO et al., 2013). Using a NFAT-luciferase assay in HEK-293T cells transfected with cDNAs of both receptors to examine PLC and PKC activation (reflects a G<sub>q</sub> activity increase), a left-shift and increase in the 5HT concentration response curve was observed in D2R-5HT2AR cells treated with QP, reflecting an

increased potency and efficacy of 5HT to elicit  $G_q$  activity. In the same assay, QP increased both 5HT- and TCB2-induced  $G_q$  activity (Borroto-Escuela DO et al., 2010). A Fluo-4 calcium assay in the same cells showed a left-shift and increase in the 5HT concentration response curve when QP was applied, again reflecting an increased potency and efficacy of 5HT to elicit  $G_q$  activity (Borroto-Escuela DO et al., 2010).

Changes in co-localization due to drug-induced allosterism were examined by FRET in HEK-293 cells transfected with CFP-tagged 5HT2AR and YFP-tagged D2R. DOI or QP significantly decreased FRET efficiency, reflecting weaker co-localization, while ketanserin or butaclamol (D2R antagonist) increased FRET efficiency, reflecting stronger co-localization (Lukasiewicz S et al., 2010). In a second similar study by the same group, the same constructs were tested and the results were similar: DOI or QP significantly decreased FRET efficiency, reflecting weaker co-localization, while ketanserin or butaclamol increased FRET efficiency, reflecting stronger co-localization. In addition, haloperidol (D2R antagonist and typical APD) and a high concentration of clozapine (5HT2AR/D2R antagonist and atypical APD) did not change the FRET efficiency, but a low concentration of clozapine reduced the FRET efficiency (Lukasiewicz S et al., 2011).

Competition binding assays between radio-labeled ketanserin and DOI showed similar results in mouse striatum and HEK-293 cells transfected with D2R and 5HT2AR cDNAs. The addition of QP changed the concentration response curves in both cases to a two-site model and increased the potency of the high affinity site, while raclopride (D2R antagonist) reversed the effect in mouse striatum. When transfected with 5HT2AR cDNA alone, the QP response is not present (Albizu L et al., 2011). Saturation binding experiments in rat striatum showed increased binding of radio-labeled raclopride when DOI or LSD was applied followed by a complete

reversal with the addition of ketanserin. However, competition binding in rat striatum between radio-labeled raclopride and LSD showed that at higher concentrations of LSD, the binding of raclopride was reduced to nearly 10% (Borrito-Escuela DO et al., 2013). In competition binding between radio-labeled ketanserin and haloperidol in HEK-293 cells transiently transfected with 5HT2AR or both receptors' cDNAs, the concentration response curve was shifted right with the presence of both receptors compared to only 5HT2AR. In the same study, competition binding between radio-labeled ketanserin and clozapine showed a small right shift of the concentration response curve, but also a loss of a second higher affinity binding site when the D2R was added (Lukasiewicz S et al., 2011).

A straightforward functional signaling experiment was performed measuring  $G_q$ -induced  $IP_3$  production of the 5HT2AR alone and with the D2R present. DOI was applied to the 5HT2AR, then the D2R was added and through lateral allostery the  $G_q$  activity increased. Finally, the further addition of QP to the D2R decreased the  $IP_3$  levels back below the original homomeric levels (**Fig. 1.8**) (Albizu L et al., 2011).

### **1.7. *In Vivo* and *Ex Vivo* Studies**

Behavioral models provide an *in vivo* method of examination, looking at both direct and indirect interactions between the involved receptors. Transgenic mice have been developed to help ascertain the relationship and interaction between the mGlu2R and 5HT2AR. Knockouts of D2R, mGlu2R, or 5HT2AR, as well as heterozygous receptor knockdowns, provide insight into behavior and expression linked to the involved receptors. Transgenic mice also serve as negative controls for other experiments, such as co-IP, western blotting, and  $GTP\gamma S$  binding (Fribourg M et al., 2011; Moreno JL et al., 2012; Moreno JL et al., 2016).

Wild-type mice dosed with LY34 (mGlu2R inverse agonist) exhibited an increased total locomotion distance and vertical activity. However, in 5HT2AR-KO mice, the total distance was decreased and vertical activity was returned to untreated values, suggesting LY34 only affects locomotion when the 5HT2AR is present (Gonzalez-Maeso J et al., 2008). An MK-801 (NMDAR antagonist)-induced psychotic mouse model increases total horizontal locomotion activity which is significantly reversed by the administration of LY37 (mGlu2R agonist) or clozapine (5HT2AR inverse agonist and atypical APD). However, in 5HT2AR-KO and mGlu2R-KO mice, LY37 and clozapine, respectively, do not reverse the locomotion increases, again reflecting the need for both receptors to be present for anti-psychotic effects (Fribourg M et al., 2011).

DOI is used to induce a head-twitch mouse model of psychosis via a post-synaptic 5HT2AR-specific pathway. Herpes simplex 2 virus (HSV2) tagged with GFP was used to reintroduce mGlu2R into mGlu2R-KO mice. After DOI administration, the HSV-GFP mice exhibited no head-twitch symptoms. The HSV-mGlu2R mice showed a high amount of head-twitches which was not present in HSV-mGlu2R $\Delta$ 4N, the construct with the three alanine motif missing (Moreno JL et al., 2012). Both receptors were present, but the mutated construct disabled heteromer formation. When the mGlu2R-5HT2AR heteromer is not optimally expressed, the head-twitch response is weaker or non-existent.

As for D2R and 5HT2AR relationships, 5HT2AR knockout mice did not exhibit the anti-psychotic effects of haloperidol, a D2R antagonist and typical APD. An MK-801-induced psychotic mouse model in wild-type mice increased horizontal locomotion activity, which haloperidol reversed. Without the 5HT2AR, haloperidol had no noticeable effect (Albizu L et al., 2011).

Wild-type mice can also be used to examine possible D2R-5HT2AR interactions. D2R family (D2R, D3R, D4R) antagonists, some being APDs and some being D2R-specific, reduced or eliminated the DOI-induced head-twitch response in mice (Rangel-Barajas C et al., 2014). The possibility exists that the ligands are eliciting a response through a direct interaction between the D2R and the 5HT2AR

### **1.8. Trafficking and Expression Effects on mGlu2R-5HT2AR Formation**

As of yet, trafficking and expression have not been explored for the D2R-5HT2AR, but some insight has been obtained for the mGlu2R-5HT2AR. As mentioned, expression of mGlu2R and 5HT2AR in post-mortem schizophrenic brains is altered (Gonzalez-Maesó J et al., 2008), which may alter mGlu2R-5HT2AR heteromer expression as well. This result is supported by GTP $\gamma$ S binding in post-mortem schizophrenic brains showing a lack of G<sub>q</sub> activity increase by LY37 (Moreno JL et al., 2016). If the expression of the individual GPCRs is altered, it is expected that the heteromer expression would be altered as well.

In order to simulate a schizophrenic mGlu2R and 5HT2AR receptor profile, as well as the subsequent presumed sub-optimal heteromer expression, *Xenopus* oocyte injection ratios of mGlu2R:5HT2AR cRNA were varied. At a 1:2 ng/oocyte cRNA injection ratio, lateral and drug-induced allosterism were observed. However, changing the cRNA injection ratio to 1:1 or 1:3 ng/oocyte removed the lateral and drug-induced (by clozapine and LY37) allosteric effects (**Fig. 1.9A**) (Fribourg M et al., 2011). A surface expression assay using chemiluminescence and HA- or c-myc-tagged receptors showed similar expression levels of the individual receptors compared to when both receptors were present at the 1:2 ratio. At the 1:1 or 1:3 ratios, individual

expression levels were dissimilar compared to when both receptors were present (**Fig. 1.9B**) (Fribourg M et al., 2011).

The process starting at the mRNA level and progressing to protein expression is important; small changes along the way can have an impact on heteromer expression and function. Supporting this hypothesis is the development of a line of HEK-293 cells stably-transfected with 5HT2AR, mGlu2R, and a reporter ion channel, GIRK1/4. The resulting clones exhibited a range of heteromer classified as high to low, as assessed by extensive experiments. Through the development of each individual clone, the receptor or heteromer trafficking and expression was different, resulting in different phenotypes. The ratio of levels of mGlu2R protein expressed at the surface membrane normalized to its own mRNA levels and 5HT2AR protein expressed at the surface membrane normalized to its own mRNA levels clearly delineated the clonal phenotypes (**Fig. 1.9C**) (Baki L et al., 2016).

A pre-clinical study examined a rat model of psychosis to determine the effects of small doses of atypical and potential glutamate agonist APDs. When one drug was administered at a time, the anti-psychotic effects were minimal, but the co-administration of both drugs was significantly greater than one at a time (Uslaner JM, 2009). At the 1:2 cRNA injection ratio in oocytes, a concurrent application of LY37, clozapine, and the neurotransmitters does not increase the drug-induced cross-signaling any further. However, at the 1:1 or 1:3 ratios, the concurrent application of LY37, clozapine, and the neurotransmitters overcomes the presumably sub-optimal heteromer expression and increases the activity of both receptors which was not possible applying one drug at a time (**Fig. 1.9D**) (Fribourg M et al., 2011).

Mice heterozygous for mGlu2R or 5HT2AR possess lower levels of receptor expression. After developing heterozygous mice, psychosis was induced by MK-801. Neither LY37 nor clozapine administration alone could decrease the resulting total horizontal locomotion activity, but in combination, the two drugs lowered the locomotion significantly in both mouse lines (Fribourg M et al., 2011). We do not know the exact mechanisms involved in heteromer trafficking and expression, but the sub-optimal mGlu2R-5HT2AR heteromer phenotypes and their symptoms can be overcome by a combinatorial drug approach.

### **1.9. Hypothesis**

There exists much evidence in support of mGlu2R-5HT2AR and D2R-5HT2AR heteromerization and resulting conformational changes which lead to changes in allosteric signaling effects. The importance of these three GPCRs in schizophrenia is well documented, as many anti-psychotic treatments target GPCR function. We hypothesize that mGlu2R-5HT2AR heteromerization allosteric effects in *Xenopus* oocytes are similar in relevant mammalian cells. Furthermore, the D2R-5HT2AR heteromer will exhibit allosteric signaling changes upon heteromerization, possibly unique to itself. We set out to examine allosteric changes upon heteromerization using electrophysiological approaches designed to measure the effects of anti-psychotic drugs on the involved GPCRs and the heteromers they form.

**Figure 1.1. Key dopamine pathways in the brain.** The neuroanatomy of dopamine neuronal pathways in the brain can explain the symptoms of schizophrenia as well as the therapeutic effects and side effects of antipsychotic drugs. **(a)** Nigrostriatal dopamine pathway **(b)** Mesolimbic dopamine pathway **(c)** Mesocortical dopamine pathway **(d)** Tuberoinfundular dopamine pathway **(e)** Brainstem projections to the Thalamus (Stahl SM, 2013).

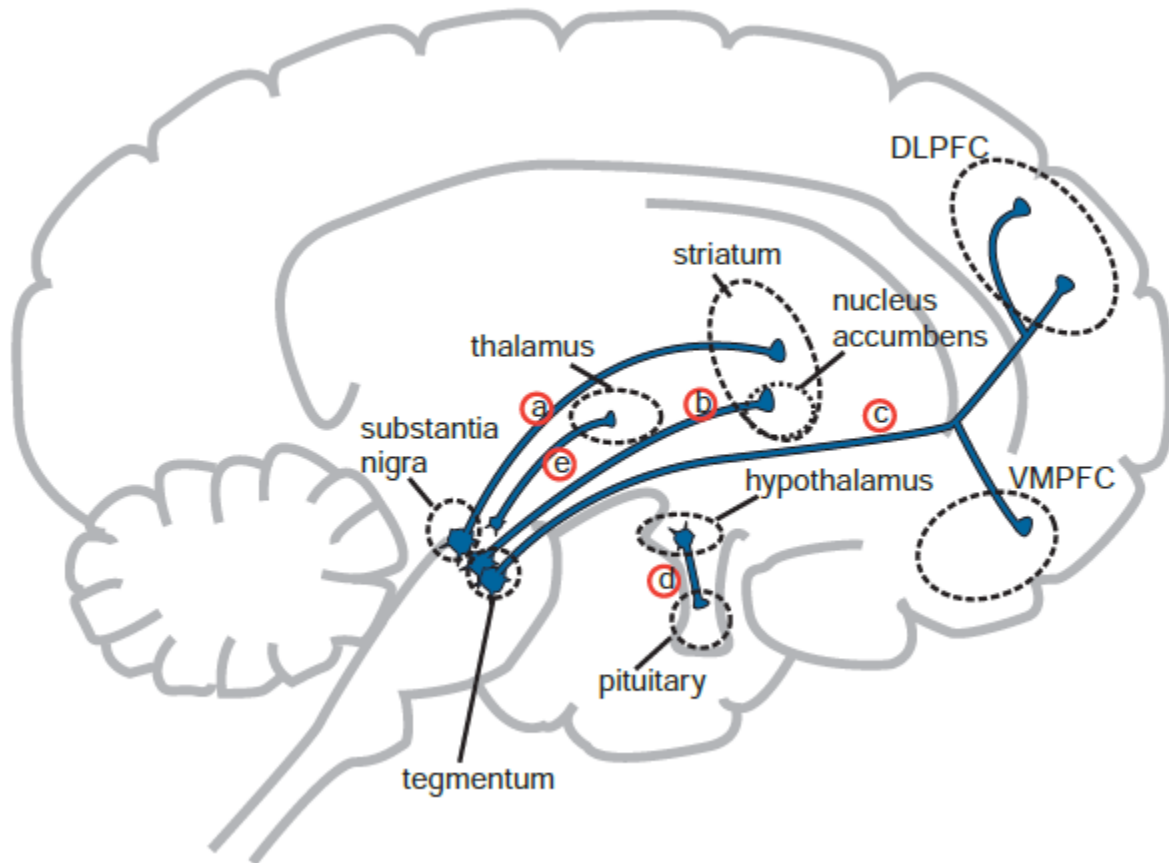


**Figure 1.2. Key glutamate pathways in the brain.** Although glutamate can have actions at virtually all neurons in the brain, there are key glutamate pathways particularly relevant to schizophrenia. **(a)** Cortico-brainstem glutamate pathway **(b)** Cortico-striatal and cortico-accumbens glutamate pathway **(c)** Hippocampal-striatal glutamate pathway **(d)** Thalamo-cortical glutamate pathway **(e)** Cortico-thalamic glutamate pathway **(f)** Direct cortico-cortical glutamate pathway **(g)** Indirect cortico-cortical glutamate pathway **(h)** GABAergic neurons in (c) and (g) also play a role in the NMDAR hypothesis (Stahl SM, 2013).

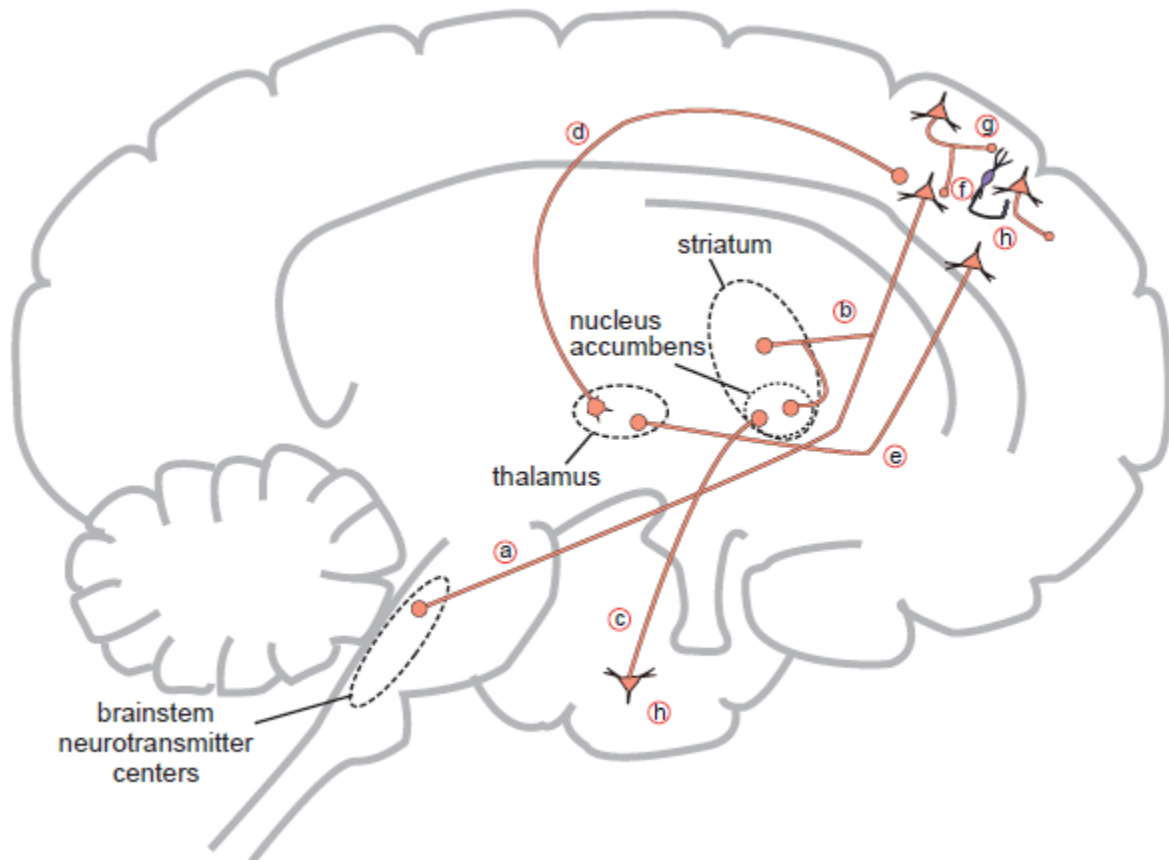


**Figure 1.3. GPCR Signaling.** (A)  $G_i$ - and (B)  $G_q$ -coupled signaling pathways consist of complex downstream signals (Huang Y et al., 2009).

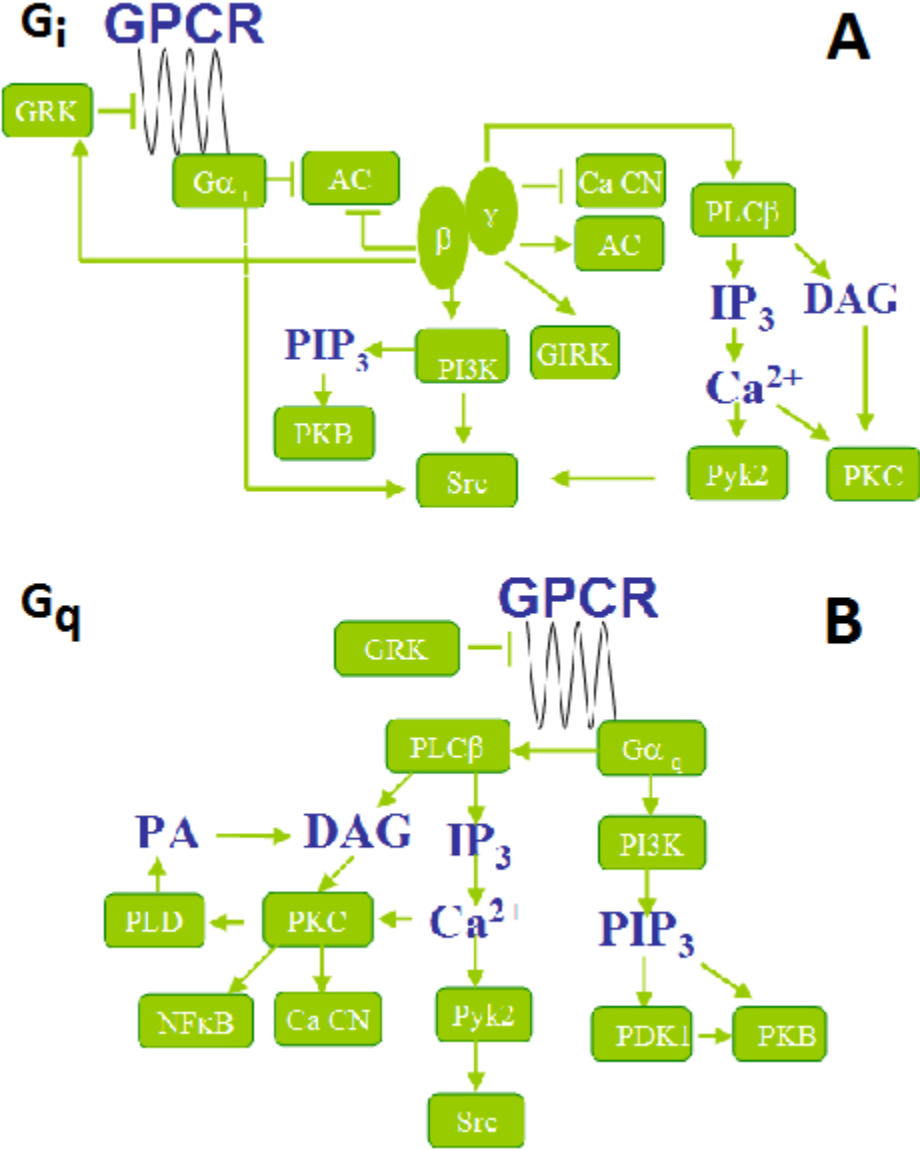


**Table 1.1. GPCRs integral to schizophrenia.** Three GPCRs: Isoforms, similarities, and differences.

<b>GPCR</b>	<b>Class</b>	<b>G-Protein Signal Path</b>	<b>Length (Amino Acids)</b>	<b>Size (kDa)</b>	<b>Loop and Termini Length Analysis Differences</b>
<b>D2R<sub>LONG</sub></b>	<b>A</b>	<b>G<sub>i</sub></b>	<b>444</b>	<b>~45</b>	<b>Long IC3 loop</b>
<b>D2R<sub>SHORT</sub></b>	<b>A</b>	<b>G<sub>i</sub></b>	<b>415</b>	<b>~42</b>	<b>Short IC3 loop – 29 residues</b>
<b>5HT2AR</b>	<b>A</b>	<b>G<sub>q</sub></b>	<b>471</b>	<b>48</b>	<b>Short N-terminus</b>
<b>mGlu2R</b>	<b>C</b>	<b>G<sub>i</sub></b>	<b>872</b>	<b>118</b>	<b>Very long N-terminus in Venus flytrap domain (VFTD); long EC2 loop</b>

**Figure 1.4. Direct evidence for mGlu2R-5HT2AR heteromerization.** (A) Three mGlu2R residues at the intracellular end of TM4 mediate mGlu2R-5HT2AR heteromerization. Chimeric constructs replaced mGlu2R residues Ala-677<sup>4.40</sup>, Ala-681<sup>4.44</sup>, and Ala-685<sup>4.48</sup> with mGlu3R Ser-686<sup>4.40</sup>, Phe-690<sup>4.44</sup>, and Gly-694<sup>4.48</sup>, respectively (HA-mGlu2RΔTM4N). Keeping the three alanines (HA-mGlu2RΔTM4C) pulls both receptors down significantly more than does the loss of the three alanine residues (Moreno JL et al., 2012). (B) 5HT2AR TM4 mediates mGlu2R-5HT2AR heteromerization. Chimeric constructs between 5HT2AR and 5HT2CR combined 5HT2AR TM2-7 along with 5HT2CR TM1 (c-myc-5HT2ARΔTM1) and 5HT2AR TM1-3, 5-7 along with 5HT2CR TM4 (c-myc-5HT2ARΔTM4). The c-myc-5HT2ARΔTM4 chimera did not pull down HA-mGlu2R, but the c-myc-5HT2ARΔTM1 did (Moreno JL et al., 2016).

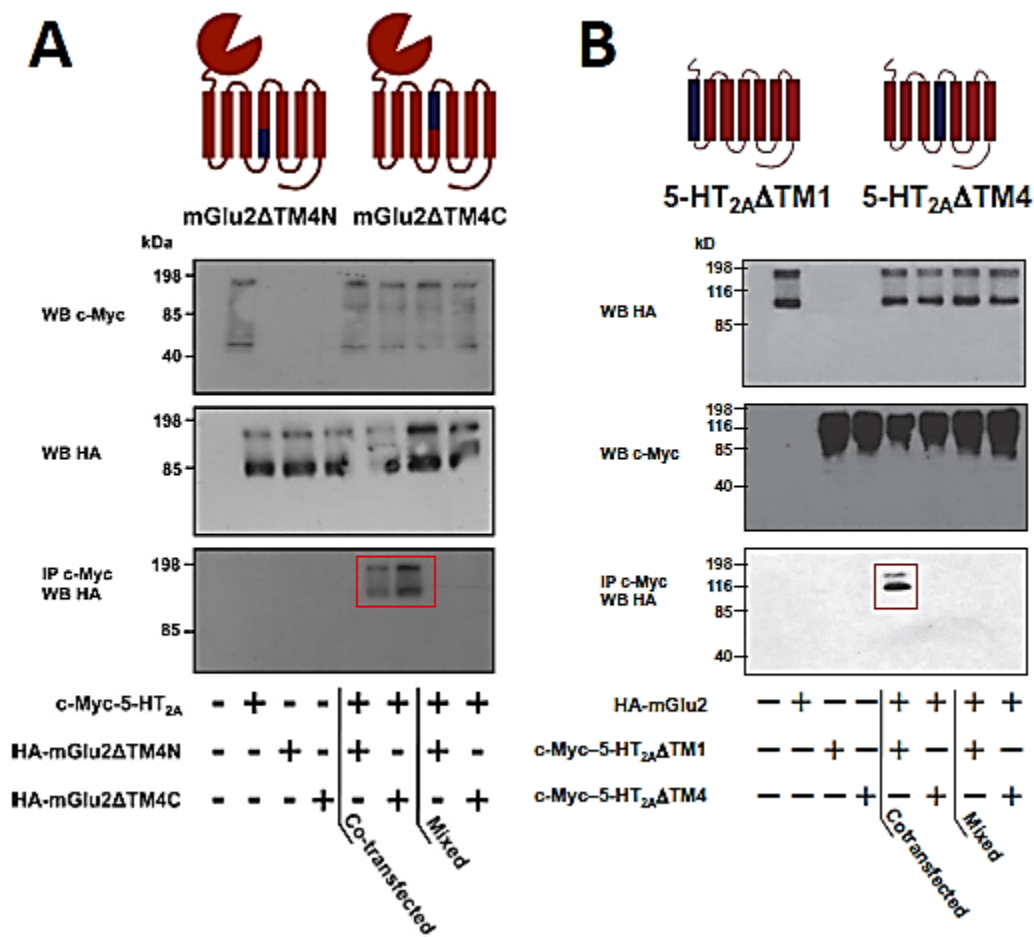


**Figure 1.5. Direct evidence for D2R-5HT2AR heteromerization.** A six positive-residue epitope in the IC3 of D2R and a two negative-residue epitope in the 5HT2AR C-terminal tail mediate D2R-5HT2AR heteromerization. In HEK-293 cells transfected with the appropriate constructs, using confocal microscopy overlays and single-cell FRET, the more positive residues in the D2R IC3 that were mutated to alanines or when the two negative residues in the 5HT2AR C-terminus tail were mutated to alanines, FRET levels decreased until the six-alanine D2R mutant showed significantly less strong interaction with 5HT2AR (Lukasiewicz S et al., 2010).

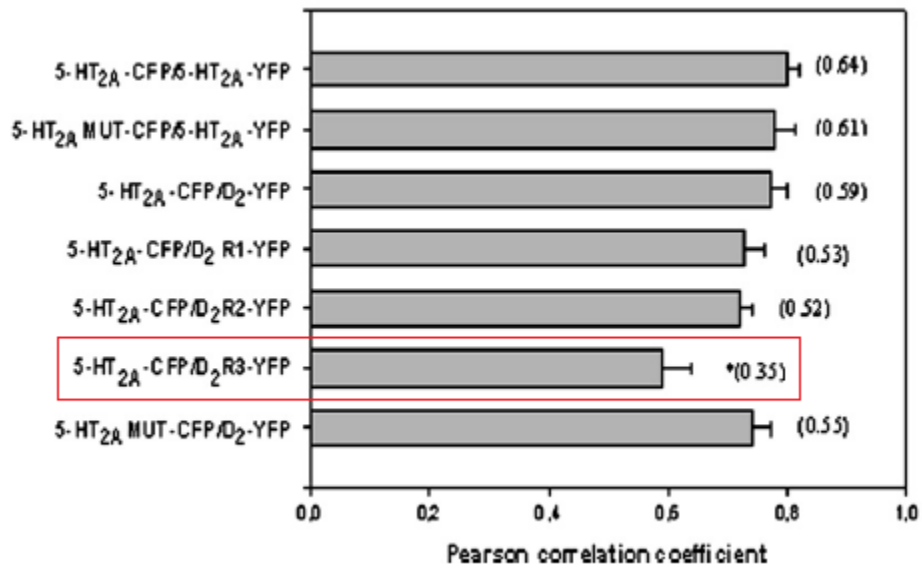


**Figure 1.6. Ion channel reporters for G-protein activity.** (A)  $G_i\beta\gamma$  directly enhances the current through GIRK4\*. PTX can then block the activity of the  $G_i$  protein. (B) IRK3 is activated by  $PIP_2$  (GIRK4\* is also activated by  $PIP_2$ ).  $G_q\alpha$  activates PLC- $\beta_1$ , which hydrolyses  $PIP_2$ , inhibiting IRK3 current. RGS2 can then block the activity of the  $G_q$  protein (Fribourg M et al., 2011; HatcherSolis C et al., 2014)

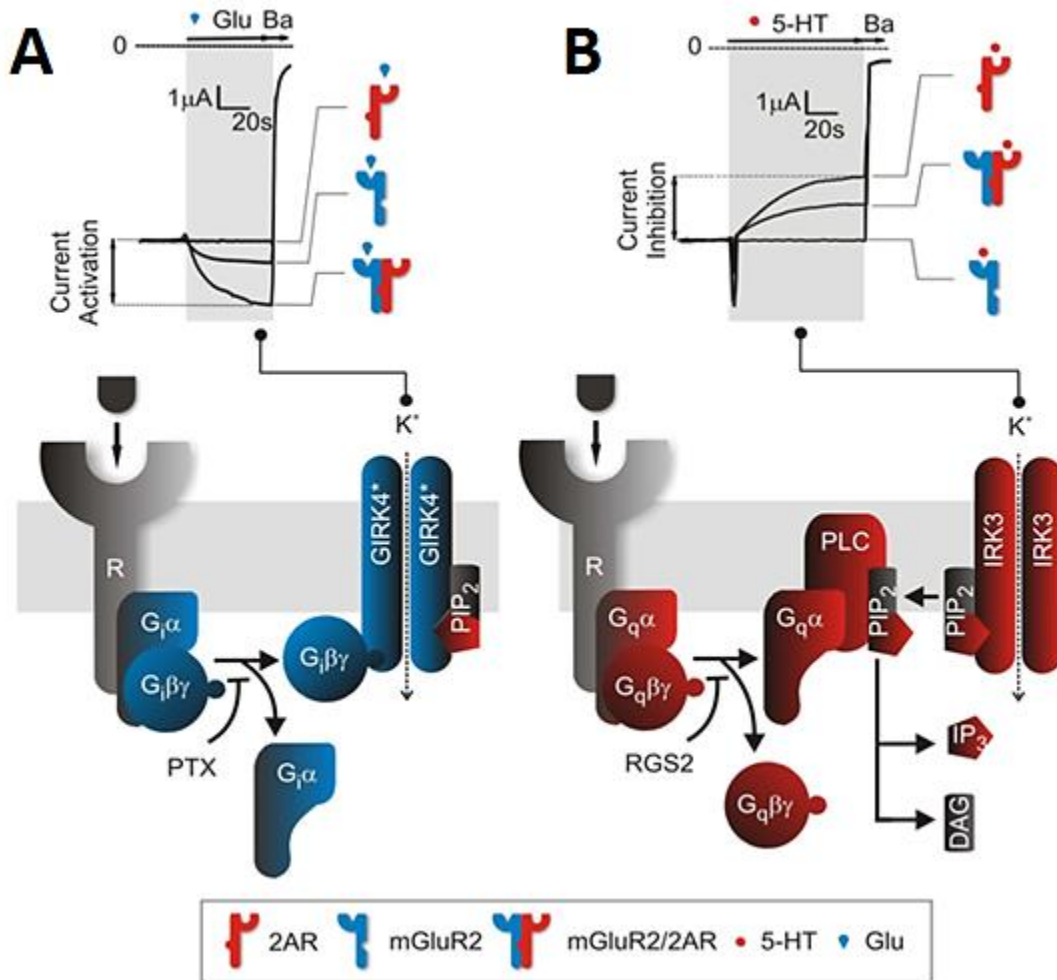


**Figure 1.7. Allosteric effects upon mGlu2R-5HT2AR heteromerization. (A)** Lateral allosterism upon mGlu2R-5HT2AR heteromerization: glutamate-induced  $G_i$  activity increased by ~100% and 5HT-induced  $G_q$  activity decreased by ~50% when compared to the G-protein activities of the homomeric receptors. **(B-C)** Drug-induced allosterism upon mGlu2R-5HT2AR heteromerization: 5HT and glutamate applied concurrently in the presence of both receptors does not change the G-protein activities further. Glutamate and methysergide or 5HT and e-glu applied concurrently in the presence of both receptors also did not change the G-protein activities further. However, glutamate and DOI or 5HT and LY37 applied concurrently in the presence of both receptors decreases the endogenous ligand-induced G-protein activity (drug-induced allosterism). Furthermore, glutamate and clozapine or 5HT and LY34 applied concurrently in the presence of both receptors increases the endogenous ligand-induced G-protein activity (Fribourg M et al., 2011).

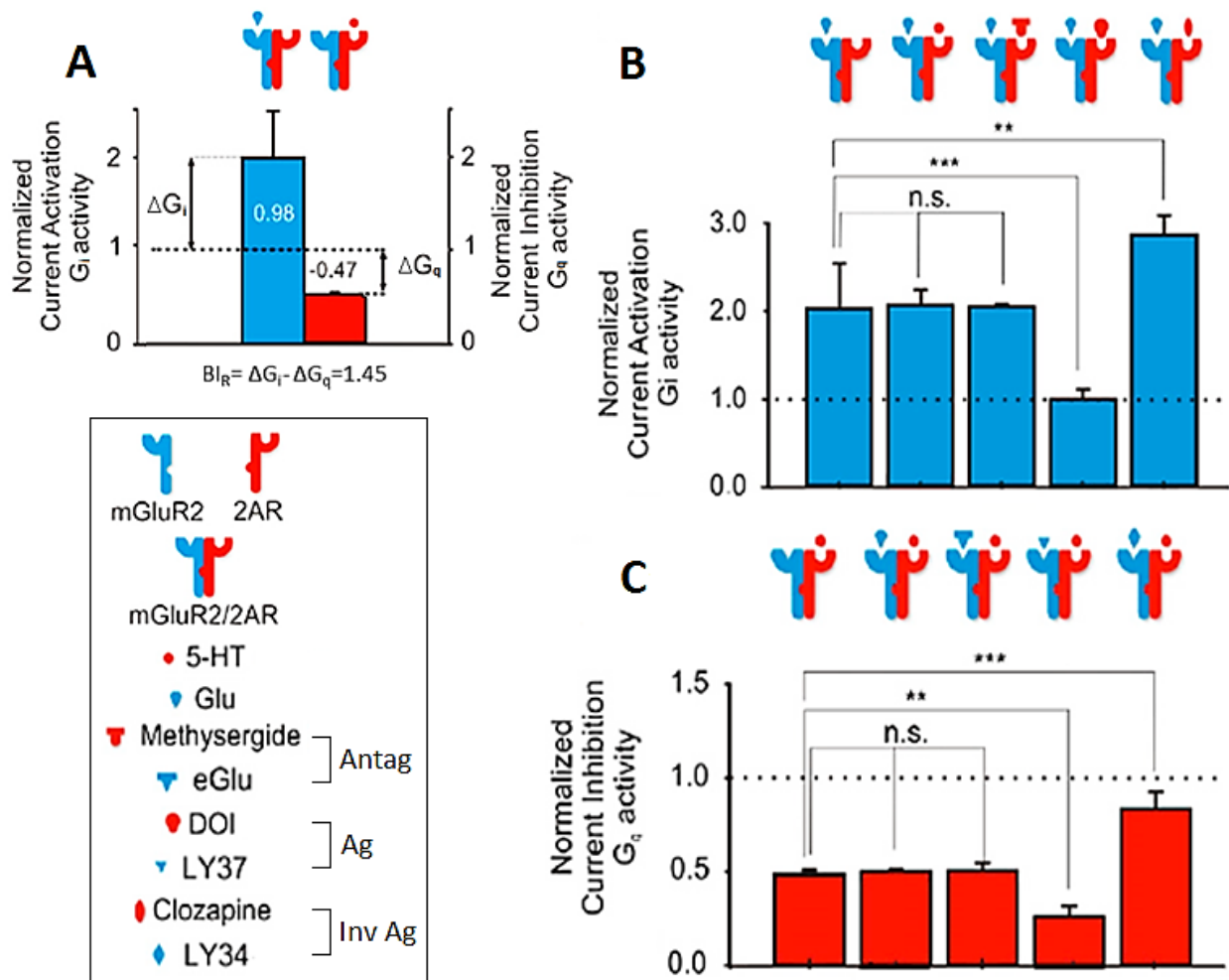


**Figure 1.8. Allosteric effects upon D2R-5HT2AR heteromerization.** A model of lateral and drug-induced allosterism and changes in affinity and  $G_q$  signaling in the D2R-5HT2AR heteromer. DOI was applied to the 5HT2AR to elicit a  $G_q$  signal. The addition of the D2R decreased 5HT2AR affinity for DOI, but increased the  $G_q$  signal. Finally, the further addition of QP to the D2R increased 5HT2AR affinity for DOI, but decreased the  $G_q$  signal (Albizu L et al., 2011).

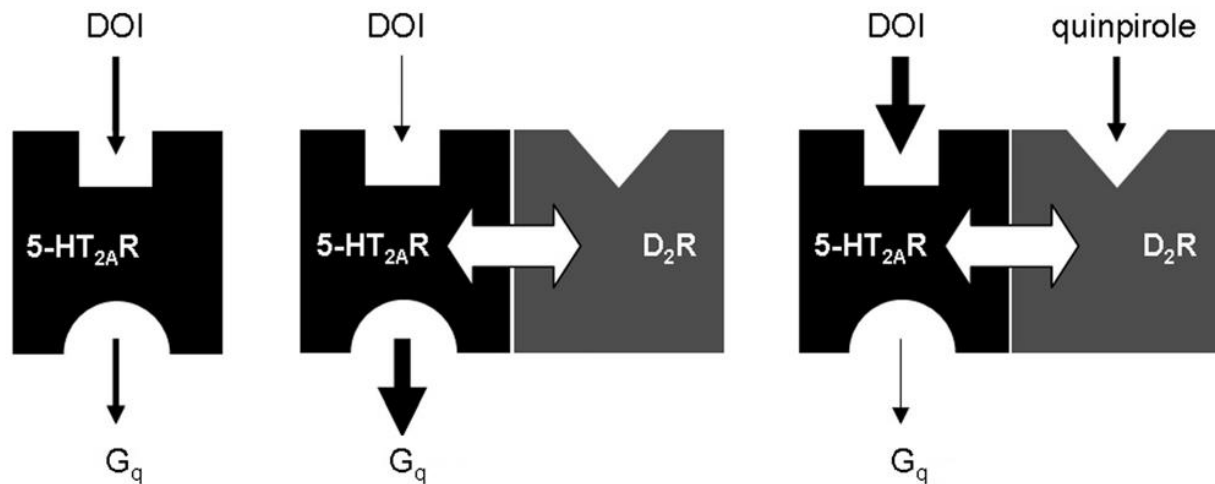
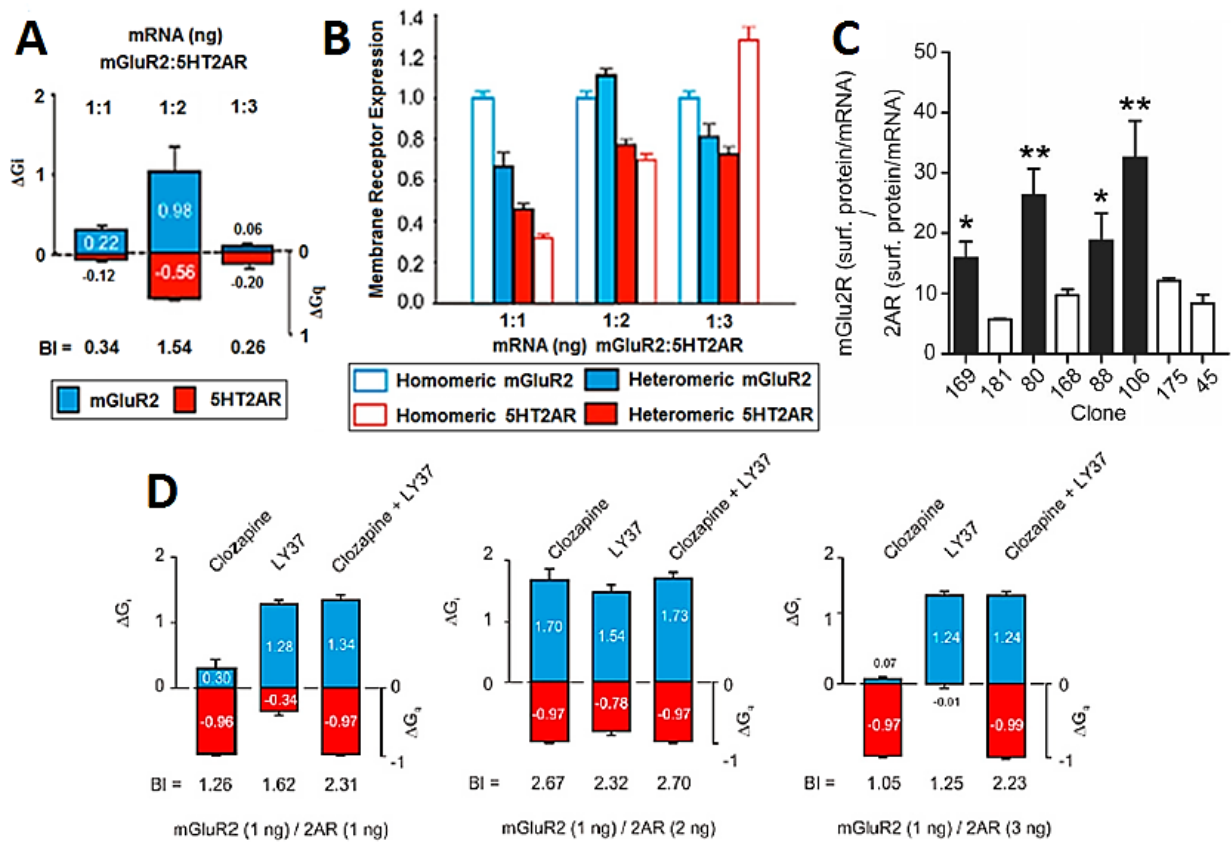


**Figure 1.9. Heteromer trafficking and expression effects.** **(A)** *Xenopus* oocyte injection ratios of mGlu2R:5HT2AR cRNA affect lateral allosterism. At a 1:2 ng/oocyte cRNA injection ratio, lateral allosterism was observed. However, changing the cRNA injection ratio to 1:1 or 1:3 ng/oocyte removed the lateral allosteric effects (Fribourg M et al., 2011). **(B)** A surface expression assay revealed similar expression levels of the individual receptors compared to when both receptors were present at the 1:2 ratio. At the 1:1 or 1:3 ratios, individual expression levels were dissimilar compared to when both receptors were present (Fribourg M et al., 2011). **(C)** Clonal lines of HEK-293 cells stably-transfected with 5HT2AR and mGlu2R exhibited a range of heteromer from low to high. The ratio of levels of mGlu2R protein expressed at the surface membrane normalized to its own mRNA levels and 5HT2AR protein expressed at the surface membrane normalized to its own mRNA levels clearly delineated the clonal phenotypes (Baki L et al., 2016) **(D)** Drug-induced allosterism exists at the 1:2 cRNA injection ratio in oocytes, but a concurrent application of LY37 or clozapine plus the respective neurotransmitters does not increase the cross-signaling any further. However, at the 1:1 or 1:3 ratios, the concurrent application of LY37 and clozapine plus the respective neurotransmitters overcomes the presumably sub-optimal heteromer expression and increases the activity of both receptors which was not possible when applying one drug at a time (Fribourg M et al., 2011).



## Chapter 2: MATERIALS AND METHODS

### 2.1: Molecular Biology

For expression in *Xenopus* oocytes, the following vectors were used: pGEMHE (for GIRK4\*, IRK3, PTX, and D2R) and pXoom (for mGlu2R, 5HT2AR, 5HT2AR (2A), and RGS2). All DNAs were human except for mouse D2R. Point mutations were introduced using standard *Pfu*-based mutagenesis techniques according to the QuikChange protocol (Agilent Technologies) and mutations were verified by sequencing (Genewiz). Plasmids were linearized and purified. *In vitro* transcription was performed using a commercially available T7 mRNA transcription kit followed by a final purification.

### 2.2: Drugs and Chemicals

L-glutamic acid, dopamine hydrochloride, serotonin hydrochloride, 2,5-Dimethoxy-4-iodoamphetamine (DOI) hydrochloride, and amisulpride were purchased from Sigma. LY341495 (LY34) disodium salt, LY379268 (LY37), R-quinpirole hydrochloride, amperozide hydrochloride, and paliperidone were purchased from Tocris. Pimavanserin was purchased from MedChem Express.

### **2.3: Cells and Transfections**

HEK-293 cells were maintained in Dulbecco's modified Eagle's medium (DMEM, Invitrogen, Carlsbad, CA) supplemented with 10 % (v/v) fetal bovine serum at 37 °C in a 5 % CO<sub>2</sub> humidified atmosphere. Transfections were performed using Lipofectamine 2000 reagent (Invitrogen) according to the manufacturer's instructions. For selection of the stably transfected GIRK clones, the pPUR selection vector (Clontech Laboratories, Inc., Catalog # 631601) was co-transfected with the pBI-CMV1-GIRK1-GIRK4 construct in a 1:20 ratio. Stable clones of HEK-GIRK cells were selected, and maintained thereafter, in puromycin-containing medium (500 ng puromycin/ml). For selection and maintenance of HEK-GIRK-mGlu2R clones, G418 (500 µg/ml) was included in the above medium, whereas HEK-GIRK-mGlu2R-2AR clones were selected and maintained in the presence of the above antibiotics plus hygromycin (200 µg/ml) (Baki L et al., 2016).

### **2.4: Oocyte Preparation and Injection**

Oocytes from *Xenopus laevis* were surgically removed and subjected to collagenase treatment according to standard protocols. Once defolliculated, oocytes were transferred to OR2 solution supplemented with Ca<sup>2+</sup> and Penicillin/Streptomycin antibiotics. Stage V or VI oocytes were injected with 50 nL of cRNA resuspended in DEPC water.

### **2.5: Two-Electrode Voltage Clamp and Analysis**

Whole-cell currents were measured by conventional two-electrode voltage clamp (TEVC) with a GeneClamp 500 amplifier (Axon Instruments, Union City, CA). A high-potassium (HK) solution was used to superfuse cRNA-injected oocytes expressing the appropriate proteins to obtain a reversal potential for potassium of zero. The HK contained in millimolar (96 KCl, 1

NaCl, 1 MgCl<sub>2</sub>, 5 KOH/HEPES, pH 7.4). Inwardly rectifying potassium currents through GIRK4\* and IRK3 were obtained by clamping the cells at a voltage ramp from -80 to +80 mV. In order to isolate the G<sub>i</sub> signal, GIRK4\* was co-expressed with RGS2 in order to eliminate the G<sub>q</sub> component of the current. In order to isolate the G<sub>q</sub> signal, GIRK4\* was co-expressed with PTX in order to eliminate the G<sub>i</sub> component of the current. Basal IRK3 and GIRK4\* currents were defined as the difference between inward currents obtained at -80 mV in the presence of 3mM BaCl<sub>2</sub> in HK solution and those in the absence of Ba<sup>2+</sup> and measured for each trace. Current inhibition and current activation were measured respectively and normalized to basal current to compensate for size variability in oocytes.

## **2.6: Whole-Cell Patch Clamp Recordings**

Whole-cell patch-clamp current recordings were performed with Patch Clamp L/M-EPC7, Axopatch 200A, and Axopatch 200B amplifiers and Axon 8.1 software (Axon Instruments, Union City, CA). HEK-293 cells were trypsinized, resuspended in DMEM medium, and placed in the incubator for at least 3 hours for recovery. After recovery, cells were placed on poly-D-lysine-doped coverslips, left to attach for ~15 min, and transferred to the chamber of the patch-clamp setup with external solution containing in millimolar: 140 potassium gluconate, 2 CaCl<sub>2</sub>, 5 EGTA/K, 10 glucose, 10 HEPES-K, and 1 MgCl<sub>2</sub>. The composition of the internal solution was in millimolar: 140 potassium gluconate, 2 CaCl<sub>2</sub>, 5 EGTA/K, 10 Glucose, 10 HEPES-K, 0.3 MgCl<sub>2</sub>, 2 Na-ATP, and 0.01 GTP. In both solutions, osmolarity was 340 mOsm and pH was 7.4. Upon formation of the whole-cell configuration, a voltage ramp from -100 to +100 mV was applied and data were collected. At the end of the recordings, 4 mM BaCl<sub>2</sub> was applied to block potassium currents. The first few data points of the current versus time plot at -100 mV were averaged to obtain basal current. Similarly, agonist-induced currents were calculated by

averaging several current values at the peak of the effect. Current values were divided by the membrane capacitance (pF) to normalize for the size of each cell. For the experiments shown in Figs. 3.2 and 3.6,  $G_i$  activity was measured as GIRK current activation. Basal currents were subtracted from  $G_i$ -induced currents and the difference was divided by the basal currents. For the experiments shown in Fig. 3.4,  $G_q$  activity was measured as GIRK current inhibition.  $G_q$ -induced currents were subtracted from basal currents, and the difference was divided by the basal currents (Baki L et al., 2016).

## **2.7: Statistics**

All error bars represent the standard error of the mean (SEM). Statistical significance was assessed using Student's t-test in Excel. Statistical significance was set at  $p < 0.05$ , 0.01, or 0.001, denoted in figures by \*, \*\*, or \*\*\* asterisks, respectively. Unless otherwise noted, all experiments were repeated in at least two separate batches of oocytes.

## **Chapter 3: MGLU2R-5HT2AR SIGNALING IN MAMMALIAN CELLS**

### **3.1: Introduction**

We wanted to further substantiate in mammalian cells the relevance of the physical mGlu2R and 5HT2AR interaction for cellular signaling seen by Gonzalez-Maeso et al., 2008 and Fribourg et al., 2011. Making this goal even more relevant were the results of Delille et al., 2011, published two months after those of Fribourg et al., 2011. Overall, the studies were similar, but key elements were different. Delille et al., 2011 set out to further substantiate in mammalian cells the relevance of the physical mGlu2R and 5HT2AR interaction for cellular signaling seen by Gonzalez-Maeso et al., 2008 and Fribourg et al., 2011. Their efforts were mostly unsuccessful.

Using inducible HEK-293T cells, Delille et al., 2011 obtained results that contradicted those seen in oocytes by Fribourg et al., 2011. In cells expressing only mGlu2R or the induced mGlu2R with 5HT2AR, cAMP levels were measured and compared with ligands applied. LY37, LY35, LY40, and glutamate, all mGlu2R agonists, and LY34 and MGS0039, mGlu2R antagonists, yielded no difference in cAMP levels between mGlu2R and mGlu2R-5HT2AR cells. PAMs of mGlu2R, LY48 and BINA, yielded a slight left-shift in cAMP production

concentration curves. Next, they measured  $\text{Ca}^{2+}$  mobilization in the same mGlu2R-5HT2AR cells compared to cells expressing 5HT2AR alone. 5HT, 2MS, mescaline, R-lisuride, and DOI, all 5HT2AR agonists, and mianserin and ketanserin, 5HT2AR antagonists, yielded no difference in  $\text{Ca}^{2+}$  levels between 5HT2AR and mGlu2R-5HT2AR cells. Finally, DOI had no effect on competition binding between LY35 (mGlu2R agonist) and radio-labeled LY34 (mGlu2R inverse agonist) in rat cerebral cortex.

There are multiple reasons why the results of Delille et al., 2011 contradicted the results of Fribourg et al., 2011. Most importantly, the positive results in oocytes required a cRNA injection ratio of 1ng to 2ng mGlu2R to 5HT2AR per oocyte, otherwise lateral and drug-induced mGlu2R-5HT2AR allosteric effects in the heteromer did not occur (Fribourg M et al., 2011). Injecting oocytes with cRNA allows for tight control of protein expression levels, with translation and trafficking of the receptor being the only steps leading to expression. Having established stably transfected HEK-293T cells with 5HT2AR, Delille et al., 2011 induced mGlu2R expression. Transfection of cDNA does not provide the same tight control of expression like cRNA injection due to the added step of transcription. Also, mGlu2R expression was held constant in oocytes while 5HT2AR expression was titrated, which was not done by Delille et al., 2011. Delille et al., 2011 consistently tried to achieve the highest expression possible of both receptors, which they verified throughout and chose their induction levels accordingly. Maximal expression of mGlu2R and 5HT2AR does not lead to maximal heteromer expression or formation (Fribourg M et al., 2011).

Other key differences were the assays and ligands used. Both Delille et al., 2011 and the papers of Gonzalez-Maeso et al., 2008 and Fribourg et al., 2011 used a few of the same ligands: glutamate, 5HT, DOI, LY34, and LY37, but these ligands were utilized in different assays.

Delille et al., 2011 used mGlu2R PAMs, known in mGluRs to display different effects as compared to glutamate or other agonists as well as binding to an allosteric site (Moustaine DE et al., 2012). Emerging theories about biased agonism, functional selectivity, and even biased antagonism make comparisons between assays, drugs, and signals nearly impossible, causing the cAMP and Ca<sup>2+</sup> mobilization assays to not compare well with other assays like the ion channel reporter assay in oocytes.

Therefore, we designed part of our study to be as similar as possible to the work performed in Fribourg et al., 2011, including our choice of ligands (**Table 3.1**). Our overall goal was to create a HEK-293 stably transfected cell line expressing GIRK1/4 as a reporter ion channel, mGlu2R, and 5HT2AR which could be used in extensive testing and possibly as a future high-throughput screening assay for ligands. These cells could then be whole-cell patch clamped in a method similar to that used in oocytes.

First, HEK-293 cells were stably transfected with GIRK1/4. Dozens of clones were then selected for testing based on western blotting for channel protein. The clone showing the best response to GTP $\gamma$ S application inside the pipette during whole-cell patch clamp and possessing a strong barium-sensitive current was chosen for the next step (clone 31). Next, clone 31 was stably transfected with mGlu2R. Dozens of clones were selected for testing based on western blotting for receptor protein. The clone showing the best response to glutamate application during whole-cell patch-clamp and possessing a strong barium-sensitive current was chosen for the next step (clone 59). Finally, clone 59 was stably transfected with 5HT2AR. Dozens of clones were selected for testing based on western blotting for receptor protein (Baki L et al., 2016).

Multiple clones were now available for mGlu2R-5HT2AR heteromeric allosterism experiments, each with a unique phenotype.  $\text{Ca}^{2+}$  mobilization was measured using the ratiometric dye Fura-2 while either 5HT or 5HT plus LY34 was being applied. Cells showing an increase in  $\text{Ca}^{2+}$  levels due to LY34 application were termed 'cross-talk positive' while cells not displaying a  $\text{Ca}^{2+}$  increase were termed 'cross-talk negative.' The established phenotypes represented a range of mGlu2R-5HT2AR heteromer formation and expression from high to low. Clone phenotypes dictated the cells to be used in further studies (Baki L et al., 2016).

Experimental and analytical differences exist between our stably-transfected HEK-293 cells and oocytes. The ability to block one receptor activity while recording current elicited by the second receptor with RGS2 or PTX is not available, therefore the whole-cell current is a total representative signal of all G-protein activity. GIRK1/4 is an inherently different ion channel than GIRK4\*, making differences in activation and inhibition a possibility. Barium sensitive currents are erratic in these cells and this assay, so we normalized G-protein-induced currents differently. First we normalized to cell size represented by membrane capacitance, which is the typically used method to represent current density. Second, instead of normalizing to barium-sensitive current, we normalized to basal currents which were a more consistent measurement. Lateral allosterism cannot be examined in these cells since the heteromer is a stable entity with no homomer to which it can be compared. Clone 59 expresses only GIRK1/4 and mGlu2R, but its glutamate-induced  $G_i$  activity is higher than the heteromeric cells, nullifying true comparisons that would be involved in examining lateral allosterism. We designed our experiments and analysis with these differences in mind.

### **3.2: Results**

### **3.2.1: Effects of 5HT2AR ligands on G<sub>i</sub> signaling of mGlu2R**

We began by examining the G<sub>i</sub> signal of the mGlu2R, intending to replicate the effects of an atypical APD, clozapine, as seen in Fribourg et al., 2011, namely an increase in glutamate-induced G<sub>i</sub> activity upon application of clozapine. Clozapine was used throughout the oocyte work, but early in our overall study, clozapine presented issues when used in conjunction with certain dyes. To maintain consistency across assays with our chosen ligands, we switched to paliperidone, another atypical APD used to show cross-signaling in oocytes similar to that shown by clozapine (Fribourg M et al., 2011). Two mGlu2R-5HT2AR heteromer clones were chosen to be tested: cross-talk positive clone 80 and cross-talk negative clone 45.

During the whole-cell patch clamp process, we first applied 500nM glutamate, a concentration chosen to be similar to an EC<sub>20</sub> – high enough to result in a current increase, but low enough to allow potentiation of the current increase. Second, we applied 500nM glutamate plus 50uM paliperidone. Finally, the application of barium reduced the signal to less than basal current (**Fig. 3.1**). The further addition of paliperidone resulted in a significant G<sub>i</sub>-induced increase in negative current through GIRK1/4 in clone 80, but not in clone 45 (**Fig. 3.2**) or the mGlu2R and GIRK1/4 clone 59 (**Fig. A1.1A**). The cross-signaling elicited by paliperidone was similar to that seen with clozapine in oocytes (Fribourg M et al., 2011).

### **3.2.2: Effects of mGlu2R ligands on G<sub>q</sub> signaling of 5HT2AR**

Again in clones 80 and 45, we examined the G<sub>q</sub> signal of the 5HT2AR, intending to replicate the effects of a mGlu2R inverse agonist, LY34, as seen in Fribourg et al., 2011, namely an increase in 5HT-induced G<sub>q</sub> activity upon application of LY34. Cells with constitutive G<sub>q</sub>

activity displayed relatively small currents, but we were nonetheless able to analyze viable  $G_q$  activity.

During the whole-cell patch-clamp process, we first applied 20nM 5HT, a concentration chosen to be similar to an EC20 – high enough to result in a current decrease, but low enough to allow potentiation of the current decrease. Second, we applied 20nM 5HT plus 100uM LY34. Finally, the application of barium reduced the signal even more (**Fig. 3.3**). The further addition of LY34 resulted in a significant  $G_q$ -induced decrease in negative current through GIRK1/4 in clone 80, but not in clone 45 (**Fig. 3.4**). The cross-signaling elicited by LY34 was similar to that seen with LY34 in oocytes (Fribourg M et al., 2011).

### **3.2.3: Combinatorial Effects of mGlu2R and 5HT2AR ligands on $G_i$ signaling of mGlu2R**

We again examined clones 80 and 45. However, using a combination of synthetic drugs, specifically LY37 (mGlu2R agonist and potential APD) and paliperidone, we expected opposite results than in section 3.2.1. The potent agonist LY37 was expected to induce a maximal heteromeric  $G_i$  signal in clone 80 that could not be increased by paliperidone, whereas the LY37-induced  $G_i$  signal in heteromeric clone 45 would be increased, overcoming a sub-optimal mGlu2R-5HT2AR heteromer formation and expression.

During the whole-cell patch-clamp process, we first applied 50nM LY37, a concentration chosen to be similar to an EC20 – high enough to result in a current increase, but low enough to allow potentiation of the current increase. Second, we applied 50nM LY37 plus 50uM paliperidone. Finally, the application of barium reduced the signal to less than basal current (**Fig. 3.5**). The further addition of paliperidone resulted in a significant  $G_i$ -induced increase in negative current through GIRK1/4 in clone 45, but not in clone 80 (**Fig. 3.6**) or the mGlu2R and

GIRK1/4 clone 59 (**Fig. A1.1B**). The cross-signaling elicited by paliperidone was similar to that seen with clozapine in oocytes (Fribourg M et al., 2011). Also, LY37 at a lower concentration than glutamate induced a higher  $G_i$  activity, supporting its role as a strong agonist.

### **3.3: Discussion**

Our whole-cell patch clamp results displayed by stably-transfected HEK-293 cells are similar to those seen using TEVC in injected oocytes (**Table 3.2**). An atypical APD cross-signals and increases glutamate-induced  $G_i$  activity of the mGlu2R with the 5HT2AR co-expressed in cells with high mGlu2R-5HT2AR heteromer expression, but not in cells with low mGlu2R-5HT2AR heteromer expression. LY34, a mGlu2R inverse agonist, cross-signals and increases 5HT-induced  $G_q$  activity of the 5HT2AR with the mGlu2R co-expressed in cells with high mGlu2R-5HT2AR heteromer expression, but not in cells with low mGlu2R-5HT2AR heteromer expression. Finally, an atypical APD cross-signals and increases LY37-induced  $G_i$  activity of the mGlu2R with the 5HT2AR co-expressed in cells with low mGlu2R-5HT2AR heteromer expression, but not in cells with high mGlu2R-5HT2AR heteromer expression.

These results establish relevance of the mGlu2R-5HT2AR heteromer allosteric effects in a mammalian cell line, but are just a portion of those found in Baki et al., 2016. Co-localization and heteromerization were studied in detail to establish not only phenotypes of stably-transfected HEK-293 clonal cells, but in order to find a bio-fingerprint related to mRNA and protein expression levels. The ratio of levels of mGlu2R protein expressed at the surface membrane normalized to its own mRNA levels and 5HT2AR protein expressed at the surface membrane normalized to its own mRNA levels served as the desired bio-fingerprint to predict clones with high or low mGlu2R-5HT2AR heteromer formation and expression. The differences between

clonal cell lines is presumably due to natural trafficking and expression mechanisms starting at cDNA transfection and ending with protein expression at the plasma membrane.

To discuss the pertinent question of relevance to psychosis, we must look at the schizophrenia-related neuro-circuitry. In **Figure 3.7** pathway number two, we envision a population of mGlu2R-5HT2AR heteromers on post-synaptic dendrites of a cortico-striatal pyramidal neuron. Maximal heteromer formation and expression exists, resulting in higher  $G_i$  signaling and lower  $G_q$  signaling compared to the respective homomers. The high  $G_i:G_q$  ratio will result in less neuronal excitement in the neuron projecting to the striatum, which will lower or maintain the low excitation of neurons in the striatum. The resulting dopamine levels will be regulated and presumably be physiologically optimal.

However, in a psychotic condition, either schizophrenia or possibly after abuse of a pro-psychotic drug, mGlu2R and 5HT2AR expression levels are changed in the PFC and/or the  $G_i:G_q$  ratio will be lower. The experiments in Fribourg et al., 2011 and Baki et al., 2016 clearly show that mGlu2R-5HT2AR heteromer formation and expression are optimized only when the two receptors exist in a tightly-regulated ratio involving mRNA and protein. Without the heteromer expressed at optimal levels, the cortico-striatal neuron will be more active and the dopamine levels in the striatum will rise. High dopamine levels are a symptom of schizophrenia and integral to the dopamine hypothesis of schizophrenia, which means increasing an already high level of dopamine will exacerbate the condition. Atypical APDs or potential mGlu2R APDs have the ability to reinforce or even reestablish the high  $G_i:G_q$  ratio, whether they are used alone or in combination. These treatments can then be used to lower the abnormally high dopamine levels in the striatum.

In **Figure 3.7** pathway 4, we consider the same population of post-synaptic mGlu2R-5HT2AR heteromers, but in this case the neuron is an inter-cortical projection to an inhibitory GABAergic neuron. Any low heteromer situation will again increase excitability of the projecting neuron. As part of the NMDAR hypothesis of schizophrenia, the already dysfunctional NMDAR receptors that would be activated by glutamate release from the now-overactive projecting neuron could possibly be restored to normal activity levels. The sub-optimal heteromer formation and expression in this case may serve to hide the effects of dysfunctional NMDARs and resulting symptoms.

In summary, the mGlu2R-5HT2AR heteromer has similar allosteric effects in mammalian cells as compared to *Xenopus* oocytes. Now that we have established the relevance of allosteric effects upon mGlu2R-5HT2AR heteromerization in HEK-293 cells, future experiments will involve neuronal cell lines and more detailed behavioral studies. The discussed scenarios are just two out of many possible ones. If the 5HT2AR is discovered to exist at greater levels pre-synaptically in the PFC, then even more scenarios will arise. The effect of homomeric populations as a mixture with the heteromeric population also needs to be examined. In the next chapter we will explore a second heteromer implicated in psychosis that may play a role in the same brain regions as well as synaptic terminals as the mGlu2R-5HT2AR heteromer.

**Table 3.1. Properties of mGlu2R and 5HT2AR ligands.** The ligands used in Chapter 3 experiments and their properties (Affinities taken from Corena-McLeod M, 2015; Southan C et. Al., 2016).

<b>Ligand</b>	<b>Target GPCR</b>	<b>Off-Target Interactions</b>	<b>Pharmacology</b>	<b>Affinity for Target GPCR (pK<sub>i</sub>/pK<sub>d</sub> values)</b>
<b>Glutamate</b>	<b>mGlu2R</b>	<b>All mGluRs, iGluRs</b>	<b>Endogenous agonist</b>	<b>5.4-5.9</b>
<b>LY379268 (LY37)</b>	<b>mGlu2R</b>	<b>mGlu3R, Group I and III mGluRs (high nM-low uM)</b>	<b>Synthetic agonist</b>	<b>7.9</b>
<b>LY341495 (LY34)</b>	<b>mGlu2R</b>	<b>mGlu3R, Group I and III mGluRs (high nM-low uM)</b>	<b>Antagonist/inverse agonist</b>	<b>7.7-9.0</b>
<b>5HT</b>	<b>5HT2AR</b>	<b>All 5HTRs</b>	<b>Endogenous agonist</b>	<b>8.9</b>
<b>Paliperidone (Pal)</b>	<b>5HT2AR</b>	<b>5HT1B-1CR, 5HT2CR, 5HT7R, D1-5R, H1-2R, α1-2R (low nM); 5HT1AR, 5HT1ER, 5HT4-6R (high nM-low uM)</b>	<b>Anti-psychotic drug, antagonist/inverse agonist</b>	<b>8.9-9.0</b>

**Figure 3.1. An atypical APD increases glutamate-induced mGlu2R signaling.** Representative barium-sensitive GIRK1/4 current trace obtained in response to 500nM glutamate (Glu) followed by 500nM Glu plus 50uM paliperidone (Pal) applied to stably-transfected HEK-293 cells (cross-talk positive clone 80) expressing mGlu2R+5HT2AR.

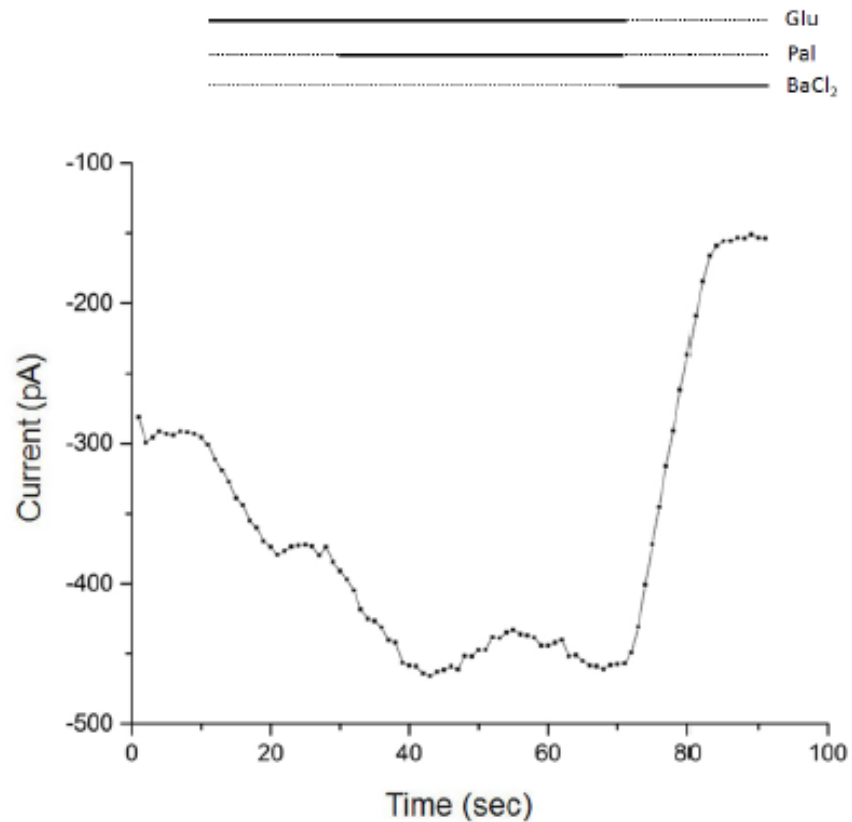


**Figure 3.2. The atypical APD paliperidone increases glutamate-induced mGlu2R signaling in positive but not negative cross-talk clones.** Summary bar graph from whole-cell patch clamp recordings of GIRK1/4 currents in cross-talk positive clone 80 and cross-talk negative clone 45 of HEK-293 cells expressing mGlu2R and 5HT2AR exposed to 500nM glutamate (Glu) followed by 500nM Glu plus 50uM paliperidone (Pal). (N = numbers inside the bars/condition, Data were normalized to basal activity and are mean  $\pm$  SEM, \* $p \leq 0.05$ ).

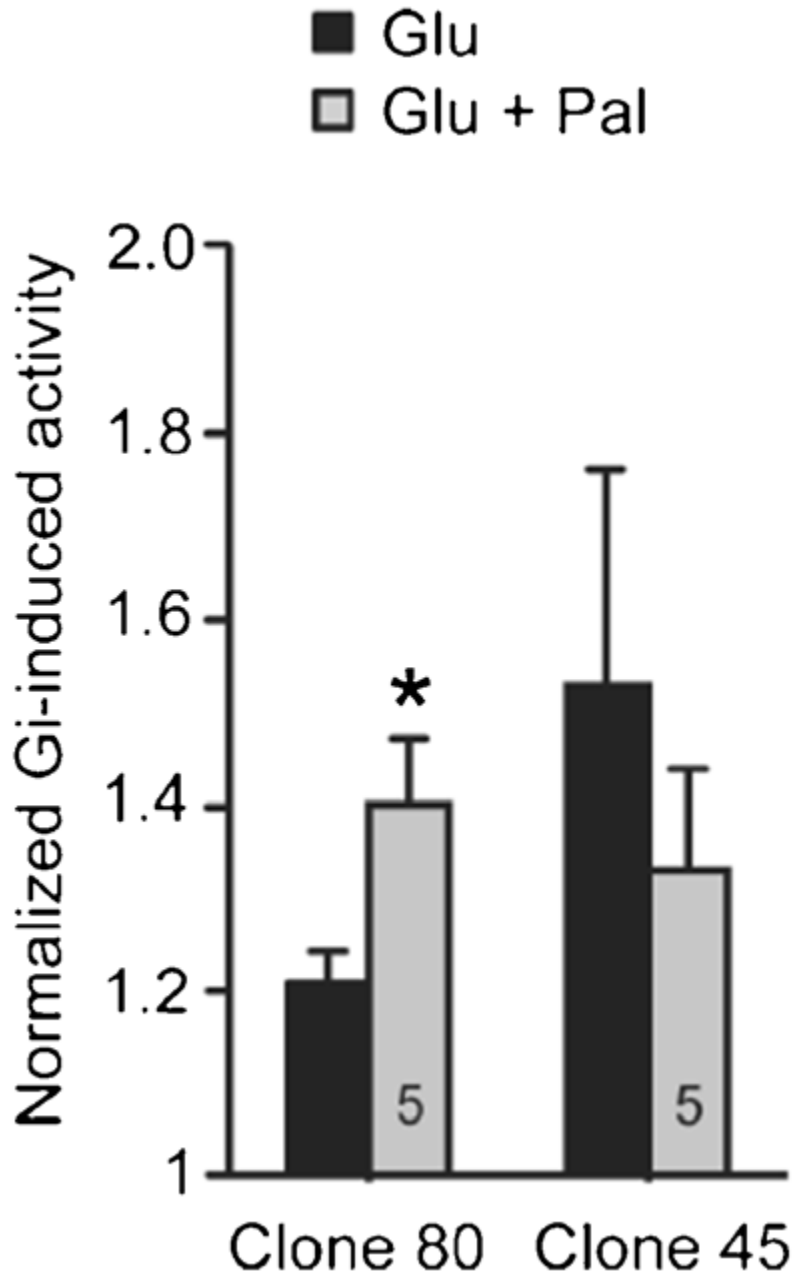


**Figure 3.3. An mGlu2R inverse agonist increases 5HT-induced 5HT2AR signaling.**

Representative barium-sensitive GIRK1/4 current trace obtained in response to 20nM 5HT followed by 20nM 5HT plus 100uM LY34 applied to stably-transfected HEK-293 cells (cross-talk positive clone 80) expressing mGlu2R+5HT2AR.

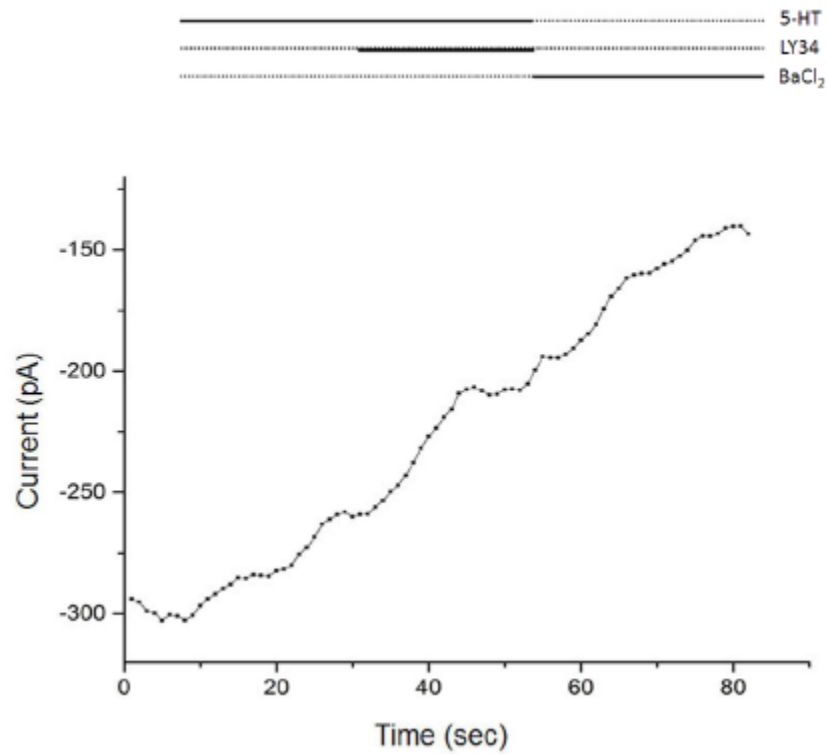


**Figure 3.4. The mGlu2R inverse agonist LY34 increases 5HT-induced 5HT2AR signaling in positive but not negative cross-talk clones.** Summary bar graph from whole-cell patch-clamp recordings of GIRK1/4 currents in cross-talk positive clone 80 and cross-talk negative clone 45 of HEK-293 cells expressing mGlu2R and 5HT2AR exposed to 20nM 5HT followed by 20nM 5HT plus 50uM LY37. (N = numbers inside the bars/condition, Data were normalized to basal activity and are mean  $\pm$  SEM, \* $p \leq 0.05$ ).

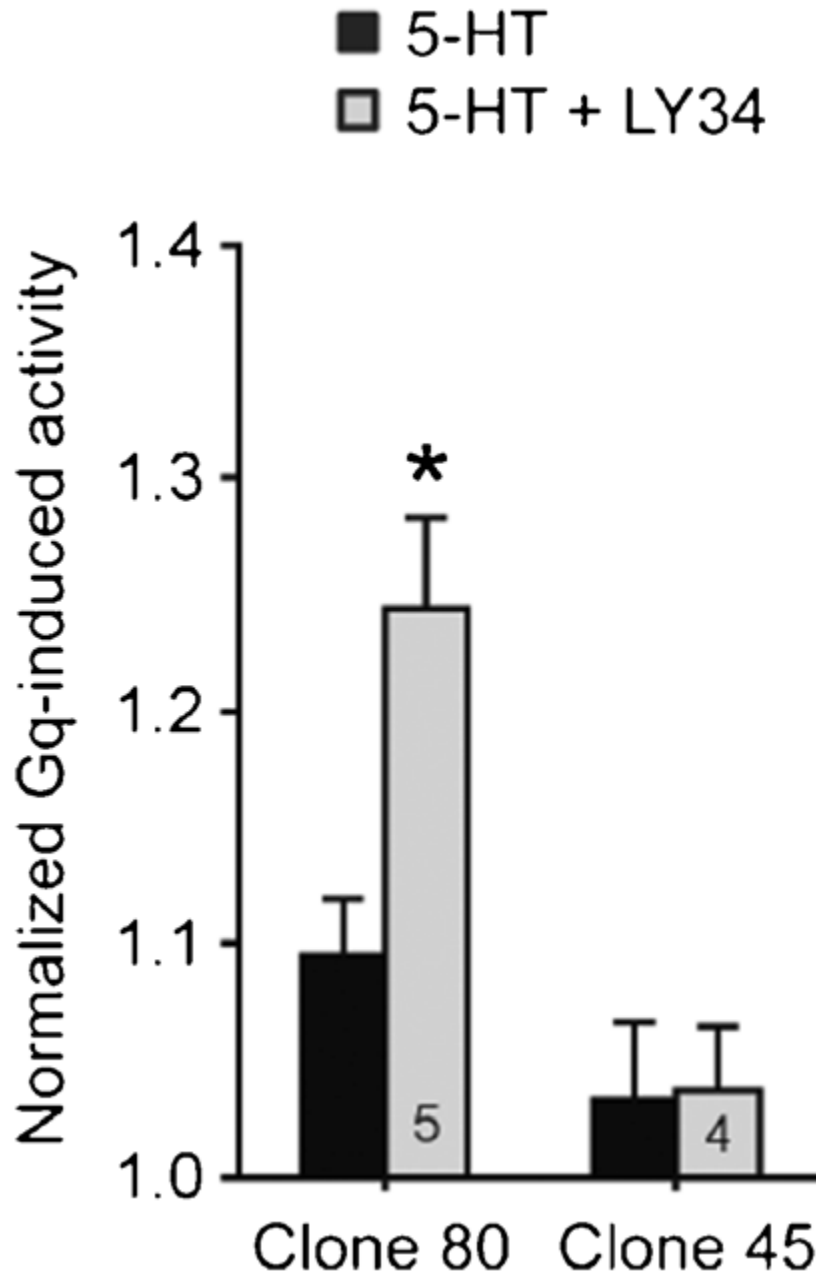


**Figure 3.5. An atypical APD increases LY37-induced mGlu2R signaling.** Representative barium-sensitive GIRK1/4 current trace obtained in response to 50nM LY37 followed by 50nM LY37 plus 50uM paliperidone (Pal) applied to stably-transfected HEK-293 cells (cross-talk negative clone 45) expressing mGlu2R+5HT2AR.

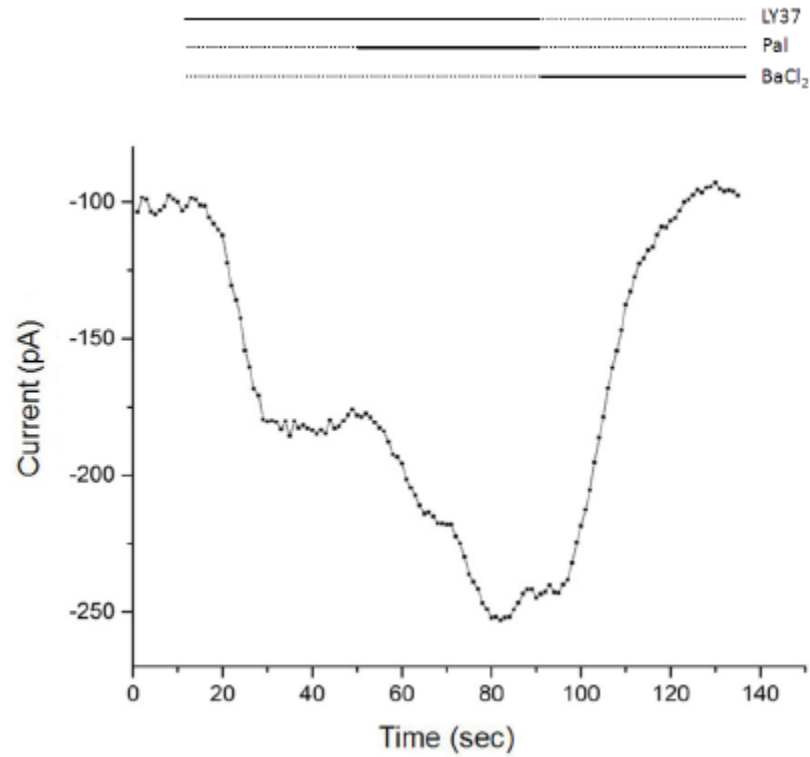


**Figure 3.6. The atypical APD paliperidone increases LY37-induced mGlu2R signaling in negative but not positive cross-talk clones.** Summary bar graph from whole-cell patch-clamp recordings of GIRK1/4 currents in cross-talk positive clone 80 and cross-talk negative clone 45 of HEK-293 cells expressing mGlu2R and 5HT2AR exposed to 50nM LY37 followed by 50nM LY37 plus 50uM paliperidone (Pal). (N = numbers inside the bars/condition, Data were normalized to basal activity and are mean  $\pm$  SEM, \* $p \leq 0.05$ ).

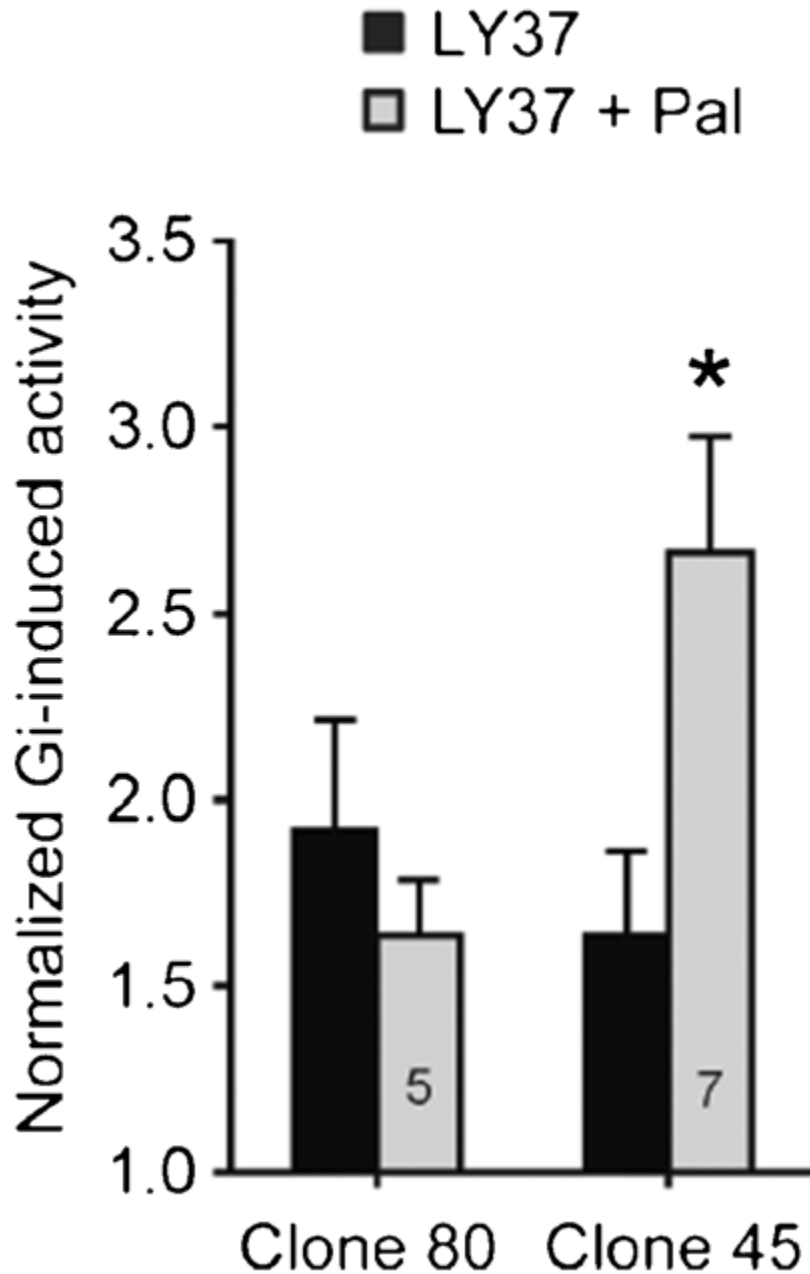
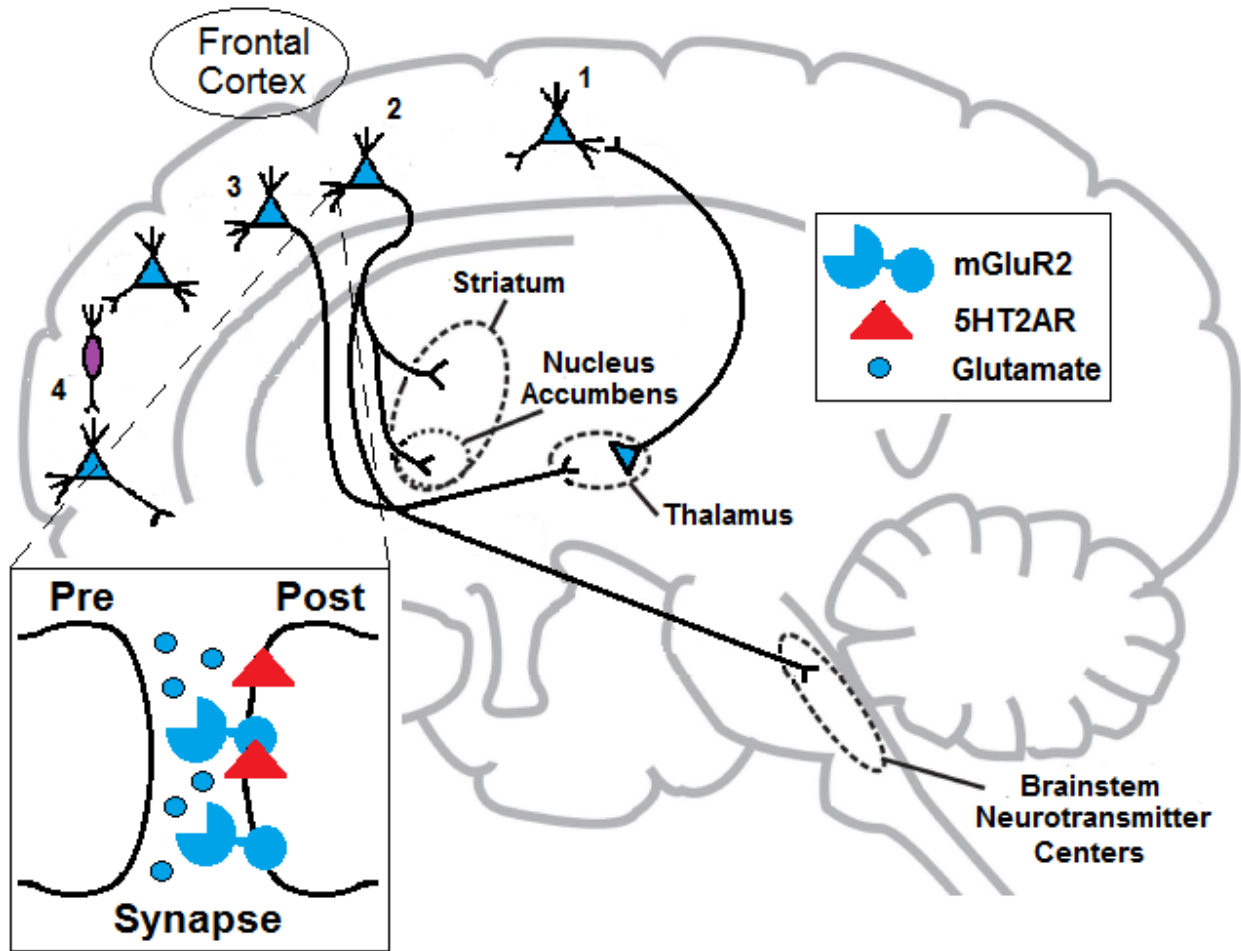


**Table 3.2. Results from mGlu2R and 5HT2AR ligand application in HEK-293 cells. The ligands used in Chapter 3 experiments and the ensuing results.**

<b>Ligand</b>	<b>Target GPCR</b>	<b>[M]</b>	<b>Effect on Target GPCR</b>	<b>Drug-induced Allosterism</b>
<b>Glutamate</b>	<b>mGlu2R</b>	<b>500nM</b>	<b>Increased G<sub>i</sub> activity</b>	<b>N/A</b>
<b>LY379268 (LY37)</b>	<b>mGlu2R</b>	<b>50nM</b>	<b>Increased G<sub>i</sub> activity (more than glutamate)</b>	<b>N/A</b>
<b>LY341495 (LY34)</b>	<b>mGlu2R</b>	<b>100uM</b>	<b>N/A</b>	<b>Increased 5HT-induced G<sub>q</sub> activity in cross-talk positive cells</b>
<b>5HT</b>	<b>5HT2AR</b>	<b>20nM</b>	<b>Increased G<sub>q</sub> activity</b>	<b>N/A</b>
<b>Paliperidone (Pal)</b>	<b>5HT2AR</b>	<b>50uM</b>	<b>N/A</b>	<b>Increased glutamate-induced G<sub>i</sub> activity in cross-talk positive cells and LY37-induced G<sub>i</sub> activity in cross-talk negative cells</b>

**Figure 3.7. The location of the mGluR2-5HT2AR heteromer determines neurotransmitter effects on brain regions.** Representative positioning of mGluR2-5HT2AR heteromers in a specific brain region and neuronal synapse. Tracing the neurocircuitry implicated in schizophrenia allows speculation on allosteric effects upon heteromerization (Adapted from Stahl SM 2013).



## Chapter 4: D2R-5HT2AR SIGNALING IN *XENOPUS* OOCYTES

### 4.1: Introduction

The mGlu2R and 5HT2AR are very different GPCRs that form a heteromer and are implicated in psychosis. The D2R is another receptor integral to schizophrenia pathways. Since the D2R forms a heteromer with the 5HT2AR, the potential exists for the D2R-5HT2AR heteromer to exhibit allosteric effects upon heteromerization that may be significant in psychosis. Further emphasizing that potential is the similar affinities APDs possess for the D2R and 5HT2AR, especially atypical APDs. The slight difference in the affinity of any atypical APD for the D2R-5HT2AR heteromer has not been properly explored as of yet.

The known data involving D2R-5HT2AR allosteric effects vary in many ways. The assays used to produce them are different (CRE-luciferase, NFAT-luciferase, calcium, FRET changes, binding, etc.), the ligands used are different (endogenous ligands, synthetic agonists, antagonists, pro-psychotics, APDs), and the different signals measured are many (Gi or Gq activity, cAMP levels, IP3 levels, binding, etc.). Interpretation of these results is difficult. As mentioned in section 3.1, emerging theories about biased agonism, functional selectivity, and even biased antagonism make comparisons between assays, drugs, and signals nearly impossible.

Our goal was to use one assay and examine the same signaling pathway throughout this project using the available range of ligands, especially the clinically-relevant APDs (**Table 4.1**). In this manner we can observe allosteric effects accurately. The D2R and 5HT2AR are class ‘A’ GPCRs, but their associated agonists, endogenous or synthetic, are selective to their target receptor, eliminating off-target binding. Early in our research, due to the D2R and 5HT2AR being G<sub>i</sub> and G<sub>q</sub> coupled receptors, respectively, we expected to see similar allosteric effects upon heteromerization as we did for the mGlu2R-5HT2AR heteromer, possibly including the same inverse functional-coupling. At the time, the only other heteromer that could be considered to be tested at a level comparable to the mGlu2R-5HT2AR was the D2R- adenosine 2A receptor (A2AR) which displayed similar allosteric effects upon heteromerization (Fuxe K et al., 2005; Fernandez-Duenas V et al., 2012; Bonaventura J et al., 2015). Any differences might be explained by the D2R-A2AR heteromer also possessing an intrinsic difference: the A2AR is a G<sub>s</sub>-coupled receptor. Therefore, we had very little information on with which to base a new hypothesis.

We wanted to examine lateral allosterism, thinking the G-protein activity of each receptor would change upon heteromerization. As we varied cRNA injection ratios of the D2R and 5HT2AR, we expected one ratio to exhibit lateral allosterism while the other ratios would not. Application of endogenous neurotransmitters, synthetic agonists, and APDs at appropriate concentrations for our oocyte system was expected to result in drug-induced allosterism, with combinations of synthetic agonists producing different results from the endogenous neurotransmitters.

## **4.2: Results**

#### 4.2.1: Lateral allosterism and effects of varying cRNA injection ratios.

We began by examining the  $G_i$  and  $G_q$  activities of the D2R and 5HT2AR alone and as a heteromer. During the TEVC process, the application of 1 $\mu$ M dopamine to the D2R produced an increase in current representing the  $G_i$  activity which was a larger change ( $\Delta G_i$ ) when both the D2R and 5HT2AR were present than when the D2R was alone (**Fig. 4.1A**). Other  $G_i$ -coupled GPCRs in our hands exhibit a current rise to a peak, but the current then stabilizes. The dopamine-induced current rose to a peak and then slowly lowered to an eventual stable level. In the literature, this is known as GIRK current relaxation, a possible voltage sensitivity of the D2R where the current through the GIRK4\* channel depolarizes the cell and differentially changes the affinity of agonists for the D2R changes (Sahlholm K et al., 2011; Sahlholm K, 2011). The stabilized current levels were variable, therefore we analyzed data at the peak current level, which can be thought of as representing a tonic release of neurotransmitter into a synapse. Interestingly, the heteromeric stabilized current levels were lower than the homomeric and were reached much faster (data not shown). The application of 1 $\mu$ M 5HT to the 5HT2AR produced a decrease in current representing the  $G_q$  activity which was a larger change ( $\Delta G_q$ ) when both the D2R and 5HT2AR were present than when the 5HT2AR was alone (**Fig. 4.1B**).

The resulting summary increases in  $G_i$  (~90%) and  $G_q$  (~50%) activities upon heteromerization (**Fig. 4.2**) happened after cRNA injections of 1:2 ng per oocyte, the same levels used by Fribourg et al., 2011. In the next experiments, we looked at changes in cRNA injection ratios and potential changes in lateral allosterism. We injected oocytes with D2R:5HT2AR cRNAs at ratios of 1:0.5, 1:1, 1:2, and 1:3 ng per oocyte, maintaining 1ng of D2R cRNA throughout. After application of 1 $\mu$ M dopamine, lateral allosterism resulted in a large increase in  $G_i$  activity from the D2R when the 5HT2AR was present at all cRNA injection ratios (**Fig. 4.3**).

This was an unexpected result. We hypothesized that the expression levels were high enough to result in maximal heteromer formation and expression, which then resulted in lateral allosterism upon heteromerization at all of the cRNA injection ratios we tested. Support was found for our hypothesis in the existing literature where much lower amounts of D2R cRNA were being injected into *Xenopus* oocytes (Sahlholm K et al., 2011; Sahlholm K, 2011). We proceeded to test lower injection levels of D2R and 5HT2AR cRNA. 1 $\mu$ M Dopamine-induced  $G_i$  activity of the D2R was comparable after 1, 0.75, 0.5, and 0.25ng of D2R cRNA was injected into oocytes and tested (**Fig. 4.4**). 1 $\mu$ M 5HT-induced  $G_q$  activity of the 5HT2AR was comparable after 2, 0.75, 0.5, 0.25, and 0.125ng of 5HT2AR cRNA was injected into oocytes and tested (**Fig. 4.5**).

Next we injected oocytes with D2R:5HT2AR cRNA ratios of 1:0.5, 1:1, 1:2, and 1:3 based on 0.25ng of D2R cRNA and applied 1 $\mu$ M dopamine (**Fig. 4.6**) or 1 $\mu$ M 5HT (**Fig. 4.7**). Maximal lateral allosterism was displayed after the 1:2 ratio injections, representing  $G_i$  or  $G_q$  activity significantly higher than that of homomeric levels. The 1:0.5 and 1:3 ratio injections resulted in  $G_i$  or  $G_q$  levels similar to the homomeric levels. Interestingly, the 1:1 ratio injections exhibited a partial lateral allosterism, whose  $G_i$  activity was significantly more than homomeric levels. While the 1:1 ratio injections resulted in a definite increase in  $G_q$  activity compared to 5HT2AR alone, the increase was not statistically significant.

#### **4.2.2: Endogenous ligand-induced allosterism and a 5HT2AR mutant**

Moving on to examine drug-induced allosterism, we first looked at the endogenous neurotransmitters. The application of both 1 $\mu$ M dopamine and 1 $\mu$ M 5HT concurrently to oocytes expressing both D2R and 5HT2AR resulted in a significantly further increase of  $G_i$  (**Fig 4.8**) and

$G_q$  (**Fig. 4.9**) activity levels beyond that resulting from lateral allosterism. Dopamine cross-signaled and increased the  $G_q$  activity of the 5HT2AR, while 5HT cross-signaled and increased the  $G_i$  activity of the D2R.

Mutants of D2R and 5HT2AR were used to abrogate D2R and 5HT2AR co-localization in HEK-293 cells (Lukasiewicz S et al., 2010). We produced two of these mutants, the D2R (6A) and 5HT2AR (2A), in order to examine their effect on allosteric effects. The D2R (6A) has 6 positively-charged residues in its IC3 which we mutated to alanines, while the 5HT2AR (2A) has two negatively-charged residues in its C-terminus tail which we mutated to alanines. So far, the D2R (6A) shows little or variable expression in oocytes. If D2R (6A) problems persist, we will produce the remaining two known mutants possessing two or four of the six positively-charged residues mutated to alanines. However, the 5HT2AR (2A) expresses robustly (**Fig. A1.2**). When co-expressed with D2R, 5HT2AR (2A) exhibits  $G_q$  activity similar to homomeric levels as well as significantly lower dopamine-induced cross-signaling (**Fig. 4.8**). These results suggest that the mutated residues in the 5HT2AR (2A) do indeed limit heteromer formation and expression.

#### **4.2.3: Synthetic agonist-induced allosterism**

Next we looked at non-endogenous ligands, or synthetic ligands. Quinpirole (QP) is an agonist at the D2R and DOI is an agonist at the 5HT2AR. While DOI is a well-known psychedelic and pro-psychotic drug, QP is only considered psychoactive and is used mostly in laboratory research. The concurrent application of 1uM dopamine with 10uM DOI to oocytes expressing both D2R and 5HT2AR resulted in a significant decrease of  $G_i$  activity levels beyond those exhibited by the D2R alone (**Fig 4.10**). DOI cross-signaled and decreased the  $G_i$  activity of the D2R. The concurrent application of 1uM 5HT with 10uM QP to oocytes expressing both

D2R and 5HT2AR resulted in a significant decrease of  $G_q$  activity levels to levels similar to those exhibited by the D2R alone (**Fig 4.10**). QP cross-signaled and decreased the  $G_q$  activity of the 5HT2AR.

#### **4.2.4: Anti-psychotic drug-induced allosterism**

In the context of allosteric effects upon heteromerization of the D2R-5HT2AR heteromer, we wanted to examine the effects of atypical APDs. Most clinically-approved atypical APDs have similar affinities for the D2R and 5HT2AR (Arnt J and Skarsfeldt T, 1998). APDs with similar affinities to each receptor as well as more selective APDs could result in interesting heteromeric effects, but first we needed to examine the functional result of each APD at the homomeric receptor. In that effort, we chose four APDs and produced inhibition concentration responses at the D2R in the presence of 1 $\mu$ M dopamine and at the 5HT2AR in the presence of 1 $\mu$ M 5HT. The effects of the APDs were then compared to the single application of 1 $\mu$ M dopamine to the D2R or 1 $\mu$ M 5HT to the 5HT2AR and are represented by the dotted lines in **Figs. 4.11, 13, 15 and 17**, all equal to 100%. The resulting concentration responses allowed us to choose concentrations of the APD for one receptor that would not have functional efficacy at the second receptor. Our intention was very specific to determine this APD concentration to test cross-signaling, not to fully characterize the drugs' effects at the receptors. However, we did see interesting results along the way. We could then test the chosen concentration for cross-signaling to the other receptor.

We chose to examine pimavanserin, amisulpride, amperozide, and paliperidone. These choices were based on requiring a 5HT2AR-selective APD, a D2R-selective APD, and two

‘dirty’ APDs that possess similar affinities for both receptors. Also, three out of the four are clinically or potentially clinically relevant.

Pimavanserin (PIMA) is a 5HT<sub>2A</sub>R-selective potential atypical APD presently in clinical trials (Garay RP et al., 2016). 5HT<sub>2A</sub>R selectivity compared to D<sub>2</sub>R is uncommon, making pimavanserin unique as a potential APD. We concurrently applied 1 $\mu$ M dopamine to oocytes expressing D<sub>2</sub>R or 1 $\mu$ M 5HT to oocytes expressing 5HT<sub>2A</sub>R with increasing concentrations of PIMA (**Fig. 4.11**). PIMA applied to the D<sub>2</sub>R had no concentration-dependent response on G<sub>i</sub> activity inhibition. PIMA did inhibit G<sub>q</sub> activity of the 5HT<sub>2A</sub>R with an IC<sub>50</sub> of approximately 1 $\mu$ M and a 70% range of efficacy. We chose a high concentration of an approximate IC<sub>80</sub> of 5 $\mu$ M PIMA for further testing due to PIMA not affecting D<sub>2</sub>R.

We concurrently applied 1 $\mu$ M dopamine with 5 $\mu$ M PIMA to oocytes expressing both D<sub>2</sub>R and 5HT<sub>2A</sub>R which resulted in a significant decrease of G<sub>i</sub> activity levels to levels similar to those exhibited by the D<sub>2</sub>R alone (**Fig 4.12**). The application of 5 $\mu$ M PIMA and 1 $\mu$ M dopamine to the homomeric D<sub>2</sub>R was no different than 1 $\mu$ M dopamine alone, suggesting PIMA possesses no efficacy for the D<sub>2</sub>R at that concentration, which leads us to conclude that PIMA cross-signaled and decreased the G<sub>i</sub> activity of the D<sub>2</sub>R. However, we cannot rule out a hypothesis that heteromerization increases D<sub>2</sub>R affinity for PIMA. This hypothesis exists for all four APDs we tested and will discuss in this section. In the future we plan to use binding assays to investigate this possibility.

Amisulpride (AMIS) is known as a D<sub>2</sub>R-selective atypical APD and is used clinically in some countries, but not the United States. As an atypical APD, D<sub>2</sub>R-selectivity is uncommon, making amisulpride a curious and unique drug (Kang SG et al., 2015). We concurrently applied

1 $\mu$ M dopamine to oocytes expressing D2R or 1 $\mu$ M 5HT to oocytes expressing 5HT2AR with increasing concentrations of AMIS (**Fig. 4.13**). AMIS applied to the D2R inhibited 1 $\mu$ M dopamine-induced G<sub>i</sub> activity with an approximate IC<sub>50</sub> of 700nM and an efficacy range of 100%. AMIS applied to the 5HT2AR inhibited G<sub>q</sub> activity of the 5HT2AR with an IC<sub>50</sub> of approximately 15 $\mu$ M and an 80% range of efficacy. Contrary to known data, amisulpride does possess efficacy at the 5HT2AR in our assay. As seen in **Figs. 4.13 and 17**, percentages above 100% and below 0% can occur due to variability. Further, percentages less than 0% suggest a possible inverse agonist activity. We chose a concentration of 300nM AMIS for further testing.

We concurrently applied 1 $\mu$ M 5HT with 300nM AMIS to oocytes expressing both D2R and 5HT2AR which resulted in a significant decrease of G<sub>q</sub> activity levels to levels similar to those exhibited by the 5HT2AR alone (**Fig 4.14**). The application of 300nM AMIS and 1 $\mu$ M 5HT to the homomeric 5HT2AR was no different than 1 $\mu$ M 5HT alone, suggesting AMIS possesses no efficacy for the 5HT2AR at that concentration, which leads us to conclude that AMIS cross-signaled and decreased the G<sub>q</sub> activity of the 5HT2AR.

Amperozide (AMP) is known to be a slightly more 5HT2AR-selective atypical APD although it has never been tested in clinical trials. It is used mostly by veterinarians as a sedative (Chang PY et al., 2008). We concurrently applied 1 $\mu$ M dopamine to oocytes expressing D2R or 1 $\mu$ M 5HT to oocytes expressing 5HT2AR with increasing concentrations of AMP (**Fig. 4.15**). AMP applied to the D2R inhibited 1 $\mu$ M dopamine-induced G<sub>i</sub> activity with an approximate IC<sub>50</sub> of 2 $\mu$ M and an efficacy range of 80%. AMP applied to the 5HT2AR inhibited G<sub>q</sub> activity of the 5HT2AR with an IC<sub>50</sub> of approximately 300nM and a 40% range of efficacy. In our assay, amperozide is more potent at the 5HT2AR, but not very efficacious, while it is the opposite at the D2R. We chose a concentration of 300nM AMP for further testing.

We concurrently applied 1 $\mu$ M dopamine with 300nM AMP to oocytes expressing both D2R and 5HT2AR which resulted in a significant decrease of G<sub>i</sub> activity levels to levels similar to those exhibited by the D2R alone (**Fig 4.16**). The application of 300nM AMP and 1 $\mu$ M dopamine to the homomeric D2R was no different than 1 $\mu$ M dopamine alone, suggesting AMP possesses no efficacy for the D2R at that concentration, which leads us to conclude that AMP cross-signaled and decreased the G<sub>i</sub> activity of the D2R.

Paliperidone (PAL) is known as a slightly more 5HT2AR-selective atypical APD and is clinically relevant (Clarke WP et al., 2013; Corena-McLeod M, 2015). We concurrently applied 1 $\mu$ M dopamine to oocytes expressing D2R or 1 $\mu$ M 5HT to oocytes expressing 5HT2AR with increasing concentrations of PAL (**Fig. 4.17**). PAL applied to the D2R inhibited 1 $\mu$ M dopamine-induced G<sub>i</sub> activity with an approximate IC<sub>50</sub> of 320nM and an efficacy range of 110%. PAL applied to the 5HT2AR inhibited G<sub>q</sub> activity of the 5HT2AR with an IC<sub>50</sub> of approximately 370nM and a 60% range of efficacy. Contrary to known data, paliperidone is more potent in our assay at the D2R than the 5HT2AR, even displaying inverse agonism at the D2R. We chose a concentration of 100nM PAL for further testing.

We concurrently applied 1 $\mu$ M 5HT with 100nM PAL to oocytes expressing both D2R and 5HT2AR which resulted in a significant decrease of G<sub>q</sub> activity levels to levels similar to those exhibited by the 5HT2AR alone (**Fig 4.18**). The application of 100nM PAL and 1 $\mu$ M 5HT to the homomeric 5HT2AR was no different than 1 $\mu$ M 5HT alone, suggesting PAL possesses no efficacy for the 5HT2AR at that concentration, which leads us to conclude that PAL cross-signaled and decreased the G<sub>q</sub> activity of the 5HT2AR.

#### **4.2.5: Effects of drug combinations**

As discussed in section 1.8, a combination of LY37 (mGlu2R agonist) and clozapine (5HT2AR inverse agonist and atypical APD) can overcome a non-human schizophrenic phenotype and symptoms as they relate to the mGlu2R-5HT2AR heteromer. Since mGlu2R synthetic agonists and PAMs are not yet clinically approved, clinicians cannot combine these potential APDs with atypical APDs. However, combinations of typical and atypical APDs are regularly prescribed. The reasons are many: trying to limit positive, negative, or extra-pyramidal symptoms, inherited co-prescriptions, decreasing total medications, and transitioning from one APD to another (Sernyak MJ and Rosenheck R, 2004). When assessing cross-signaling in the D2R-5HT2AR heteromer using APDs, we cannot combine two APDs because there would be a decreased signal to start from both receptors. The resulting mixed signal would be uninterpretable.

Therefore, we decided to replicate an experiment that involved the two synthetic agonists we had already tested for cross-signaling in the D2R-5HT2AR heteromer, quinpirole (QP) and DOI. Using an IP<sub>3</sub> assay, Albizu et al., 2011 saw a DOI-induced increase in G<sub>q</sub> activity followed by a concurrent application of DOI with QP and a decrease in G<sub>q</sub> activity beyond homomeric 5HT2AR levels. We concurrently applied 1uM QP with 10uM DOI to oocytes expressing both D2R and 5HT2AR which resulted in a significant decrease of G<sub>q</sub> activity levels to levels similar to those exhibited by the 5HT2AR alone (**Fig 4.19**). QP cross-signaled and decreased the G<sub>q</sub> activity of the 5HT2AR, similar to the results seen by Albizu et al., 2011.

### **4.3: Discussion**

Our TEVC results from oocytes suggest a unique set of allosteric responses upon D2R-5HT2AR heteromerization (**Table 4.2**). D2R-5HT2AR lateral allosterism results in an increased

$G_i$  and  $G_q$  activity. D2R to 5HT2AR cRNA injection ratios based on lower levels of GPCR expression lead to a 1:2 ratio displaying maximal lateral allosterism, 1:1 ratio displaying a partial lateral allosterism, and other ratios displaying G-protein activity similar to homomeric levels. Addition of the second endogenous neurotransmitter further increases  $G_i$  and  $G_q$  activity via cross-signaling. The concurrent application of a synthetic agonist to one receptor with the endogenous neurotransmitter of the second receptor decreases the G-protein activity of the second receptor. Concentration responses of atypical or potential atypical APDs inhibiting the G-protein activity of each homomer revealed interesting new results not suggested in the literature. The concurrent application of a variety of atypical or potential atypical APDs to one receptor with the endogenous neurotransmitter of the second receptor decreases the G-protein activity of the second receptor. Finally, a combination of synthetic agonists applied concurrently decreases the  $G_q$  activity of the 5HT2AR, similar to synthetic agonists paired with endogenous neurotransmitters.

As a control experiment, we ensured all ligands applied at concentrations used in chapter four did not significantly affect GIRK4\* currents (**Figure A1.3**). Further controls applying these same ligands and concentrations to the off-target receptor resulted in no change in GIRK4\* current except in the case of QP (**Figures A1.4A-B**). Surprisingly, 10uM QP activated the 5HT2AR to approximately 80% of  $G_q$  activity as compared to 1uM 5HT. The cross-signaling results of 10uM QP application resulting in a decrease in  $G_q$  activity could in part be to a partial agonist activity at the 5HT2AR or a competition between QP and 5HT binding to the 5HT2AR. However, we would not expect the decrease in  $G_q$  activity to be as strong as was seen, suggesting the presence of a cross-signaling component. The QP effect at 5HT2AR needs to be investigated further due to there being only two apparent examples in the literature examining QP binding at

the 5HT2AR and both result in a relatively high  $K_i$  of 7 $\mu$ M or more (Knight AR, et al., 2004; Millan MJ et al., 2002).

The results found in chapter four possess similarities and differences when compared to previous results in different assays. Much of the existing results examining the D2R-5HT2AR heteromer involved binding assays, which do not necessarily reflect function, as evidenced by Albizu et al., 2011 and the experiment we replicated functionally (**Figs.1.8 and 4.20**). Lateral allosterism resulted in an increase in DOI-induced  $G_q$  activity, but the 5HT2AR affinity for DOI decreased. The addition of QP decreased the signal, but the 5HT2AR affinity for DOI increased. Results like this pinpoint the complications of comparing binding and function.

Differences include experiments where synthetic agonists LSD and DOI increased while 5HT decreased the QP-induced  $G_i$  activity of the D2R (Borroto-Escuela DO et al., 2010; Borroto-Escuela DO et al., 2013) which is the opposite of what we would predict from our results. However, we have not tested cross-signaling to a QP-bound D2R, and our assay examines specific interaction with an ion channel whereas theirs looks at a downstream transcription factor. QP increased both 5HT- and TCB2-induced  $G_q$  activity, but again in an assay looking at a transcription factor (Borroto-Escuela DO et al., 2010). These differences highlight the need to carefully consider functional selectivity when comparing results from different assays.

Our results can be compared to results found in native systems like the VTA of rats. Presynaptic D2Rs on dopaminergic neurons act as autoreceptors, receiving a dopamine signal and subsequently reducing neurotransmission. Measured electrophysiologically, the application of dopamine decreases the neuron firing rate. With lower concentrations of dopamine, the

inhibition is much less. This allows the addition of 5HT concurrently with low dopamine concentrations, which results in a stronger inhibition of firing rate (Brodie MS and Bunney EB, 1996). This may reflect an increased  $G_i$  signal due to 5HT-induced cross-signaling through the 5HT2AR to the D2R, similar to our results.

Extended exposure of dopaminergic neurons to moderate concentrations of dopamine results in a time-dependent decrease in sensitivity of dopaminergic neurons to dopamine inhibition, a process called dopamine inhibition reversal (DIR) (Nimitvilai S and Brodie M, 2010; Nimitvilai S et al., 2012). Looking at rat VTA neurons over a longer time-frame of QP exposure, 5HT reverses the QP-induced inhibition, similar to DIR (Nimitvilai S et al., 2012). This result is in the opposite direction from the previous one, but was performed in a longer time-frame. This may suggest a difference between a short and long application of ligands. The Brodie group's ongoing studies with atypical APDs more selective for the 5HT2AR, specifically pimavanserin and amperozide, is providing results similar to ours (personal communication).

To discuss the pertinent question of relevance to psychosis, we must look at the schizophrenia-related neuro-circuitry. In **Fig. 4.20** pathway number four, we envision a population of presynaptic D2Rs in spiny neurons signaling to meso-limbic neurons. Maximal D2R-5HT2AR heteromer formation, expression, and lateral allosterism exists, resulting in higher  $G_i$  and  $G_q$  signaling compared to the respective homomers. The larger increase in  $G_i$  than  $G_q$  activity will result in less neurotransmitter release to the meso-limbic neuron projecting to the striatum, which will lower the excitability of the meso-limbic neuron, finally lowering or maintaining the low excitation of neurons in the striatum. The resulting dopamine levels will be regulated and presumably be physiologically optimal.

However, in a psychotic condition, either schizophrenia or possibly after abuse of a pro-psychotic drug, the D2R-5HT2AR may be dysregulated. Our experiments show that D2R-5HT2AR heteromer lateral allosterism is maximal when the two receptors are expressed at a specific cRNA ratio. Without the heteromer expressed at maximal levels, the nigro-striatal neuron will be more active and the dopamine levels in the striatum will rise. High striatal dopamine levels are a symptom of schizophrenia and integral to the dopamine hypothesis of schizophrenia, which means increasing an already high level of dopamine will exacerbate the condition. Atypical APDs will lower the G-protein activity of both receptors, especially at higher doses, further lowering the expression and lateral allosterism of the D2R-5HT2AR. These treatments applied to this area will not improve psychotic symptoms. This is but one example of the importance of location. Synaptic terminals, brain regions, and neurocircuitry will all play a part in determining the overall effects of allosterism upon heteromerization.

We can postulate hypotheses as to the importance of different locations. In our experiments, we used the D2R<sub>L</sub> which is predominantly found post-synaptically. D2R-5HT2AR heteromeric allosterism may not apply or be beneficial on a presynapse. The D2R<sub>S</sub>, predominantly found presynaptically, may not form a heteromer with the 5HT2AR. The mGlu2R-5HT2AR heteromer does not appear to be widespread, but the D2R-5HT2AR could be located in many regions and various synaptic terminals. Allosteric changes upon D2R-5HT2AR heteromerization will affect a large variety of neurons differently.

Now we will envision a population of D2R-5HT2AR in pathway four of **Fig. 4.20** again, only this time the heteromer is found on the postsynapse of the meso-limbic neuron. Again, the neuron will be less excited in its normal state, delivering an optimal amount of dopamine to neurons in the striatum. In a psychotic state, the heteromer will be dysregulated while dopamine

levels are known to be high. Now, the application of atypical APDs will lower the excitation of the meso-cortical neuron which will lower dopamine release in the striatum, helping to correct the psychotic symptoms. Meso-cortical neurons would have the opposite effect on the psychotic symptoms originating from the PFC. The lowering of excitation relaying from the VTA to the PFC would lower the already low levels of dopamine, exacerbating the condition.

To allow for quick and easy speculation about the D2R-5HT2AR in specific locations, we can view D2R-5HT2AR heteromeric allosterism as a simple three-level model of G-protein activity. Level one is the homomeric  $G_i$  and  $G_q$  activity with dopamine and 5HT present. At level two, imagine one neurotransmitter being present at a time when the heteromer forms, allowing lateral allosterism to raise the  $G_i$  levels by 90% and the  $G_q$  levels by 50%. At level three, both neurotransmitters are present at physiological concentrations and both G-protein levels increase to an equilibrium level. We can envision a population of D2R-5HT2AR heteromers in a specific location, including pre-or post-synapse. Then we can mentally apply synthetic agonists, APDs, or different levels of dopamine or 5HT. If the  $G_i$  and  $G_q$  activity levels become too high or unbalanced, a psychotic state exists. APDs will lower the G-protein activity levels and reestablish the equilibrium, possibly near levels two or even one. APDs will not necessarily restore the equilibrium at level three, which could play a role in the side effects associated with APDs. Synthetic agonists, some of which are pro-psychotics, will ruin the equilibrium and increase one G-protein activity above level three while the other level decreases to levels two or even one due to cross-signaling. The optimal goal of the D2R-5HT2AR heteromer throughout will be a G-protein activity equilibrium at level three.

In summary, the D2R-5HT2AR heteromer possesses a unique set of allosteric effects upon heteromerization. To substantiate these results, we will need to test multiple ligands and different

assays in the future, especially in neurons and behavioral studies. So far we have looked at atypical APDs and only two synthetic agonists. Typical APDs and other pro-psychotic drugs may produce allosteric effects as well. The discussed scenarios are just three out of many possible ones. Any synaptic location involved in schizophrenia should be examined. As with the mGlu2R-5HT2AR heteromer, the effect of homomeric populations as a mixture with the heteromeric population also needs to be examined. This is especially relevant in light of the partial lateral allosterism seen in **Figs. 4.6 and 4.7**. Partial allosterism may result from a population of monomers, homomers, and heteromers that is sub-optimal but still viable. It may also reflect multiple viable subunit stoichiometries, which we will also investigate in the future.

**Table 4.1. Properties of D2R and 5HT2AR ligands.** The ligands used in Chapter 4 experiments and their properties (Affinities taken from Arnt J et al.,1998; Corena-McLeod M, 2015; Southan C et al., 2016).

<b>Ligand</b>	<b>Target GPCR</b>	<b>Off-Target Interactions</b>	<b>Pharmacology for Target GPCR</b>	<b>Affinity for Target GPCR (pK<sub>i</sub>/pK<sub>d</sub> values)</b>
<b>Dopamine</b>	<b>D2R</b>	<b>All dopamine receptors</b>	<b>Endogenous agonist</b>	<b>4.7-7.2</b>
<b>Quinpirole</b>	<b>D2R</b>	<b>D3R, D5R (low nM)</b>	<b>Synthetic agonist</b>	<b>4.9-7.7</b>
<b>Amisulpride</b>	<b>D2R</b>	<b>D3R, 5HT2BR, 5HT7R (low nM); D4R, α2R, 5HT1BR, 5HT1DR, 5HT6R (high nM-low uM)</b>	<b>Anti-psychotic drug, antagonist/ inverse agonist</b>	<b>7.8-8.0</b>
<b>Paliperidone (Pal)</b>	<b>D2R</b>	<b>5HT1B-1CR, 5HT2AR, 5HT2CR, 5HT7R, D1R, D3-5R, H1-2R, α1-2R (low nM); 5HT1AR, 5HT1ER, 5HT4-6R (high nM-low uM)</b>	<b>Anti-psychotic drug, antagonist/ inverse agonist</b>	<b>8.9-9.0</b>
<b>5HT</b>	<b>5HT2AR</b>	<b>All 5HT receptors</b>	<b>Endogenous agonist</b>	<b>8.9</b>
<b>DOI</b>	<b>5HT2AR</b>	<b>5HT2B-2CR (low nM); 5HT1A-1FR, 5HT5R (high nM-low uM)</b>	<b>Synthetic agonist</b>	<b>7.1-9.2</b>
<b>Pimavanserin</b>	<b>5HT2AR</b>	<b>5HT2CR, σ-1R (low nM)</b>	<b>Anti-psychotic drug, antagonist/ inverse agonist</b>	<b>9.3</b>
<b>Amperozide</b>	<b>5HT2AR</b>	<b>D1-2R, 5HT2CR, 5HT6R α1R (low nM); 5HT1AR, H1R, α2R, 5HT7R (high nM-low uM)</b>	<b>Anti-psychotic drug, antagonist/ inverse agonist</b>	<b>7.9</b>

**Figure 4.1. Upon D2R-5HT2AR heteromerization,  $G_i$ -induced currents increase while  $G_q$ -induced currents decrease. (A)** Representative barium-sensitive GIRK4\* current traces obtained in response to 1uM dopamine (DA) applied to oocytes expressing D2R alone or D2R+5HT2AR.  $\Delta G_i$  is analyzed at the peak  $G_i$ -induced current – fast desensitization is due to GIRK current relaxation. **(B)** Representative barium-sensitive GIRK4\* current traces obtained in response to 1uM serotonin (5HT) applied to oocytes expressing 5HT2AR alone or D2R+5HT2AR.  $\Delta G_q$  is analyzed at the lowest stable  $G_q$ -induced current.

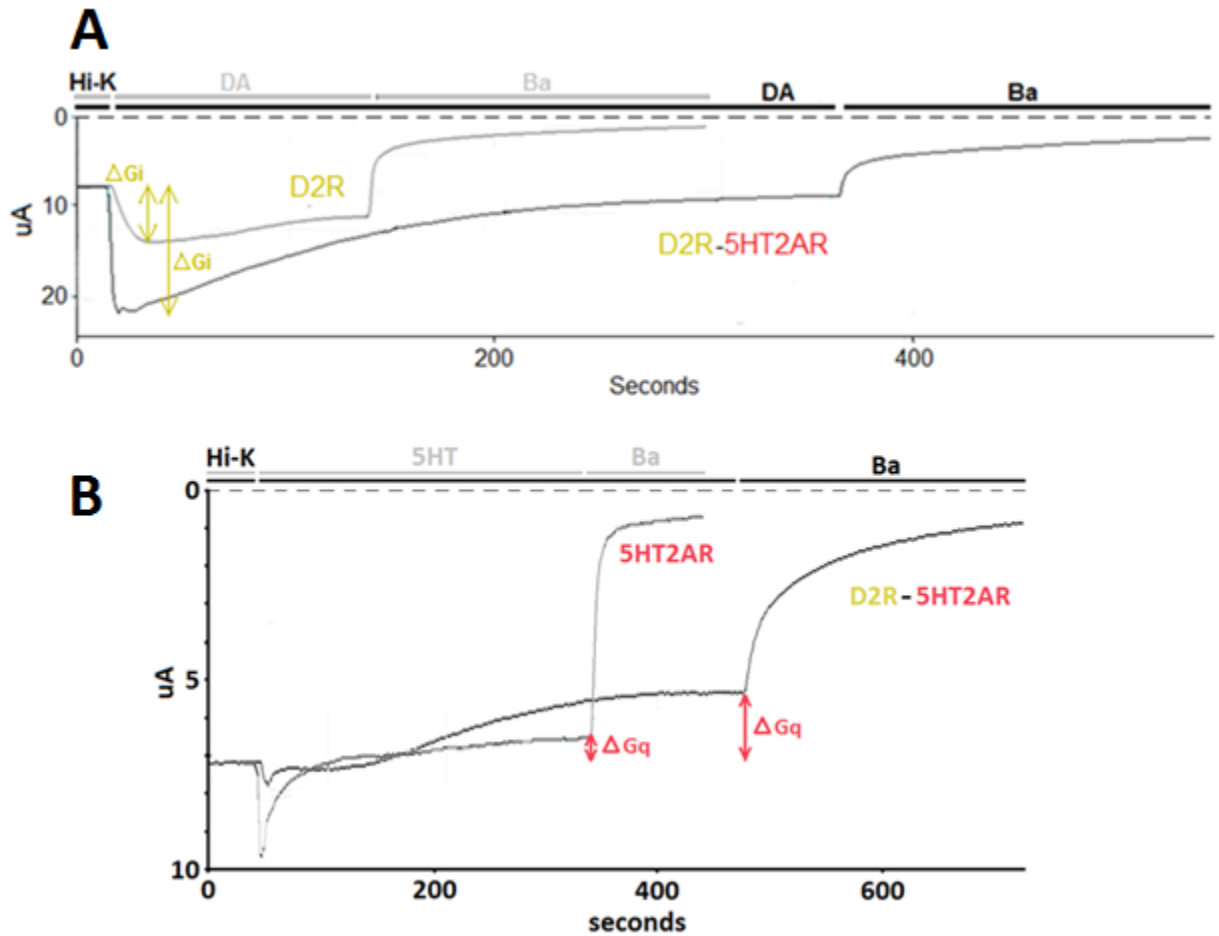


**Figure 4.2. Lateral Allosterism upon D2R-5HT2AR heteromerization.** Summary bar graph of  $G_i$  and  $G_q$  activity measured in oocytes: The addition of 1 $\mu$ M DA or 1 $\mu$ M 5HT increases  $G_i$  and  $G_q$  activity of the D2R-5HT2AR as compared to D2R or 5HT2AR alone. (N = 36-38/condition, Dotted line = 1 or 100%, Data are mean  $\pm$  SEM, \*\*\* $p$ <0.001)  
cRNA injections (1ng:2ng D2R:5HT2AR): GIRK4\*, RGS2 or PTX, plus D2R, 5HT2AR, or D2R+5HT2AR

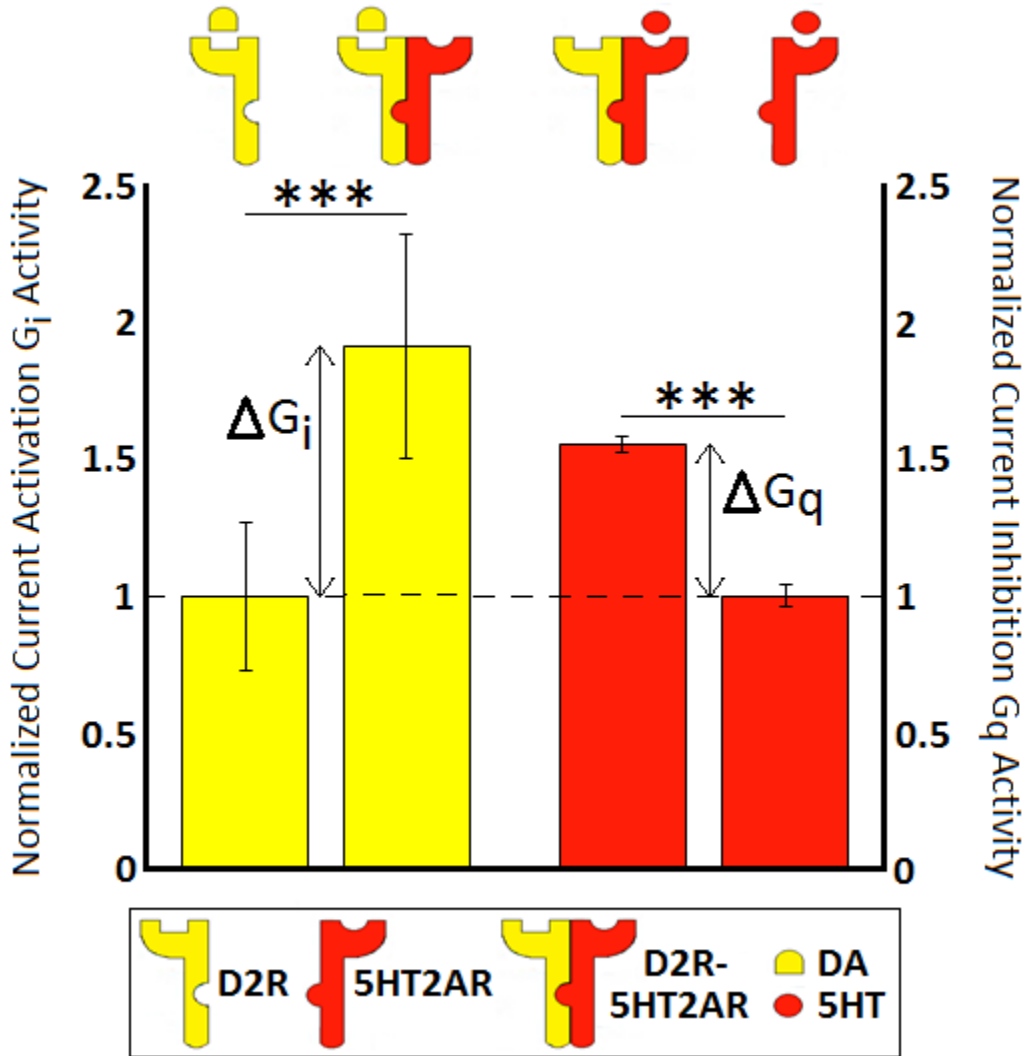


**Figure 4.3. Lateral Allosterism upon D2R-5HT2AR heteromerization at different cRNA injection ratios based on 1ng/oocyte.** Summary bar graph of  $G_i$  activity measured in oocytes: The addition of 1 $\mu$ M DA in the presence of D2R and 5HT2AR increases  $G_i$  activity compared to the D2R. (N = 7-10/condition, Dotted line = 1 or 100%, Data are mean  $\pm$  SEM)  
cRNA injections (1ng:xng D2R:5HT2AR): GIRK4\*, RGS2, plus D2R or D2R+5HT2AR

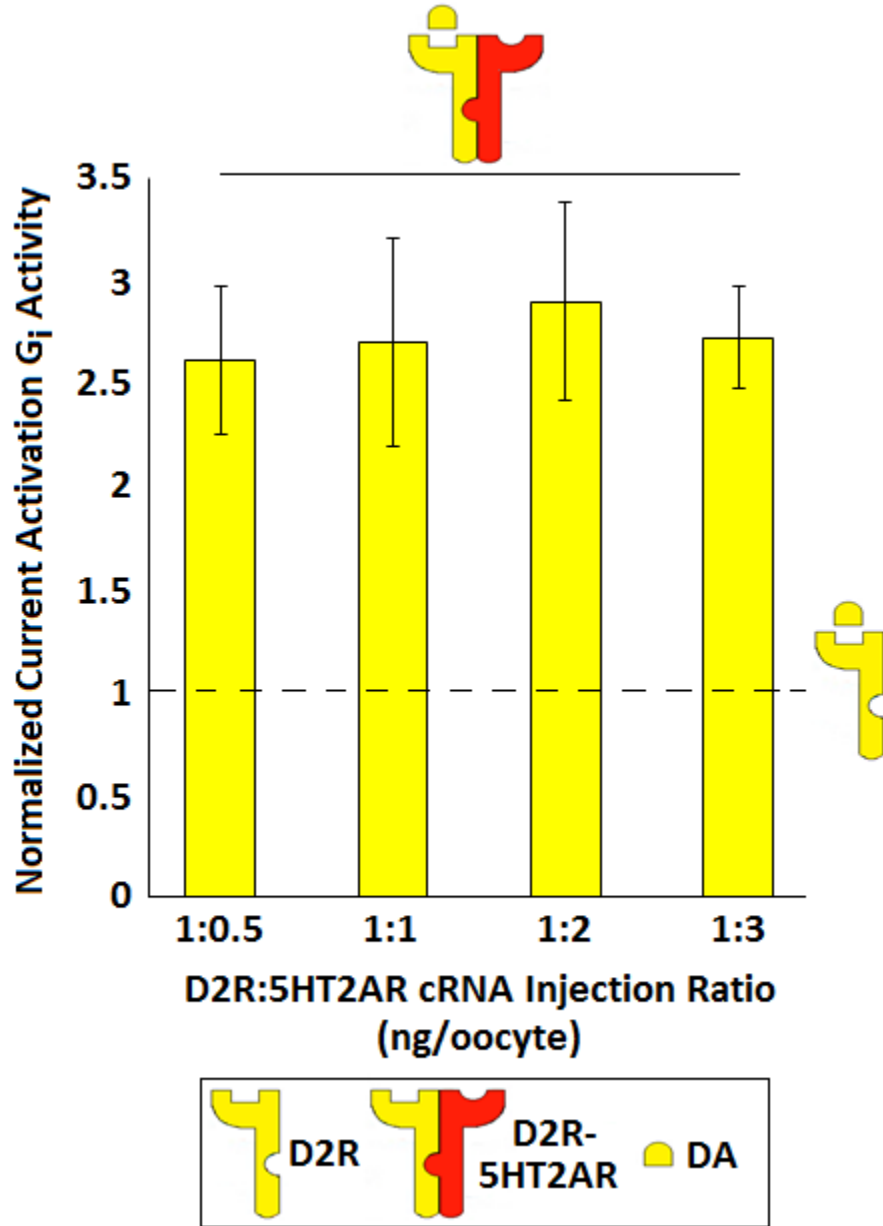


**Figure 4.4. Verification of G<sub>i</sub> signal at ≤ 1ng/oocyte cRNA injection levels.** Summary bar graph of G<sub>i</sub> activity measured in oocytes: The addition of 1uM DA in the presence of D2R increases G<sub>i</sub> activity. (N = 2-3/condition, Performed in one batch of oocytes, Dotted line = 1 or 100%, Data are mean ± SEM)  
cRNA injections (xng D2R): GIRK4\*, RGS2, plus D2R

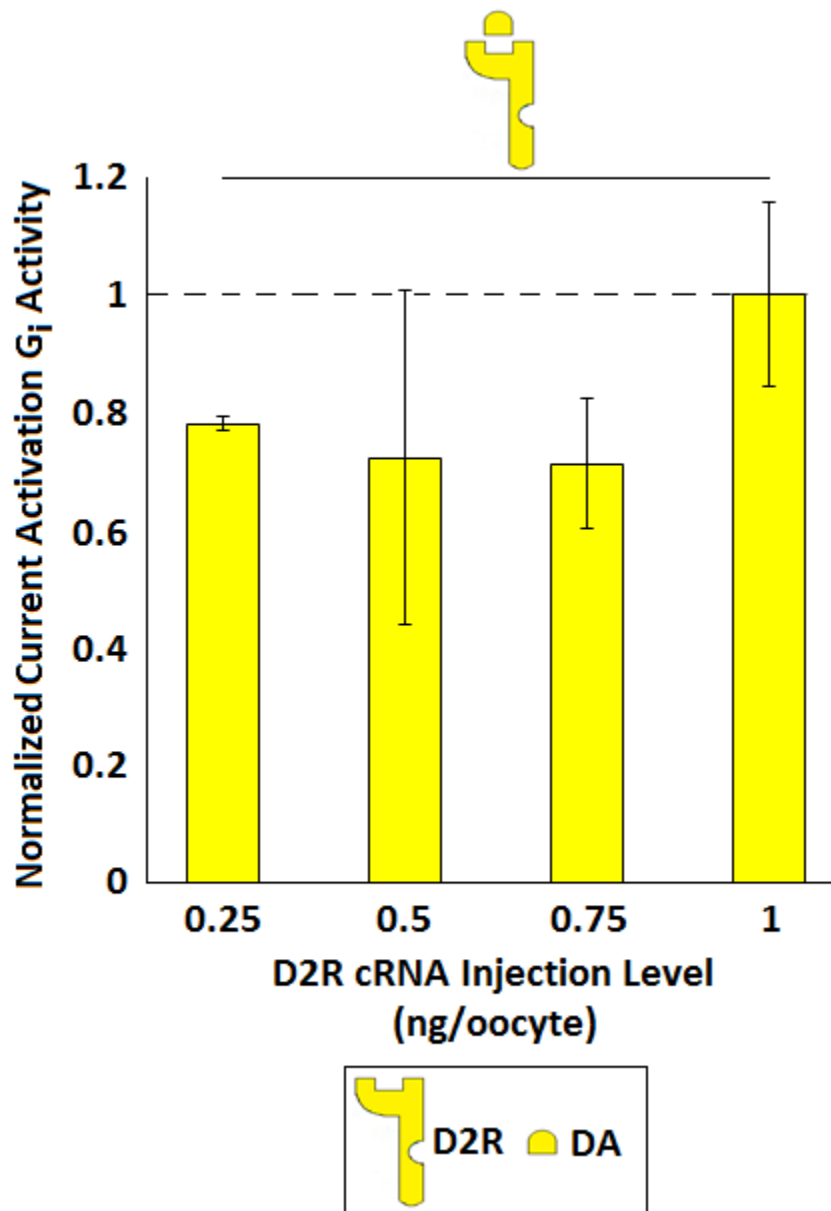


**Figure 4.5. Verification of G<sub>q</sub> signal at ≤ 2ng/oocyte cRNA injection levels.** Summary bar graph of G<sub>q</sub> activity measured in oocytes: The addition of 1μM 5HT in the presence of 5HT2AR increases G<sub>q</sub> activity. (N = 3-4/condition, Performed in one batch of oocytes, Dotted line = 1 or 100%, Data are mean ± SEM)

cRNA injections (xng 5HT2AR): GIRK4\*, PTX, plus 5HT2AR

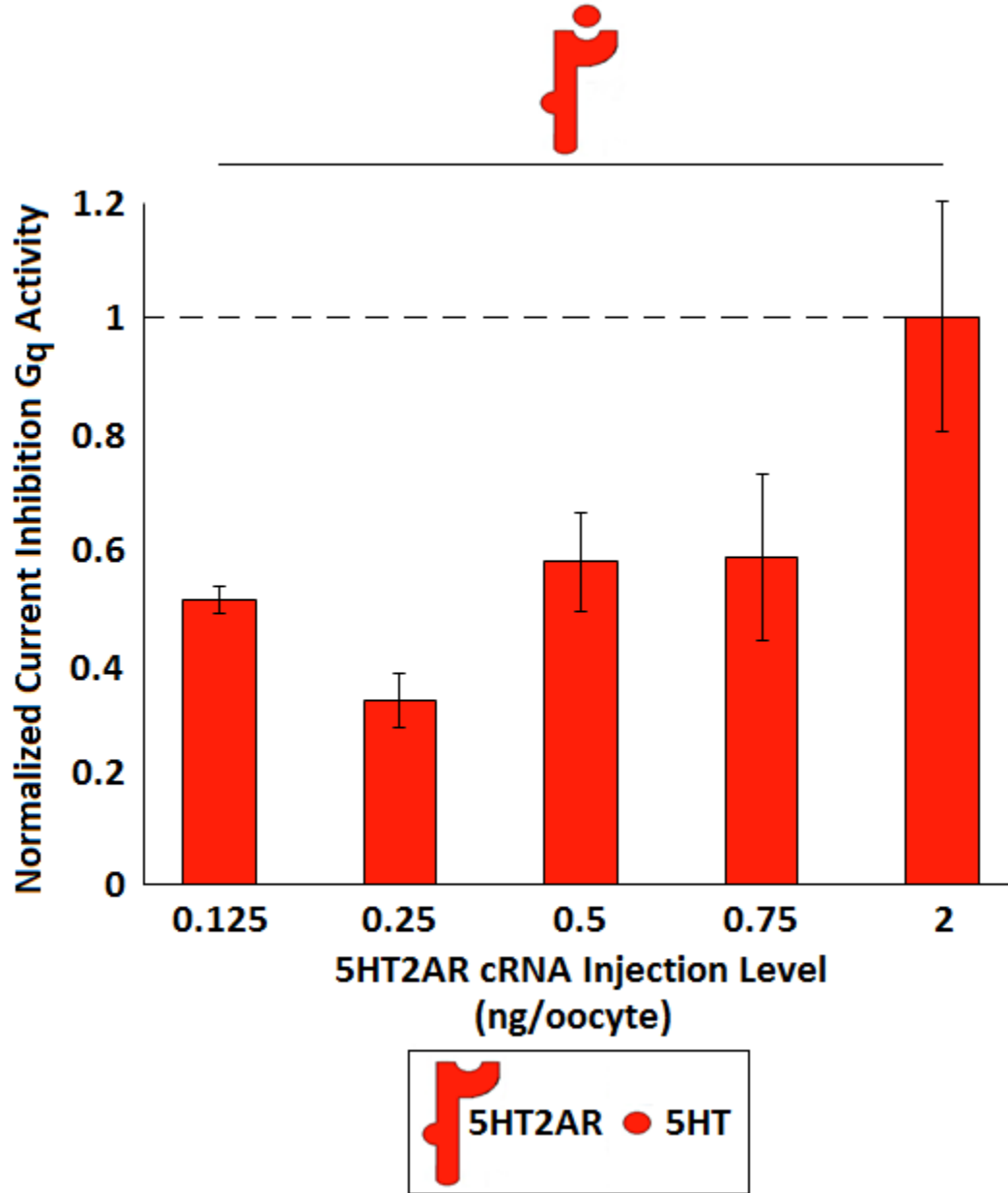


**Figure 4.6. Lateral allosterism at lower cRNA amounts and corresponding cRNA ratios:  $G_i$  activity.** Summary bar graph of  $G_i$  activity measured in oocytes: The addition of 1 $\mu$ M DA in the presence of D2R and 5HT2AR increases  $G_i$  activity compared to the D2R. (N = 7-8/condition, Dotted line = 1 or 100%, Data are mean  $\pm$  SEM, \* $p$ <0.05, \*\* $p$ <0.01, no horizontal significance line = compared to homomer)

cRNA injections (0.25ng:xng D2R:5HT2AR): GIRK4\*, RGS2, plus D2R or D2R+5HT2AR

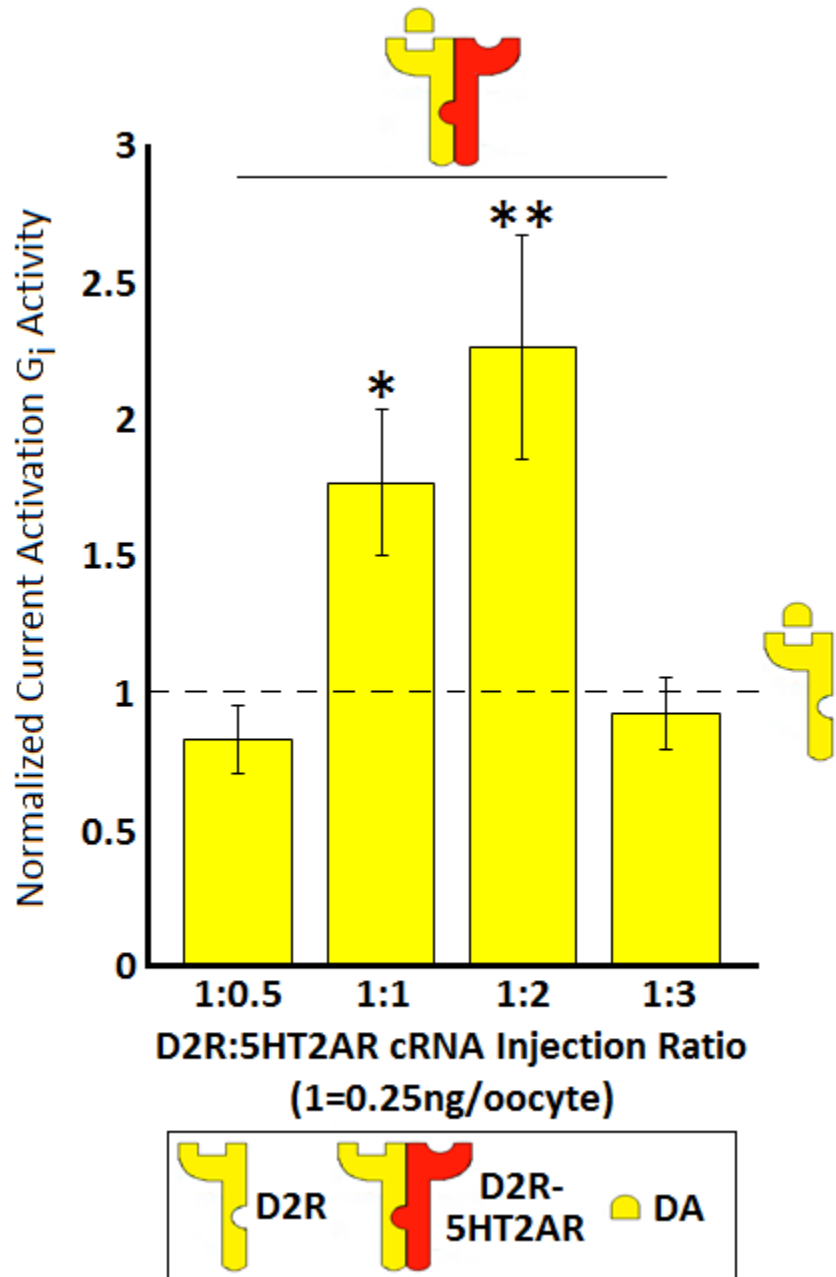


**Figure 4.7. Lateral allosterism at lower cRNA amounts and corresponding cRNA ratios: G<sub>q</sub> activity.** Summary bar graph of G<sub>q</sub> activity measured in oocytes: The addition of 1uM 5HT in the presence of D2R and 5HT2AR increases G<sub>q</sub> activity compared to the 5HT2AR. (N = 8/condition, Dotted line = 1 or 100%, Data are mean ± SEM, \*\**p*<0.01, no horizontal significance line = compared to homomer)

cRNA injections (0.25ng:xng D2R:5HT2AR): GIRK4\*, PTX, plus 5HT2AR or D2R+5HT2AR

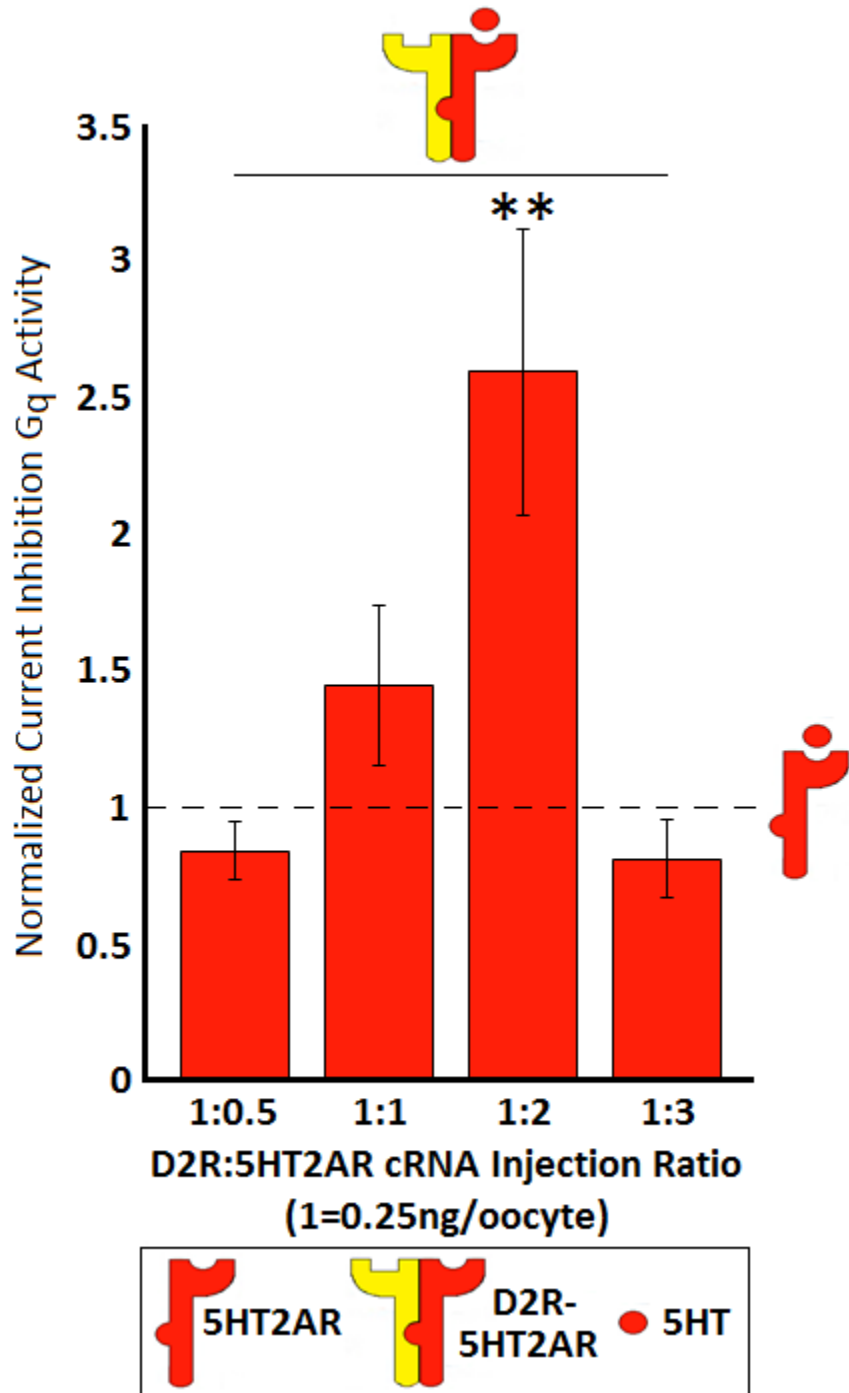


**Figure 4.8. The endogenous neurotransmitter 5HT cross-signals and increases the activity of the non-target receptor while the 5HT2AR 2-alanine mutant abrogates lateral and drug-induced allosterism.** Summary bar graph of  $G_i$  activity measured in oocytes: The addition of 1 $\mu$ M 5HT with 1 $\mu$ M DA allosterically cross-signals and increases  $G_i$  activity of the endogenous neurotransmitter DA. When the 5HT2AR is replaced with the 5HT2AR (2A) mutant, lateral allosterism is lost and the addition of 1 $\mu$ M 5HT with 1 $\mu$ M DA does not allosterically cross-signal and increase  $G_i$  activity of the endogenous neurotransmitter DA (N = 8-14/condition, Dotted line = 1 or 100%, Data are mean  $\pm$  SEM, \* $p$ <0.05, \*\* $p$ <0.01, #: no significance compared to homomer, no horizontal significance line = compared to homomer)  
cRNA injections (1ng:2ng D2R:5HT2AR): GIRK4\*, RGS2, plus D2R, 5HT2AR, D2R+5HT2AR or D2R+5HT2AR (2A)

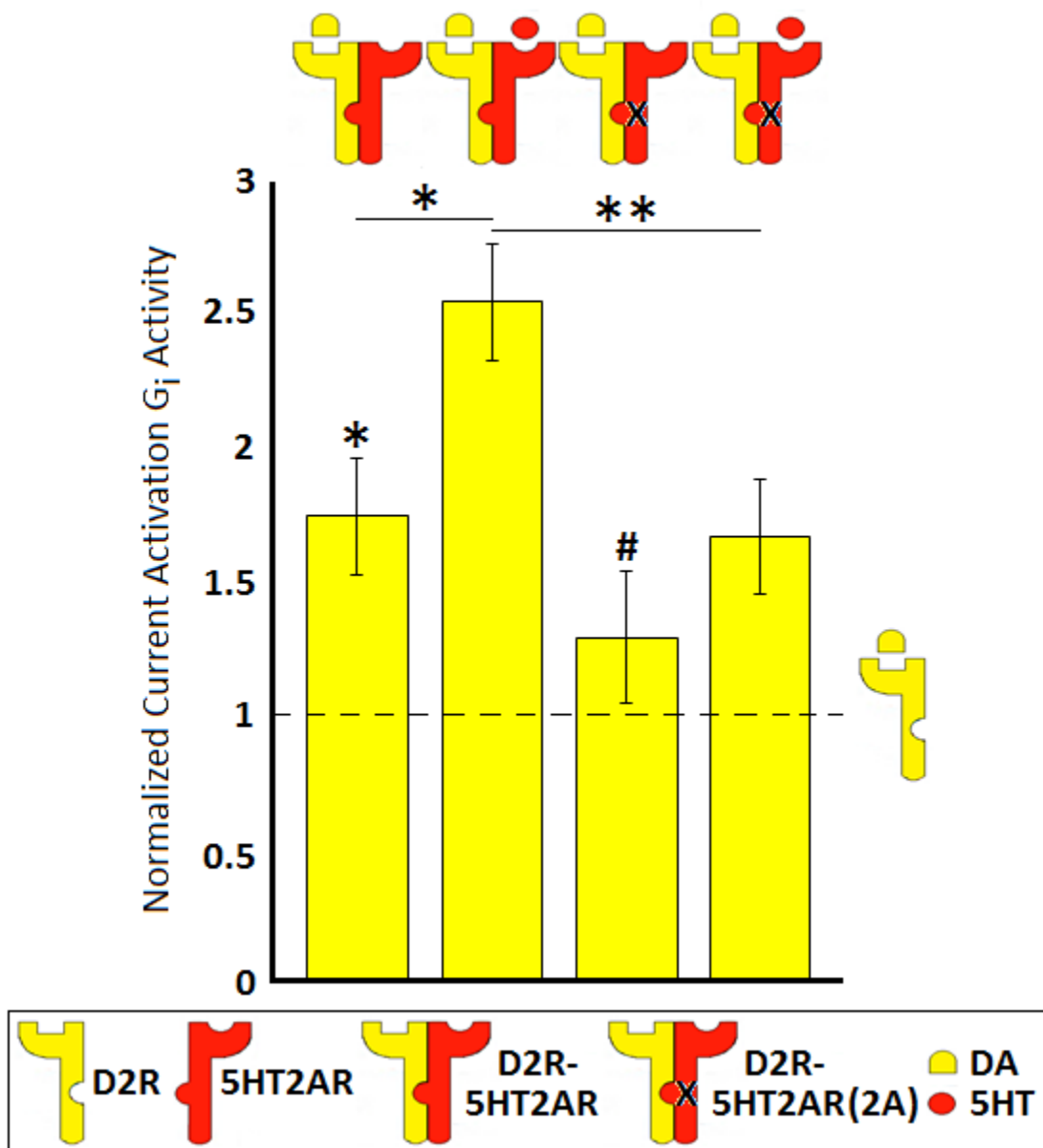


**Figure 4.9. The endogenous neurotransmitter dopamine cross-signals and increases the activity of the non-target receptor.** Summary bar graph of  $G_q$  activity measured in oocytes: The addition of 1 $\mu$ M DA with 1 $\mu$ M 5HT allosterically cross-signals and increases  $G_q$  activity of the endogenous neurotransmitter 5HT2AR. (N = 8/condition, Dotted line = 1 or 100%, Data are mean  $\pm$  SEM, \* $p$ <0.05, \*\* $p$ <0.01, no horizontal significance line = compared to homomer) cRNA injections (1ng:2ng D2R:5HT2AR): GIRK4\*, PTX, plus 5HT2AR or D2R+5HT2AR

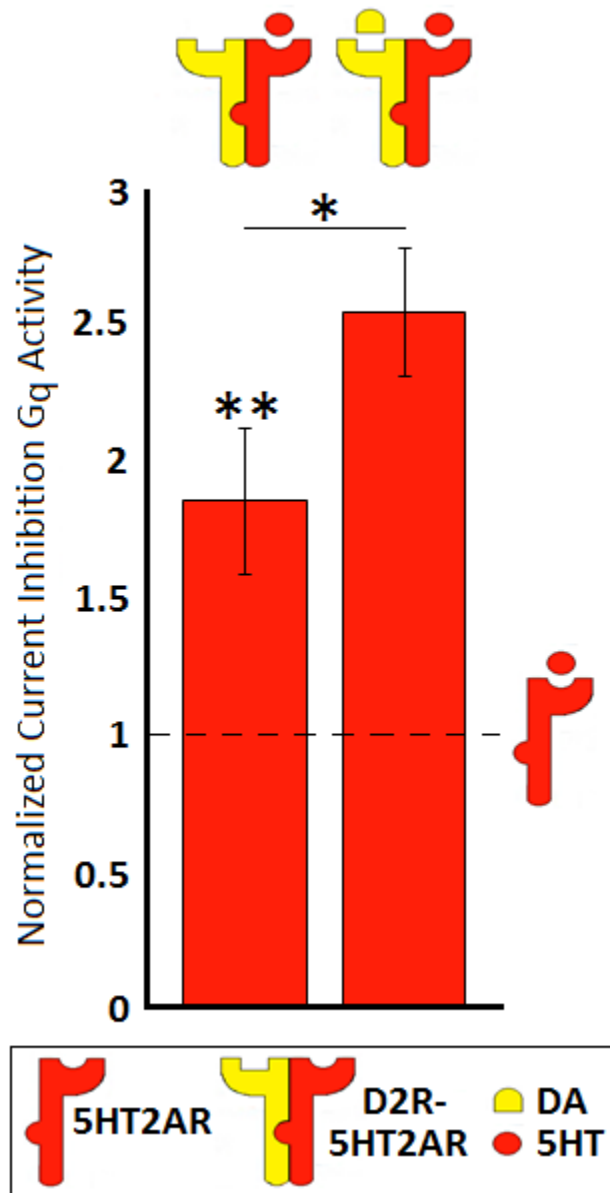


**Figure 4.10. Synthetic agonists cross-signal and decrease the activity of the non-target receptor.** Summary bar graph of  $G_i$  and  $G_q$  activity measured in oocytes: The addition of 10uM DOI with 1uM DA or 10uM QP with 1uM 5HT allosterically cross-signals and decreases  $G_i$  and  $G_q$  activity of the endogenous ligand. (N = 7-8/condition, Dotted line = 1 or 100%, Data are mean  $\pm$  SEM, \* $p$ <0.05, \*\* $p$ <0.01, no horizontal significance line = compared to homomer) cRNA injections (1ng:2ng D2R:5HT2AR): GIRK4\*, RGS2 or PTX, plus D2R, 5HT2AR, or D2R+5HT2AR

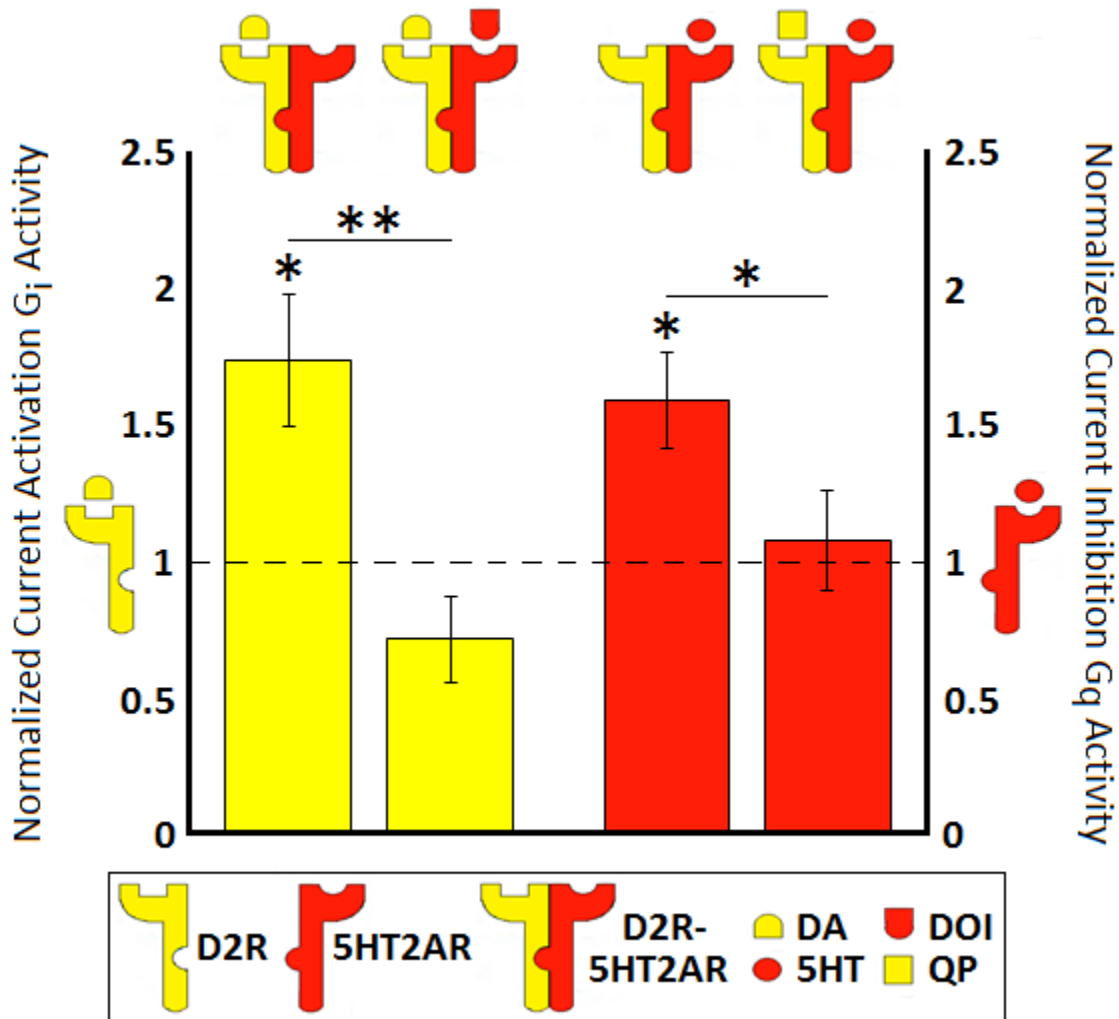


**Figure 4.11. Concentration responses of Pimavanserin as dopamine or 5HT antagonists at the D2R or 5HT2AR.** Concentration response curves of either 1uM DA G<sub>i</sub> or 1uM 5HT G<sub>q</sub> activity with increasing concentrations of the potential atypical anti-psychotic pimavanserin (PIMA) measured in oocytes. The addition of PIMA with dopamine (DA) to the D2R decreases G<sub>i</sub> activity or with serotonin (5HT) to the 5HT2AR decreases G<sub>q</sub> activity. (G<sub>i</sub> activity normalized to 1uM DA response, G<sub>q</sub> activity normalized to 1uM 5HT response, N = 7-11/condition, Dotted line = 1 or 100%, Data are mean ± SEM, Curve was fit by eye)  
cRNA injections: GIRK4\*, RGS2 or PTX, plus D2R or 5HT2AR

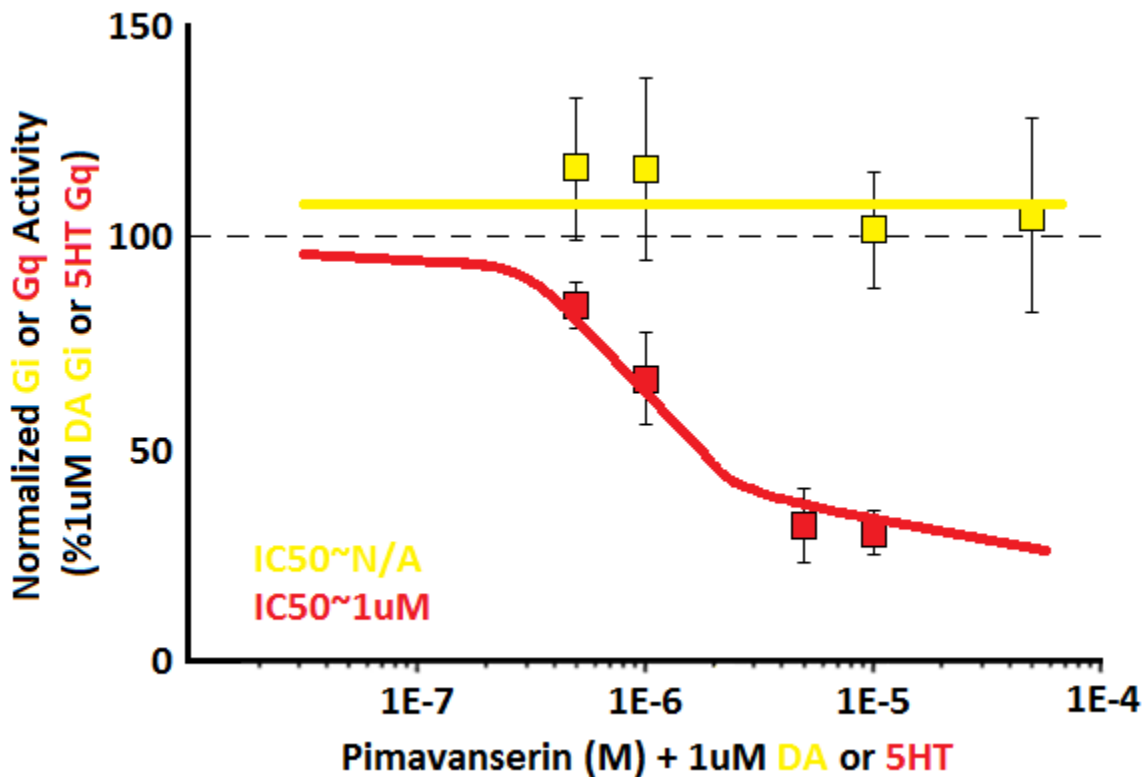


**Figure 4.12. 5HT2AR-selective potential APD Pimavanserin cross-signaling to the D2R.**  
 Summary bar graph of  $G_i$  activity measured in oocytes: The addition of 5uM PIMA with 1uM DA in the presence of both D2R and 5HT2AR allosterically cross-signals and decreases  $G_i$  activity of the endogenous ligand. The addition of 5uM PIMA with 1uM DA to D2R does not change  $G_i$  activity. (N = 7-8/condition, Dotted line = 1 or 100%, Data are mean  $\pm$  SEM, \*\*\* $p$ <0.001, no horizontal significance line = compared to homomer)  
cRNA injections (1ng:2ng D2R:5HT2AR): GIRK4\*, RGS2, plus D2R, or D2R+5HT2AR

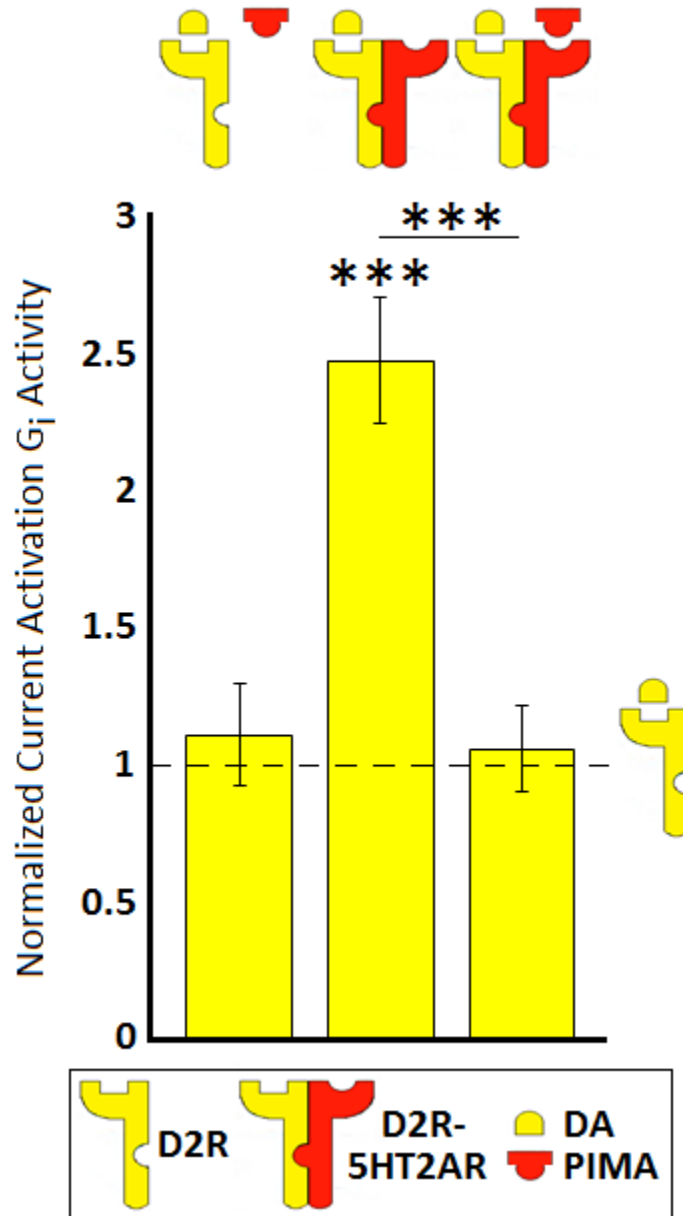


**Figure 4.13. Concentration responses of Amisulpride as dopamine or 5HT antagonists at the D2R or 5HT2AR.** Concentration response curves of either 1uM DA  $G_i$  or 1uM 5HT  $G_q$  activity with increasing concentrations of the atypical anti-psychotic amisulpride (AMIS) measured in oocytes. The addition of AMIS with dopamine (DA) to the D2R decreases  $G_i$  activity or with serotonin (5HT) to the 5HT2AR decreases  $G_q$  activity. ( $G_i$  activity normalized to 1uM DA response,  $G_q$  activity normalized to 1uM 5HT response, N = 8/condition, Dotted line = 1 or 100%, Data are mean  $\pm$  SEM, Curve was fit by eye)  
cRNA injections: GIRK4\*, RGS2 or PTX, plus D2R or 5HT2AR

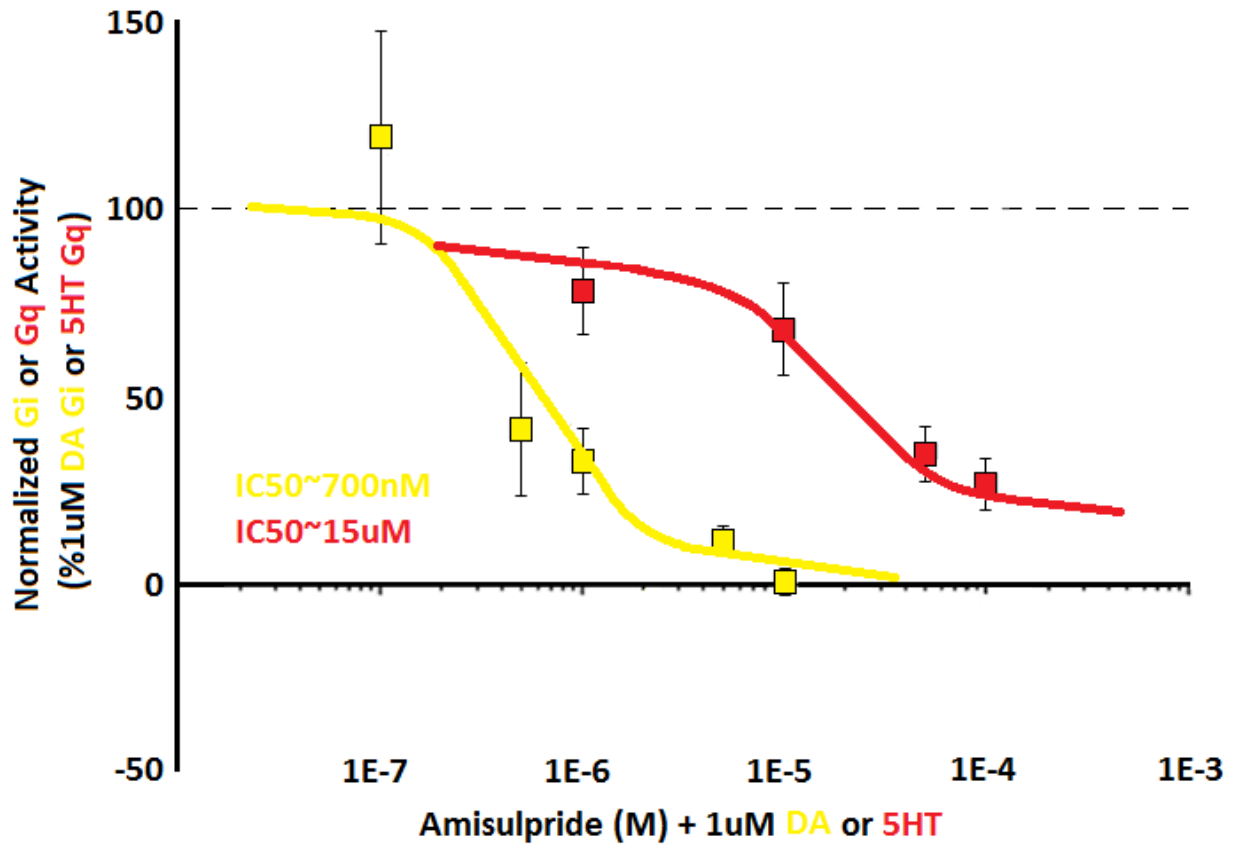


**Figure 4.14. D2R-selective APD Amisulpride cross-signaling to the 5HT2AR.** Summary bar graph of  $G_q$  activity measured in oocytes: The addition of 300nM AMIS with 1uM 5HT in the presence of both D2R and 5HT2AR allosterically cross-signals and decreases  $G_q$  activity of the endogenous ligand. The addition of 300nM AMIS with 1uM 5HT to 5HT2AR does not change  $G_q$  activity. (N = 8/condition, Dotted line = 1 or 100%, Data are mean  $\pm$  SEM,  $**p < 0.01$ ,  $***p < 0.001$ , no horizontal significance line = compared to homomer) cRNA injections (1ng:2ng D2R:5HT2AR): GIRK4\*, PTX, plus 5HT2AR, or D2R+5HT2AR

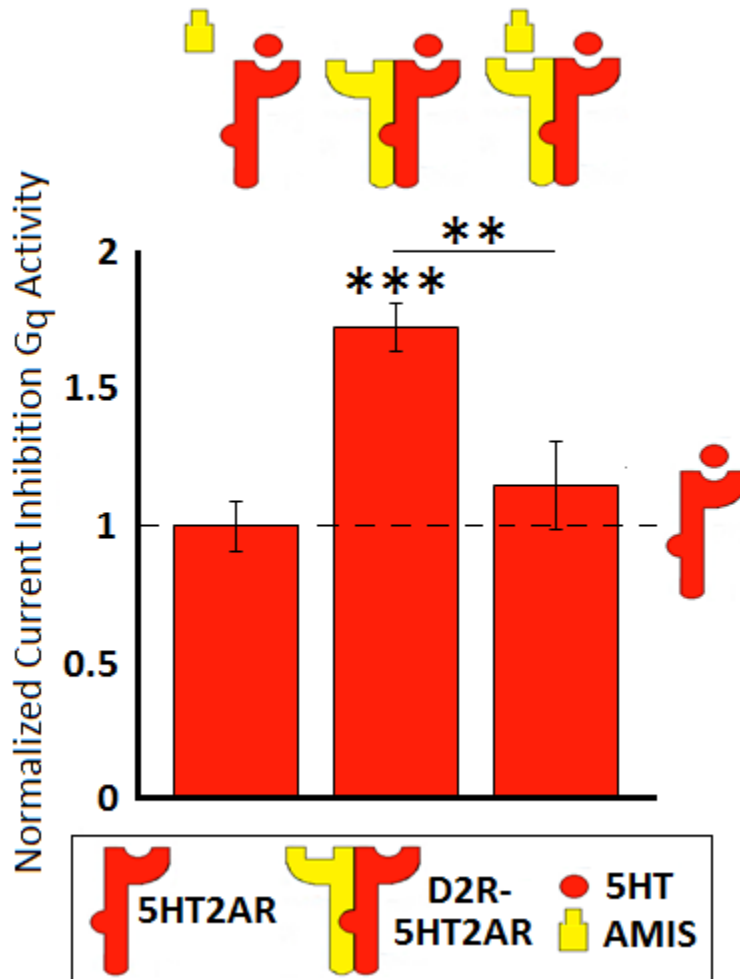


**Figure 4.15. Concentration responses of Amperozide as dopamine or 5HT antagonists at the D2R or 5HT2AR.** Concentration response curves of either 1uM DA  $G_i$  or 1uM 5HT  $G_q$  activity with increasing concentrations of the potential atypical anti-psychotic amperozide (AMP) measured in oocytes. The addition of AMP with dopamine (DA) to the D2R decreases  $G_i$  activity or with serotonin (5HT) to the 5HT2AR decreases  $G_q$  activity. ( $G_i$  activity normalized to 1uM DA response,  $G_q$  activity normalized to 1uM 5HT response, N = 8/condition, Dotted line = 1 or 100%, Data are mean  $\pm$  SEM, Curve was fit by eye)  
cRNA injections: GIRK4\*, RGS2 or PTX, plus D2R or 5HT2AR

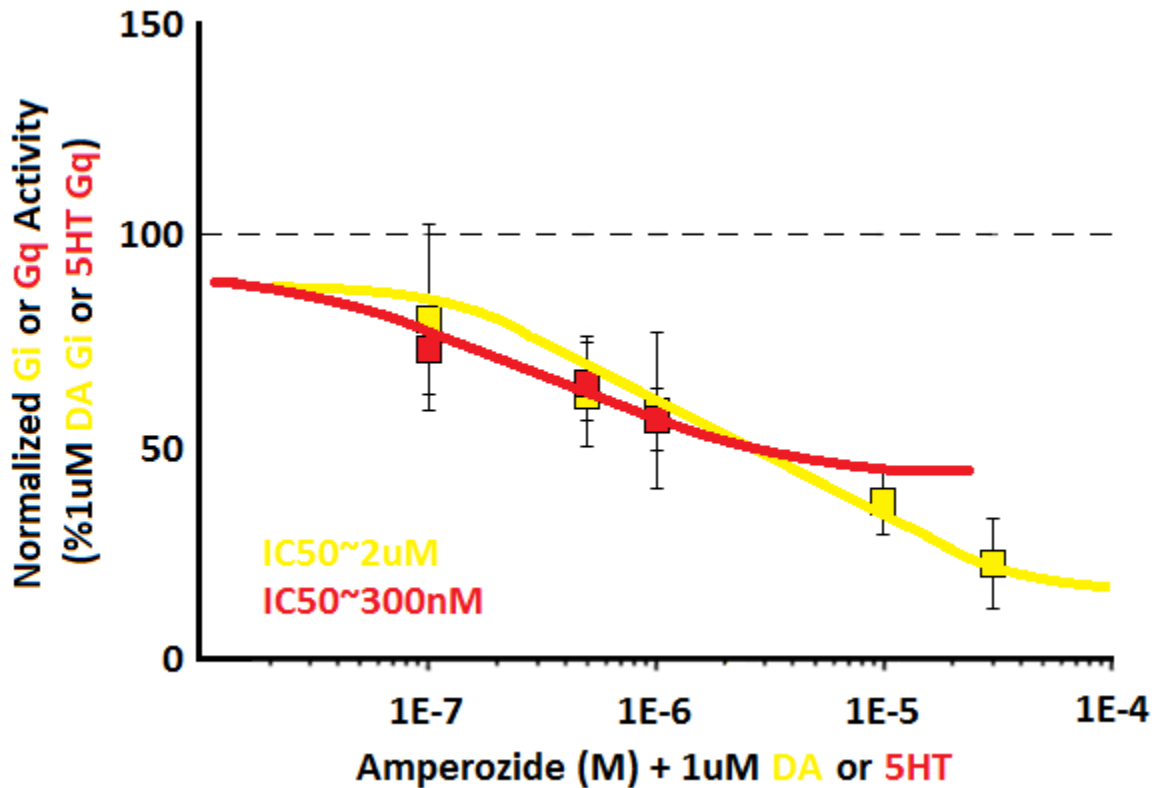


**Figure 4.16. Non-selective APD Amperozide cross-signaling to the D2R.** Summary bar graph of  $G_i$  activity measured in oocytes: The addition of 300nM AMP with 1uM DA in the presence of both D2R and 5HT2AR allosterically cross-signals and decreases  $G_i$  activity of the endogenous ligand. The addition of 300nM AMP with 1uM DA to D2R does not change  $G_i$  activity. (N = 8-9/condition, Dotted line = 1 or 100%, Data are mean  $\pm$  SEM,  $**p < 0.01$ , no horizontal significance line = compared to homomer)

cRNA injections (1ng:2ng D2R:5HT2AR): GIRK4\*, RGS2, plus D2R, or D2R+5HT2AR

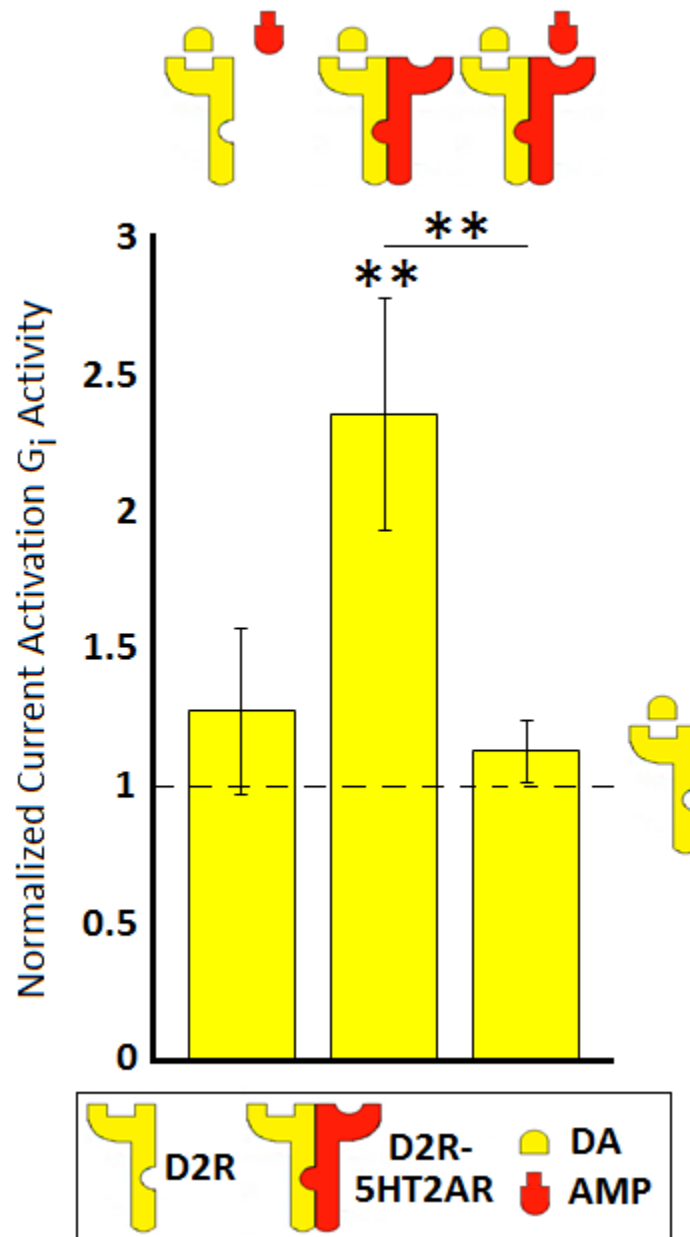


**Figure 4.17. Concentration responses of Paliperidone as dopamine or 5HT antagonists at the D2R or 5HT2AR.** Concentration response curves of either 1uM DA G<sub>i</sub> or 1uM 5HT G<sub>q</sub> activity with increasing concentrations of the atypical anti-psychotic paliperidone (PAL) measured in oocytes. The addition of PAL with dopamine (DA) to the D2R decreases G<sub>i</sub> activity or with serotonin (5HT) to the 5HT2AR decreases G<sub>q</sub> activity. (G<sub>i</sub> activity normalized to 1uM DA response, G<sub>q</sub> activity normalized to 1uM 5HT response, N = 6-8/condition, Dotted line = 1 or 100%, Data are mean ± SEM, Curve was fit by eye)  
cRNA injections: GIRK4\*, RGS2 or PTX, plus D2R or 5HT2AR

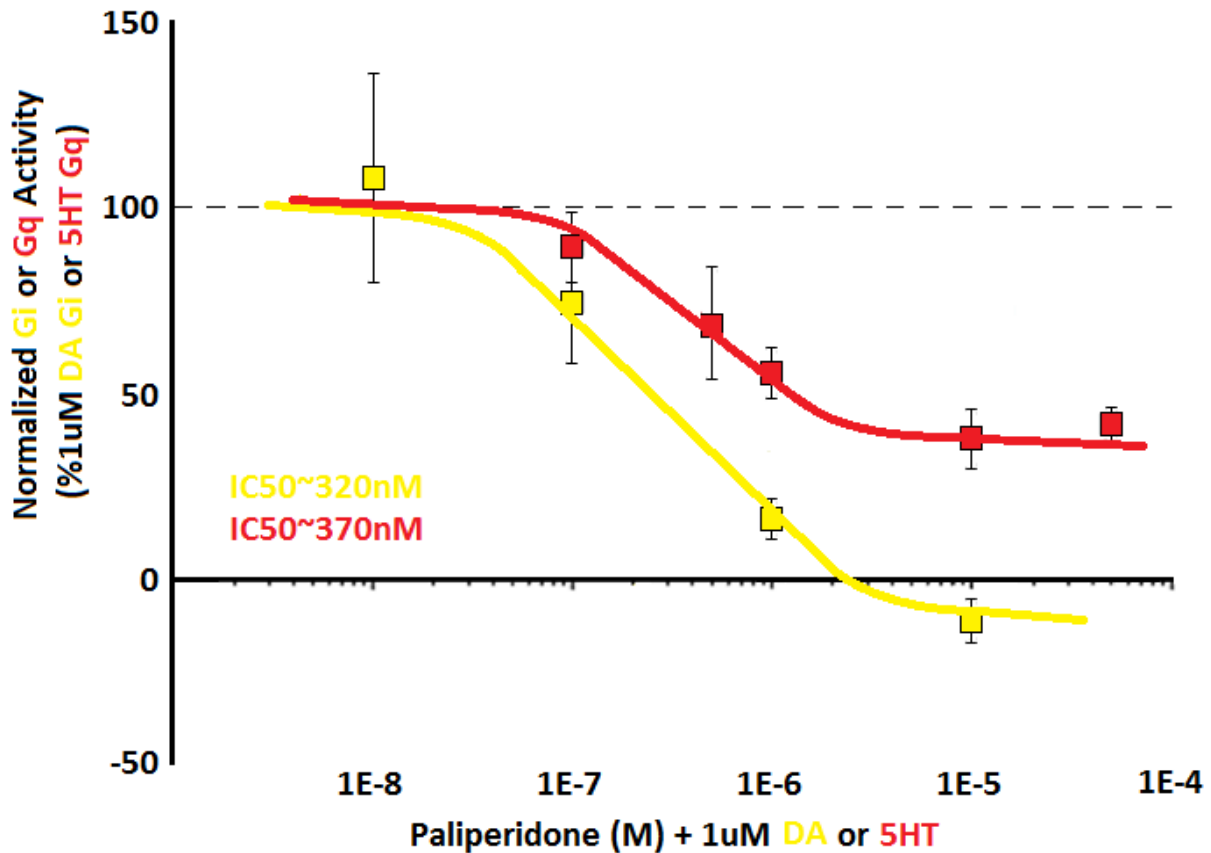


**Figure 4.18. Non-selective APD Paliperidone cross-signaling to the 5HT2AR.** Summary bar graph of  $G_q$  activity measured in oocytes: The addition of 100nM PAL with 1 $\mu$ M 5HT in the presence of both D2R and 5HT2AR allosterically cross-signals and decreases  $G_q$  activity of the endogenous ligand. The addition of 100nM AMIS with 1 $\mu$ M 5HT to 5HT2AR alone does not change  $G_q$  activity. (N = 8/condition, Dotted line = 1 or 100%, Data are mean  $\pm$  SEM, \* $p$ <0.05, \*\* $p$ <0.01, no horizontal significance line = compared to homomer) cRNA injections (1ng:2ng D2R:5HT2AR): GIRK4\*, PTX, plus 5HT2AR, or D2R+5HT2AR

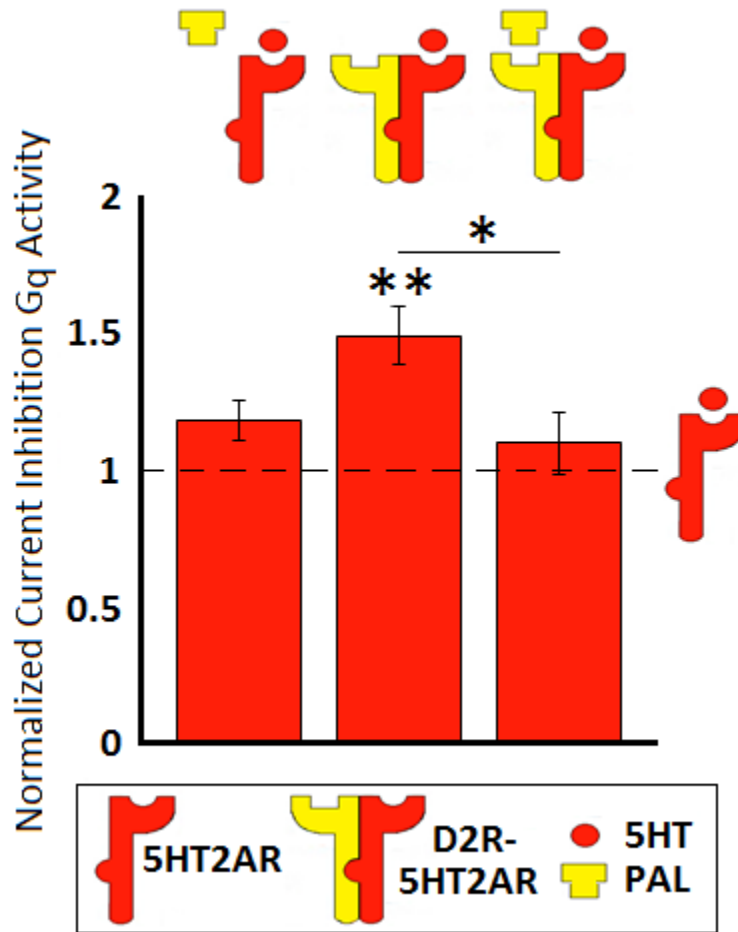


**Figure 4.19. Effects of drug combinations.** Summary bar graph of  $G_q$  activity measured in oocytes: The addition of QP with DOI allosterically cross-signals and decreases  $G_q$  activity of the endogenous neurotransmitter 5HT2AR. (N = 5-7/condition, Performed in one batch of oocytes, Dotted line = 1 or 100%, Data are mean  $\pm$  SEM,  $**p < 0.01$ ,  $***p < 0.001$ , no horizontal significance line = compared to homomer)

cRNA injections (1ng:2ng D2R:5HT2AR): IRK3, PTX, plus 5HT2AR or D2R+5HT2AR

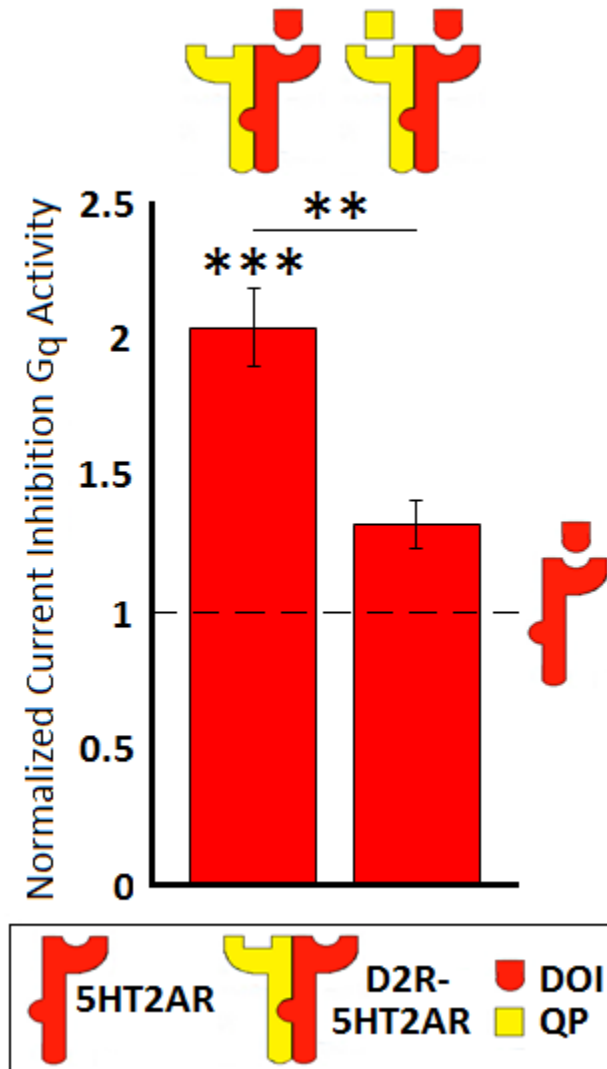
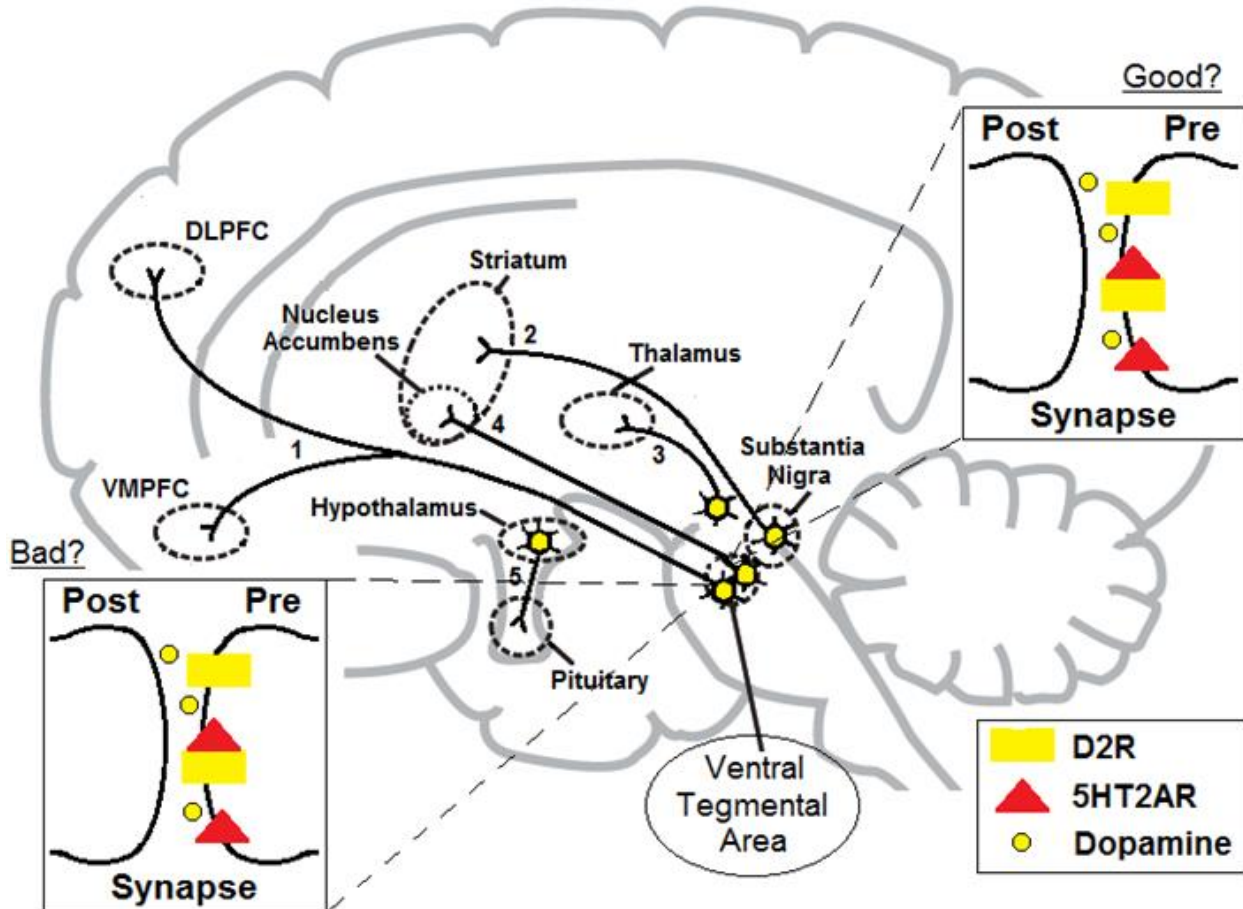


**Table 4.2. Results from D2R and 5HT2AR ligand application in *Xenopus* oocytes.** The ligands used in Chapter 4 experiments and the ensuing results.

<b>Ligand</b>	<b>Target GPCR</b>	<b>[M]</b>	<b>Lateral Allosterism</b>	<b>Drug-induced Allosterism</b>	<b>D2R vs. 5HT2AR Homomeric Effects</b>
<b>Dopamine</b>	<b>D2R</b>	<b>1uM</b>	<b>Increased G<sub>i</sub> activity (90%)</b>	<b>Increased G<sub>q</sub> activity</b>	<b>Increased G<sub>i</sub> activity of the D2R</b>
<b>Quinpirole</b>	<b>D2R</b>	<b>10uM</b>	<b>N/A</b>	<b>Decreased G<sub>q</sub> activity</b>	<b>Increased G-Protein activity of the D2R <u>and</u> 5HT2AR</b>
<b>Amisulpride</b>	<b>D2R</b>	<b>300nM</b>	<b>N/A</b>	<b>Decreased G<sub>q</sub> activity</b>	<b>IC<sub>50</sub>~700nM at D2R; IC<sub>50</sub>~15uM at 5HT2AR</b>
<b>Paliperidone (Pal)</b>	<b>D2R</b>	<b>100nM</b>	<b>N/A</b>	<b>Decreased G<sub>q</sub> activity</b>	<b>IC<sub>50</sub>~320nM at D2R and acts as inverse agonist; IC<sub>50</sub>~370nM at 5HT2AR and limited efficacy</b>
<b>5HT</b>	<b>5HT2AR</b>	<b>1uM</b>	<b>Increased G<sub>q</sub> activity (50%)</b>	<b>Increased G<sub>i</sub> activity</b>	<b>Increased G<sub>q</sub> activity of the 5HT2AR</b>
<b>DOI</b>	<b>5HT2AR</b>	<b>10uM</b>	<b>N/A</b>	<b>Decreased G<sub>i</sub> activity</b>	<b>Increased G<sub>q</sub> activity of the 5HT2AR</b>
<b>Pimavanserin</b>	<b>5HT2AR</b>	<b>5uM</b>	<b>N/A</b>	<b>Decreased G<sub>i</sub> activity</b>	<b>IC<sub>50</sub>~1uM at 5HT2AR; No effect at D2R</b>
<b>Amperozide</b>	<b>5HT2AR</b>	<b>300nM</b>	<b>N/A</b>	<b>Decreased G<sub>i</sub> activity</b>	<b>IC<sub>50</sub>~300nM at 5HT2AR and limited efficacy; IC<sub>50</sub>~2uM at D2R</b>

**Figure 4.20. The location of the D2R-5HT2AR heteromer determines neurotransmitter effects on brain regions.** Representative positioning of D2R-5HT2AR heteromers in a specific brain region and neuronal synapse. Tracing the neuro-circuitry implicated in schizophrenia allows speculation on allosteric effects upon heteromerization (Adapted from Stahl SM 2013).



## Chapter 5: DISCUSSION AND CONCLUDING REMARKS

We had two goals in mind at the beginning of this study. First, we wanted to further substantiate in mammalian cells the allosteric effects upon mGlu2R-5HT2AR heteromerization seen in oocytes. Second, we wanted to investigate in oocytes a second heteromer, the D2R-5HT2AR, whose potential allosteric effects upon heteromerization would be relevant to psychosis.

With the mGlu2R-5HT2AR heteromer in a mammalian cell line, inverse agonists did indeed cross-signal and increase G-protein activity of the non-target receptor. A combination of an atypical APD and a potential mGlu2R APD was able to overcome low levels of heteromer formation and expression. With the D2R-5HT2AR heteromer in oocytes, lateral allosterism increased G-protein activity of both receptors, while the concurrent application of dopamine and 5HT increased G-protein activity of both receptors even further. Only one D2R to 5HT2AR cRNA injection ratio produced a maximal lateral allosterism. A two-point mutation in the 5HT2AR C-terminus tail significantly lowered or eliminated the lateral allosterism and endogenous neurotransmitter cross-signaling. Synthetic agonists and atypical APDs decreased the G-protein activity of the non-target receptors. Finally, the combination of two synthetic

agonists without any endogenous neurotransmitters behaved similarly to single synthetic agonists, decreasing the G-protein activity of the non-target receptor.

Our work with the mGlu2R-5HT2AR heteromer confirmed the *Xenopus* oocyte work and yielded no surprises, but the D2R-5HT2AR certainly did. The APDs we used showed interesting results when applied to the homomers, even reversals in affinity for the D2R and 5HT2AR compared to the existing data. The cross-signaling we examined turned out to be mostly different than we expected. Multiple basic D2R-5HT2AR allosteric functional effects are now evident from our work in oocytes and allow for conjecture as to how heteromeric formation will affect neurocircuitry.

How do the allosteric effects upon mGlu2R-5HT2AR and D2R-5HT2AR heteromerization apply to the overall neurocircuitry of our brains? In **Figs. 3.7 and 4.20**, we explored how individual neurocircuits specific to each heteromer would be affected by GPCR heteromerization. Obviously, this is a very simplistic view. The effects postulated in these two figures can also affect downstream neurocircuitry, as well as added components along the pathways.

So far we have postulated the effects of the heteromers on a single neuron. If we add interneurons to the neurocircuitry, the effects would change. In the binary digital world, interneurons would be viewed as an inverter, changing a one to a zero, or vice versa. An even number of interneurons in series would result in the same signal qualitatively, but any odd number would invert the signal. The striatum contains many interneurons as well as spiny stellate neurons. In the previous example, the D2R-5HT2AR on a pre-synaptic terminal signaling to meso-limbic neurons will regulate the dopamine release in the striatum.

Dysregulation of these heteromers will cause the dopamine levels in the striatum to increase similar to a psychotic condition. The addition of an interneuron downstream of the meso-limbic neuron will reverse this effect, adding levels of complexity to neuronal signaling. Thus, not only does the synaptic and neurocircuitry location of the D2R-5HT2AR heteromer matter in influencing downstream effects, but interneurons in series with the existing neurocircuitry will alter the overall signaling, glial cells expressing the heteromer and the associated allosteric differences will modulate the signals, and other effectors will play roles in neuronal signaling.

Next, we can look at the links between more than two brain regions. The striatal neurons from the previous paragraph will then signal back to the VTA, which acts a relay to the PFC. In the PFC, a series of pyramidal neurons and interneurons will eventually signal back to the VTA and also directly to the striatum. Along these pathways, there will be any number of interneurons involved. Two separate paths from one brain region to another could result in completely different signals, all reliant upon the heteromeric effects of the D2R-5HT2AR and mGlu2R-5HT2AR, or lack thereof in a psychotic condition.

Finally, schizophrenia is but one of many neurological diseases. The mGlu2R, D2R, and 5HT2AR are obviously widely distributed in the brain. Everywhere they are co-localized is a potential region for their heteromerization. The resulting allosteric effects will also play roles in diseases like Parkinson's, epilepsy, Alzheimer's, and IBS, just to name a few. These diseases involve similarly complex neurocircuitry like that found in schizophrenia, and the allosteric effects upon heteromerization will be just as important in the studies of these diseases.

Several open questions remain, all of which apply to future studies of the mGlu2R-5HT2AR and D2R-5HT2AR. The effects evidenced in Chapter 4 will be furthered in a

mammalian cell line similar to the experiments in Chapter 3. Transient transfections in HEK-293 cells could be used, but the development of separate stable cell lines containing 5HT2AR plus GIRK1/4, D2R plus GIRK1/4, and 5HT2AR plus D2R plus GIRK1/4 is preferred. These cells will allow consistency with previous experimental methods. Also, translationally, our stably-transfected HEK-293 cells can then be used in high-throughput screening of potential APDs. The  $G_q$  signaling of 5HT2AR can be assessed using  $Ca^{2+}$  imaging while potentiometric dyes can be used to assess the  $G_i$  signaling of mGlu2R or D2R. Thus, hundreds of compounds can be tested quickly and precisely as to their potential translational use in the treatment of schizophrenia.

However, translational studies will not be pertinent until we have identified the effects of a wider range of APDs at the mGlu2R-5HT2AR and D2R-5HT2AR heteromers. Once we know how typical and other atypical APDs affect the heteromers we can design experiments intended to improve schizophrenic treatments.

The mechanisms behind trafficking and expression and their relationship to mRNA amounts of the individual GPCRs remain elusive. We began to explore mRNA and protein relationships between mGlu2R and 5HT2AR in the Baki L et al., 2016 study, but only scratched the surface. We expect the mechanisms behind trafficking and expression and their relationship to mRNA amounts of the individual GPCRs to be just as challenging. The simplest method to explore trafficking and expression starts with fluorescently-tagged receptors and imaging. Time-resolved images of fluorescent movement corresponding to the constituent GPCRs will provide knowledge of where the involved heteromers form, whether in the endoplasmic reticulum followed by delivery to the plasma membrane or at the plasma membrane itself. Also, the use of bi-fluorescence complementation will allow us to distinguish where the heteromers are physically located along the exocytosis and endocytosis pathways.

An experiment of particular interest to us that has not been explored yet could provide insight into not only the trafficking and formation of either heteromer we have studied, but also the mechanisms involved with chronic administration of APDs. Electrophysiology, be it whole-cell patch clamp or TEVC, reflects a short time frame process, normally only several minutes per recording. APD application is therefore not a time-dependent concern. What results would an incubation of cells with APDs produce, testing either our stably-transfected HEK-293 cells or cRNA-injected oocytes? Atypical APDs clozapine (Schmid CL et al., 2014) and amperozide (Chang PY et al., 2008) are known to down-regulate the 5HT2AR. Incubation in either APD could stabilize or destabilize the heteromers, affecting either the low or high states of heteromer expression and formation. APDs in general are highly lipophilic. Given time, APDs will diffuse through the plasma membrane and bind to receptors trafficking to the membrane or in the internal organelles, possibly stabilizing or destabilizing the receptors in various membranes. These types of effects could have a profound impact on heteromerization, either during trafficking or in the plasma membrane.

It is not clear whether GPCR heteromers are formed in the ER and delivered to the plasma membrane or formed in the plasma membrane. It is also not clear how many of each receptor subunit are involved in the heteromeric complex. The subunits may exist in a fixed ratio, but they also could vary, depending on many factors. When they vary, their allosteric effects may also vary. Subunit stoichiometry is beginning to be addressed by modeling and assays combining different constructs (Moreno JL et al., 2016), but assays like single-molecule photo-bleaching could pinpoint the ratio of subunits comprising individual heteromeric molecules (Reiner A et al., 2012; Arant RJ and Ulbrich MH, 2014). GPCRs tagged with mEGFP can be photobleached in a time-resolved manner. Single-molecule photobleaching is the chemical destruction of the

fluorophore, resulting in a discrete decrease in the intensity of the fluorescence. The number of discrete decreases in a single location at molecular resolution represents the number of subunits in a complex. Using these tagged receptors, we can elucidate the number of each GPCR subunits in a given heteromer. We do not know if the result will be one stoichiometry or a mixture of different stoichiometries. Therefore, the information gleaned from these experiments will not only provide possible insights into the mechanisms of allosterism, but also knowledge of a ‘normal’ set of subunit stoichiometries. Further, information will be provided as to the relative amounts of monomers and homomers as compared to heteromers.

Along with allosteric effects upon heteromerization and physiological relevance, one of the top goals when studying GPCR heteromers is to show an unequivocal direct interaction between the GPCR constituents of a heteromer. Knowledge of the direct interaction between the constituent GPCRs of a heteromer will aid in the elucidation of the involved allosteric mechanisms. The difference between ‘co-present’ and ‘co-joined’ is subtle, but very important. In all of our experiments, we know that both receptors are expressed, but we have only bio-fingerprints to ascertain whether there is direct interaction. Unfortunately, there is no experimental method able to accomplish a perfect ‘snapshot’ of the constituent GPCRs bound together. Even a crystal structure of a GPCR heteromer would be considered artificial. For the moment, we must gather as much evidence supporting heteromer formation as possible and we will be using two methods we consider the strongest available: mutated receptors and single-TM peptides.

We showed in **Fig. 4.8** that the 5HT2AR (2A) mutant used in the literature resulted in similar heteromer abrogation effects in our system. So far we have tested the 5HT2AR (2A) mutant and its effect on the  $G_i$  signaling of the D2R. We will next examine its effect on the  $G_q$

signaling of the 5HT2AR. As for the D2R mutants in the literature, we have developed a construct that combines the 6-alanine mutation in the IC3 of the D2R used in D2R-5HT2AR heteromer experiments with the 3-alanine mutation further along the sequence of the IC3 of the D2R used in D2R-A2AR heteromer experiments. This D2R (9A) mutant construct will test the abrogation of the D2R-5HT2AR heteromer and be useable in D2R-A2AR studies. Preliminary experiments exhibit a similar Gi signal as compared to the wild-type D2R, whereas the D2R (6A) used in the literature does not express well in our system. Finally, we expect a combination of the D2R (9A) and 5HT2AR (2A) to eliminate heteromer formation entirely, resulting in no allosteric effects.

A new and strong method utilizing single-TM peptides is starting to be used to interrupt the interfaces of GPCR heteromers. Through computer modeling or chimeric-construct methods, we know the TMs involved in some heteromeric interfaces, including the mGlu2R-5HT2AR: TM4 of the mGlu2R and TM4 of the 5HT2AR. With this knowledge, we will express TM4 of 5HT2AR as a peptide that we expect to act as a sink and bind to mGlu2R, effectively blocking heteromer formation. The same will be done with TM4 of mGlu2R as it binds to 5HT2AR and blocks heteromer formation. These peptides can be used in multiple systems, including *in vivo* viral introduction. The TM interface, if it exists, between D2R and 5HT2AR is unknown. We are modeling this interface and will use similar single-TM peptides in the future.

The allosteric effects upon heteromerization of two heteromers relevant to psychosis provide a novel target for APD treatment of schizophrenia. The changes in function of one or both receptors may allow for adjustments in dosages and combining APDs to limit side effects, among many possible treatment improvements. The GPCR heteromer field remains wide open,

but the evidence supporting direct interaction of GPCRs resulting in conformational changes is ever growing, along with evidence of resulting allosteric changes upon heteromer formation.

## LITERATURE CITED

- Aizman O, Brismar H, Uhlen P, Zettergren E, Levey AI, Forsberg H, Greengard P and Aperia A.** Anatomical and physiological evidence for D1 and D2 dopamine receptor colocalization in neostriatal neurons. *Nature Neuroscience* 3: 226-230, 2000.  
doi: 10.1038/72929
- Albizu L, Holloway T, Gonzalez-Maeso J and Sealfon SC.** Functional crosstalk and heteromerization of serotonin 5-HT<sub>2A</sub> and dopamine D<sub>2</sub> receptors. *Neuropharmacology* 61: 770-777, 2011.  
doi:10.1016/j.neuropharm.2011.05.023
- American Psychiatric Association.** Diagnostic and Statistical Manual of Mental Disorders. *American Psychiatric Association*, 5<sup>th</sup> edition, Arlington, VA, 2013.  
ISBN: 0110743488109
- Arant RJ and Ulbrich MH.** Deciphering the Subunit Composition of Multimeric Proteins by Counting Photobleaching Steps. *European Journal of Chemical Physics and Physical Chemistry* 15: 600-605, 2014.  
doi: 10.1002/cphc.201301092
- Arnt J and Skarsfeldt T.** Do novel antipsychotics have similar pharmacological characteristics? A review of the evidence. *Neuropsychopharmacology* 18: 63-101, 1998.  
doi: 10.1016/S0893-133X(97)00112-7
- Baki L, Fribourg M, Younkin J, Eltit JM, Moreno JL, Park G, Vysotskaya Z, Narahari A, Sealfon SC, Gonzalez-Maeso J and Logothetis DE.** Cross-signaling in metabotropic glutamate 2 and serotonin 2A receptor heteromers in mammalian cells. *Pflugers Archive-European Journal of Physiology*: 2016 [E-pub ahead of print].  
doi: 10.1007/s00424-015-1780-7

- Ballesteros JA and Weinstein H.** Integrated methods for the construction of three-dimensional models and computational probing of structure-function relations in G protein-coupled receptors. *Methods in Neuroscience* 25: 366–428, 1995.  
doi: 10.1016/S1043-9471(05)80049-7
- Bonaventura J, Navarro G, Casado-Anguera V, Azdad K, Rea W, Moreno E, Brugarolas M, Mallol J, Canela EI, Lluís C, Cortes A, Volkow ND, Schiffmann SN, Ferre S and Casado V.** Allosteric interactions between agonists and antagonists within the adenosine A2A receptor-dopamine D2 receptor heterotetramer. *Proceedings of the National Academy of Sciences* 112: E3609-3618, 2015.  
doi: 10.1073/pnas.1507704112
- Borroto-Escuela DO, Romero-Fernandez W, Tarakanov AO, Marcellino D, Ciruela F, Agnati LF and Fuxe K.** Dopamine D2 and 5-hydroxytryptamine 5-HT<sub>2A</sub> receptors assemble into functionally interacting heteromers. *Biochemical and Biophysical Research Communications* 401: 605-610, 2010.  
doi: 10.1016/j.bbrc.2010.09.110
- Borroto-Escuela DO, Romero-Fernandez W, Garriga P, Ciruela F, Narvaez M, Tarakanov AO, Palkovits M, Agnati LF and Fuxe K.** G protein-coupled receptor heterodimerization in the brain. *Methods in Enzymology* 521: 281-294, 2013.  
doi: 10.1016/B978-0-12-391862-8.00015-6
- Borroto-Escuela DO, Romero-Fernandez W, Narvaez M, Oflijan J, Agnati LF and Fuxe K.** Hallucinogenic 5-HT<sub>2A</sub> Agonists LSD and DOI Enhance Dopamine D2R Protomer Recognition and Signaling of D2-5-HT<sub>2A</sub> Heteroreceptor Complexes. *Biochemical and Biophysical Research Communications* 443: 278-284, 2014.  
doi: 10.1016/j.bbrc.2013.11.104
- Brea J, Castro M, Giraldo J, Lopez-Gimenez JF, Padin JF, Quintian F, Cadavid MI, Vilario MT, Mengod G, Berg KA, Clarke WP, Vilardaga JP, Milligan G and Loza MI.** Evidence for distinct antagonist-revealed functional states of 5-hydroxytryptamine(2A) receptor homodimers. *Molecular Pharmacology* 75: 1380-1391, 2009.  
doi: 10.1124/mol.108.054395.
- Brodie MS and Bunney EB.** Serotonin potentiates dopamine inhibition of ventral tegmental area neurons in vitro. *Journal of Neurophysiology* 76: 2077-2082, 1996.  
PMID: 8890316 (no doi found)
- Bruno A, Guadix AE and Costantino G.** Molecular dynamics simulation of the heterodimeric mGluR2/5HT<sub>2A</sub> complex. An atomistic resolution study of a potential new target in psychiatric conditions. *Journal of Chemical Information and Modeling* 49: 1602-1616, 2009.  
doi: 10.1021/ci900067g

- Burnet PW, Eastwood SL and Harrison PJ.** 5-HT1A and 5-HT2A receptor mRNAs and binding site densities are differentially altered in schizophrenia. *Neuropsychopharmacology* 15: 442-455, 1996.  
doi: 10.1016/S0893-133X(96)00053-X
- Cao DY, Bai G, Ji Y and Traub RJ.** Epigenetic upregulation of metabotropic glutamate receptor 2 in the spinal cord attenuates oestrogen-induced visceral hypersensitivity. *Gut* 64: 1913-1920, 2015.  
doi: 10.1136/gutjnl-2014-307748
- Chang PY, Chuang CH, Chen JC and Tung CS.** Behavioral and biochemical effects of amperozide and serotonin agents on nigrostriatal and mesolimbic dopamine systems. *Chinese Journal of Physiology* 51: 106-115, 2008.  
PMID: 18666714 (no doi found)
- Chio CL, Hess GF, Graham RS and Huff RM.** A second molecular form of D2 dopamine receptor in rat and bovine caudate nucleus. *Nature* 343: 266-269, 1990.  
doi: 10.1038/343266a0
- Clarke WP, Chavera TA, Silva M, Sullivan LC and Berg KA.** Signalling profile differences: paliperidone versus risperidone. *British Journal of Pharmacology* 170: 532-545, 2013.  
doi: 10.1111/bph.12295
- Corena-McLeod M.** Comparative Pharmacology of Risperidone and Paliperidone. *Drugs in R&D* 15: 163-174, 2015.  
doi: 10.1007/s40268-015-0092-x
- Cornea-Hebert V, Riad M, Wu C, Singh SK and Descarries L.** Cellular and subcellular distribution of the serotonin 5-HT2A receptor in the central nervous system of adult rat. *Journal of Comparative Neurology* 409: 187-209, 1999.  
doi: 10.1002/(SICI)1096-9861(19990628)409:2<187::AID-CNE2>3.0.CO;2-P
- Dal Toso R, Sommer B, Ewert M, Herb A, Pritchett DB, Bach A, Shivers BD and Seeburg PH.** The dopamine D2 receptor: two molecular forms generated by alternative splicing. *European Molecular Biology Organization Journal* 8: 4025-4034, 1989.  
PMID: 2531656 (no doi found)
- Delille HK, Becker JM, Burkhardt S, Bleher B, Terstappen GC, Schmidt M, Meyer AH, Unger L, Marek GJ and Mezler M.** Heterocomplex formation of 5-HT2A-mGlu2 and its relevance for cellular signaling cascades. *Neuropharmacology* 62: 2184-2191, 2012.  
doi: 10.1016/j.neuropharm.2012.01.010
- Doherty MD and Pickel VM.** Ultrastructural localization of the serotonin 2A receptor in dopaminergic neurons in the ventral tegmental area. *Brain Research* 864: 176-185, 2000.  
doi: 10.1016/S0006-8993(00)02062-X

- Doumazane E, Scholler P, Zwier JM, Trinquet E, Rondard P and Pin JP.** A new approach to analyze cell surface protein complexes reveals specific heterodimeric metabotropic glutamate receptors. *Federation of American Societies for Experimental Biology Journal* 25: 66-77, 2011.  
doi: 10.1096/fj.10-163147
- Duffy AM, Fitzgerald ML, Chan J, Robinson DC, Milner TA, Mackie K and Pickel VM.** Acetylcholine  $\alpha 7$  nicotinic and dopamine D2 receptors are targeted to many of the same postsynaptic dendrites and astrocytes in the rodent prefrontal cortex. *Neuroscience* 252: 126–143, 2013.  
doi: 10.1016/j.neuroscience.2013.08.008
- Ellaithy A, Younkin J, González-Maeso J and Logothetis DE.** Positive allosteric modulators of metabotropic glutamate 2 receptors in schizophrenia treatment. *Trends in Neuroscience*, 38: 506-516, 2015.  
doi: 10.1016/j.tins.2015.06.002
- Fernandez-Duenas V, Gomez-Soler M, Jacobson KA, Kumar ST, Fuxe K, Borroto-Escuela DO and Ciruela F.** Molecular determinants of A2AR-D2R allosterism: role of the intracellular loop 3 of the D2R. *Journal of Neurochemistry* 123: 373-384, 2012.  
doi: 10.1111/j.1471-4159.2012.07956.x
- Ferre S, Casado V, Devi LA, Filizola M, Jockers R, Lohse MJ, Milligan G, Pin JP and Guitart X.** G protein-coupled receptor oligomerization revisited: functional and pharmacological perspectives. *Pharmacological Reviews* 66: 413-434, 2014.  
doi: 10.1124/pr.113.008052
- Fraser E, McDonagh AM, Head M, Bishop M, Ironside JW and Mann DMA.** Neuronal and astrocytic responses involving the serotonergic system in human spongiform encephalopathies. *Neuropathology and Applied Neurobiology* 29: 482–495, 2003.  
doi: 10.1046/j.1365-2990.2003.00486.x
- Fribourg M, Moreno JL, Holloway T, Provasi D, Baki L, Mahajan R, Park G, Adney SK, Hatcher C, Eltit JM, Ruta JD, Albizu L, Li Z, Umali A, Shim J, Fabiato A, MacKerell Jr AD, Brezina V, Sealfon SC, Filizola M, Gonzalez-Maeso J and Logothetis DE.** Decoding the signaling of a GPCR heteromeric complex reveals a unifying mechanism of action of antipsychotic drugs. *Cell* 147: 1011-1023, 2011.  
doi: 10.1016/j.cell.2011.09.055
- Fuxe K, Ferre S, Canals M, Torvinen M, Terasmaa A, Marcellino D, Goldberg SR, Staines W, Jacobsen KX, Lluis C, Woods AS, Agnati LF and Franco R.** Adenosine A2A and Dopamine D2 Heteromeric Receptor Complexes and Their Function. *Journal of Molecular Neuroscience* 26: 209-219, 2005.  
doi: 10.1385/JMN/26:02:209
- Fuxe K, Borroto-Escuela DO, Tarakanov AO, Romero-Fernandez W, Ferraro L,**

- Tanganelli S, Perez-Alea M, Di Palma M and Agnati LF.** Dopamine D2 heteroreceptor complexes and their receptor-receptor interactions in ventral striatum: novel targets for antipsychotic drugs. *Progress in Brain Research* 211: 113-139, 2014.  
doi: 10.1016/B978-0-444-63425-2.00005-2
- Garay RP, Bourin M, de Paillette E, Samalin L, Hameg A and Llorca PM.** Potential serotonergic agents for the treatment of schizophrenia. *Expert Opinion on Investigational Drugs* 25: 159-170, 2016.  
doi: 10.1517/13543784.2016.1121995
- Garzon M, Duffy AM, Chan J, Lynch MK, Mackie K and Pickel VM.** Dopamine D2 and Acetylcholine  $\alpha 7$  nicotinic receptors have subcellular distributions favoring mediation of convergent signaling in the mouse ventral tegmental area. *Neuroscience* 252: 126-143, 2013.  
doi: 10.1016/j.neuroscience.2013.08.008
- Gonzalez-Maeso J, Ang RL, Yuen T, Chan P, Weisstaub NV, Lopez-Gimenez JF, Zhou M, Okawa Y, Callado LF, Milligan G, Gingrich JA, Filizola M, Meana JJ and Sealfon SC.** Identification of a serotonin/glutamate receptor complex implicated in psychosis. *Nature* 452: 93-97, 2008.  
doi: 10.1038/nature06612
- Guo W, Urizar E, Kralikova M, Mobarec JC, Shi L, Filizola M and Javitch JA.** Dopamine D2 receptors form higher order oligomers at physiological expression levels. *European Molecular Biology Organization Journal* 27: 2293-2304, 2008.  
doi: 10.1038/emboj.2008.153
- Han Y, Moreira IS, Urizar E, Weinstein H and Javitch JA.** Allosteric communication between protomers of dopamine class A GPCR dimers modulates activation. *Nature Chemical Biology* 5: 688-695, 2009.  
doi: 10.1038/nchembio.199
- Hatcher-Solis C, Fribourg M, Spyridaki K, Younkin J, Ellaithy A, Xiang G, Liapakis G, Gonzalez-Maeso J, Zhang H, Cui M and Logothetis DE.** G protein-coupled receptor signaling to Kir channels in *Xenopus* oocytes. *Current Pharmaceutical Biotechnology*, 15: 987-995, 2014.  
doi: 10.2174/1389201015666141031111916
- Hersch SM, Ciliax BJ, Gutekunst CA, Rees HD, Heilman CJ, Yung KK, Bolam JP, Ince E, Yi H and Levey AI.** Electron microscopic analysis of D<sub>1</sub> and D<sub>2</sub> dopamine receptor proteins in the dorsal striatum and their synaptic relationships with motor corticostriatal afferents. *Journal of Neuroscience* 15: 5222-5237, 1995.  
doi: 10.1002/cne.23235

- Huang Y, Zheng Y, Su Z and Gu X.** Differences in duplication age distributions between human GPCRs and their downstream genes from a network prospective. *BMC Genomics* 10 Suppl 1: S14, 2009.  
doi:10.1186/1471-2164-10-S1-S14
- Kang SG, Na KS, Lee HJ, Chee IS, Lee K and Lee J.** DRD2 genotypic and haplotype variation is associated with improvements in negative symptoms after 6 weeks' amisulpride treatment. *Journal of Clinical Psychopharmacology* 35: 158-162, 2015.  
doi: 10.1097/JCP.0000000000000294
- Khan ZU, Koulen P, Rubinstein M, Grandy DK and Goldman-Rakic PS.** An astroglia-linked dopamine D2-receptor action in prefrontal cortex. *Proceedings of the National Academy of Sciences* 98:1964–1969, 2001.  
doi:10.1073/pnas.98.4.1964
- Knight AR, Misra A, Quirk K, Benwell K, Revell D, Kennett G and Bickerdike M.** Pharmacological characterisation of the agonist radioligand binding site of 5-HT<sub>2A</sub>, 5-HT<sub>2B</sub> and 5-HT<sub>2C</sub> receptors. *Naunyn-Schmiedeberg's Archives of Pharmacology* 370: 114-123, 2004.  
doi: 10.1007/s00210-004-0951-4
- Kurita M, Moreno JL, Holloway T, Kozlenkov A, Mocci G, Garcia-Bea A, Hanks JB, Neve R, Nestler EJ, Russo SJ and Gonzalez-Maeso J.** Repressive epigenetic changes at the mGlu2 promoter in frontal cortex of 5-HT<sub>2A</sub> knockout mice. *Molecular Pharmacology* 83: 1166-1175, 2013.  
doi: 10.1124/mol.112.084582
- Le Moine C and Bloch B.** D<sub>1</sub> and D<sub>2</sub> dopamine receptor gene expression in the rat striatum: sensitive cRNA probes demonstrate prominent segregation of D<sub>1</sub> and D<sub>2</sub> mRNAs in distinct neuronal populations of the dorsal and ventral striatum. *Journal of Comparative Neurology* 355: 418–426, 1995.  
doi: 10.1002/cne.903550308
- Le Moine C, Normand E, Guitteny AF, Fouque B, Theoule R and Bloch B.** Dopamine receptor gene expression by enkephalin neurons in rat forebrain. *Proceedings of the National Academy of Sciences* 87: 230–234, 1990.  
doi: 10.1111/j.1460-9568.1995.tb01092.x
- Levey AI, Hersch SM, Rye DB, Sunahara RK, Niznik HB, Kitt CA, Price DL, Maggio R, Brann II MR and Ciliax BJ.** Localization of D1 and D2 dopamine receptors in brain with subtype-specific antibodies. *Proceedings of the National Academy of Sciences* 90: 8861-8865, 1993.  
doi: 10.1073/pnas.90.19.8861
- Lopez-Gimenez JF, Villazon M, Brea J, Loza MI, Palacios JM, Mengod G and Vilaro MT.** Multiple conformations of native and recombinant human 5-hydroxytryptamine(2a)

receptors are labeled by agonists and discriminated by antagonists. *Molecular Pharmacology* 60: 690-699, 2001.  
PMID: 11562430 (no doi found)

**Lukasiewicz S, Faron-Gorecka A, Dobrucki J, Polit A and Dziedzicka-Wasylewska M.** Studies on the role of the receptor protein motifs possibly involved in electrostatic interactions on the dopamine D1 and D2 receptor oligomerization. *Federation of European Biochemical Societies Journal* 276: 760-775, 2009.  
doi: 10.1111/j.1742-4658.2008.06822.x

**Lukasiewicz S, Polit A, Kedracka-Krok S, Wedzony K, Mackowiak M and Dziedzicka-Wasylewska M.** Hetero-dimerization of serotonin 5-HT<sub>2A</sub> and Dopamine D<sub>2</sub> receptors. *Biochimica et Biophysica Acta* 1803: 1347-1358, 2010.  
doi: 10.1016/j.bbamcr.2010.08.010

**Lukasiewicz S, Faron-Gorecka A, Kedracka-Krok S and Dziedzicka-Wasylewska M.** Effect of clozapine on the dimerization of serotonin 5-HT<sub>2A</sub> receptor and its genetic variant 5-HT<sub>2A</sub>H425Y with dopamine D<sub>2</sub> receptor. *European Journal of Pharmacology* 659: 114-123, 2011.  
doi: 10.1016/j.ejphar.2011.03.038

**Marek GJ, Wright RA, Schoepp DD, Monn JA and Aghajanian GK.** Physiological antagonism between 5-hydroxytryptamine(2A) and group II metabotropic glutamate receptors in prefrontal cortex. *Journal of Pharmacology and Experimental Therapeutics* 292:76-87, 2000.  
PMID: 10604933 (no doi found)

**Meador-Woodruff JH, Damask SP, Wang J, Haroutunian V, Davis KL and Watson SJ.** Dopamine receptor mRNA expression in human striatum and neocortex. *Neuropsychopharmacology* 15: 17-29, 1996.  
doi: 10.1016/S0306-4522(02)00580-8

**Millan MJ, Maiorini L, Cussac D, Audinot V, Boutin JA and Newman-Tancredi A.** Differential Actions of Antiparkinson Agents at Multiple Classes of Monoaminergic Receptor. I. A Multivariate Analysis of the Binding Profiles of 14 Drugs at 21 Native and Cloned Human Receptor Subtypes. *Journal of Pharmacology and Experimental Therapeutics* 303: 791-804, 2002.  
doi: 10.1124/jpet.102.039867

**Miner LAH, Backstrom JR, Sanders-Bush E and Sesack SR.** Ultrastructural localization of serotonin<sub>2A</sub> receptors in the middle layers of the rat prelimbic prefrontal cortex. *Neuroscience* 116: 107-117, 2003.  
doi: 10.1016/S0306-4522(02)00580-8

**Moreno JL, Muguruza C, Umali A, Mortillo S, Holloway T, Pilar-Cuellar F, Mocci G, Seto J, Callado LF, Neve RL, Milligan G, Sealfon SC, Lopez-Gimenez JF, Meana JJ,**

- Benson DL and Gonzalez-Maeso J.** Identification of three residues essential for 5-HT<sub>2A</sub>-mGlu<sub>2</sub> receptor heteromerization and its psychoactive behavioral function. *Journal of Biological Chemistry* 287: 44301-44319, 2012.  
doi: 10.1074/jbc.M112.413161
- Moreno JL, Miranda-Azpiazu P, Garcia-Bea A, Younkin J, Cui M, Kozlenkov A, Ben-Ezra A, Voloudakis G, Fakira AK, Baki L, Ge Y, Georgakopoulos A, Moron JA, Milligan G, Lopez-Gimenez JF, Robakis NK, Logothetis DE, Meana JJ and Gonzalez-Maeso J.** Allosteric signaling through an mGlu<sub>2</sub> and 5-HT<sub>2A</sub> heteromeric receptor complex and its potential contribution to schizophrenia. *Science Signaling* 9: ra5, 2016.  
doi: 10.1126/scisignal.aab0467
- Moustaine DE, Granier S, Doumazane E, Scholler P, Rahmeh R, Bron P, Mouillac B, Baneres JL, Rondard P and Pin JP.** Distinct roles of metabotropic glutamate receptor dimerization in agonist activation and G-protein coupling. *Proceedings of the National Academy of Sciences*, 109: 16342–16347, 2012.  
doi: 10.1073/pnas.1205838109
- Nimitvilai S and Brodie MS.** Reversal of prolonged dopamine inhibition of dopaminergic neurons of the ventral tegmental area. *Journal of Pharmacology and Experimental Therapeutics* 333: 555-563, 2010.  
doi: 10.1124/jpet.109.163931
- Nimitvilai S, McElvain MA, Arora DS and Brodie MS.** Reversal of quinpirole inhibition of ventral tegmental area neurons is linked to the phosphatidylinositol system and is induced by agonists linked to G(q). *Journal of Neurophysiology* 108: 263-274, 2012.  
doi: 10.1152/jn.01137.2011
- Nocjar C, Roth BL and Pehek EA.** Localization of 5-HT(2A) receptors on dopamine cells in subnuclei of the midbrain A10 cell group. *Neuroscience* 111: 163-176, 2002.  
doi: 10.1016/S0306-4522(01)00593-0
- Ohishi H, Neki A and Mizuno N.** Distribution of a metabotropic glutamate receptor, mGlu<sub>2</sub>, in the central nervous system of the rat and mouse: an immunohistochemical study with a monoclonal antibody. *Neuroscience Research* 30: 65-82, 1998.  
doi: 10.1016/S0168-0102(97)00120-X
- Phillips T, Rees S, Augood S, Waldvogel H, Faull R, Svendsen C and Emson P.** Localization of metabotropic glutamate receptor type 2 in the human brain. *Neuroscience* 95: 1139-1156, 2000.  
doi: 10.1016/S0306-4522(99)00353-X
- Rangel-Barajas C, Malik M, Vangveravong S, Mach RH and Luedtke RR.** Pharmacological modulation of abnormal involuntary DOI-induced head twitch response in male DBA/2J mice: I. Effects of D2/D3 and D2 dopamine receptor selective compounds. *Neuropharmacology* 83: 18-27, 2014.

doi: 10.1016/j.neuropharm.2014.03.003

**Reiner A, Arant RJ and Isacoff EY.** Assembly Stoichiometry of the GluK2/GluK5 Kainate Receptor Complex. *Cell Reports 1*: 234-240, 2012.  
doi: 10.1016/j.celrep.2012.01.003

**Rodríguez JJ, Garcia DR and Pickel VM.** Subcellular distribution of 5-hydroxytryptamine<sub>2A</sub> and N-methyl-D-aspartate receptors within single neurons in rat motor and limbic striatum. *Journal of Comparative Neurology 413*: 219-231, 1999.  
doi: 10.1002/(SICI)1096-9861(19991018)413:2<219::AID-CNE4>3.0.CO;2-F

**Romano C, Yang WL and O'Malley KL.** Metabotropic glutamate receptor 5 is a disulfide-linked dimer. *Journal of Biological Chemistry 271*: 28612-28616, 1996.  
doi: 10.1074/jbc.271.45.28612

**Sahlholm K.** The role of RGS protein in agonist-dependent relaxation of GIRK currents in *Xenopus* oocytes. *Biochemical and Biophysical Research Communications 415*: 509-514, 2011.  
doi: 10.1016/j.bbrc.2011.10.106

**Sahlholm K, Barchad-Avitzur O, Marcellino D, Gomez-Soler M, Fuxe K, Ciruela F and Arhem P.** Agonist-specific voltage sensitivity at the dopamine D<sub>2S</sub> receptor--molecular determinants and relevance to therapeutic ligands. *Neuropharmacology 61*: 937-949, 2011.  
doi: 10.1016/j.neuropharm.2011.06.022

**Santana N, Mengod G and Artigas F.** Quantitative analysis of the expression of dopamine D<sub>1</sub> and D<sub>2</sub> receptors in pyramidal and GABAergic neurons of the rat prefrontal cortex. *Cerebral Cortex 19*: 849-860, 2009.  
doi: 10.1093/cercor/bhn134

**Schmid CL, Streicher JM, Meltzer HY and Bohn LM.** Clozapine acts as an agonist at serotonin 2A receptors to counter MK-801-induced behaviors through a barrestin2-independent activation of Akt. *Neuropsychopharmacology 39*: 1902-1913, 2014.  
doi: 10.1038/npp.2014.38

**Sernyak MJ and Rosenheck R.** Clinicians' reasons for antipsychotic coprescribing. *Journal of Clinical Psychiatry 65*: 1597-1600, 2004.  
PMID: 15641863 (no doi found)

**Sieler S and Milligan G.** G Protein Coupled Receptors: Structure, Signaling, and Physiology. *Cambridge University Press*, New York, NY, 2011.  
ISBN: 978-0-521-11208-6

**Southan C, Sharman JL, Benson HE, Faccenda E, Pawson AJ, Alexander SPH, Buneman OP, Davenport AP, McGrath JC, Peters JA, Spedding M, Catterall WA, Fabbro D and Davies JA.** The IUPHAR/BPS Guide to PHARMACOLOGY in 2016: towards

curated quantitative interactions between 1300 protein targets and 6000 ligands. NC-IUPHAR. *Nucleic Acids Research* 44: D1054-68, 2016.  
doi: 10.1093/nar/gkv1037

**Stahl SM.** Stahl's Essential Psychopharmacology: Neuroscientific Basis and Practical Applications. *Cambridge University Press*, 4<sup>th</sup> edition, New York, NY, 2013.  
ISBN: 9781455702824

**Sun H, Calipari ES, Beveridge TJ, Jones SR and Chen R.** The brain gene expression profile of dopamine D2/D3 receptors and associated signaling proteins following amphetamine self-administration. *Neuroscience* 307: 253-261, 2015.  
doi: 10.1016/j.neuroscience.2015.08.053

**Tarakanov AO and Fuxe KG.** Triplet puzzle: homologies of receptor heteromers. *Journal of Molecular Neuroscience* 41: 294-303, 2010.  
doi: 10.1007/s12031-009-9313-5

**Taylor DL, Jones F, Kubota ES and Pocock JM.** Stimulation of microglial metabotropic glutamate receptor mGlu2 triggers tumor necrosis factor alpha-induced neurotoxicity in concert with microglial-derived Fas ligand. *Journal of Neuroscience* 25: 2952-2964, 2005.  
doi: 0.1523/JNEUROSCI.4456-04.2005

**Uslaner JM, Smith SM, Huszar SL, Pachmerhiwala R, Hinchliffe RM, Vardigan JD and Hutson PH.** Combined administration of an mGlu2/3 receptor agonist and a 5-HT 2A receptor antagonist markedly attenuate the psychomotor-activating and neurochemical effects of psychostimulants. *Psychopharmacology* 206: 641-651, 2009.  
doi: 10.1007/s00213-009-1644-y

**Vivaudou M, Chan KW, Sui JL, Jan LY, Reuveny E and Logothetis DE.** Probing the G-protein regulation of GIRK1 and GIRK4, the two subunits of the KACH channel, using functional homomeric mutants. *Journal of Biological Chemistry* 272: 31553-31560, 1997.  
doi: 10.1074/jbc.272.50.31553

**Wang X, Li F, Jose PA and Ecelbarger CM.** Reduction of renal dopamine receptor expression in obese Zucker rats: role of sex and angiotensin II. *American Journal of Physiology: Renal Physiology*, 299: 1164-1170, 2010.  
doi: 10.1152/ajprenal.00604.2009

**Xu T and Pandey SC.** Cellular localization of serotonin (2A) (5HT(2A)) receptors in the rat brain. *Brain Research Bulletin* 51: 499-505, 2000.  
doi: 10.1016/S0361-9230(99)00278-6

## APPENDIX 1: CONTROL EXPERIMENTS

**Figure A1.1. Whole-cell patch clamp controls.** Summary bar graphs from whole-cell patch-clamp recordings of GIRK1/4 currents in clone 59 of HEK-293 cells expressing mGlu2R exposed to **(A)** 500nM glutamate (Glu) followed by 500nM Glu plus 50uM paliperidone (Pal) or **(B)** 10uM LY37 followed by 10uM LY37 plus 50uM Pal (N = 4-5/condition, Data were normalized to basal activity and are mean  $\pm$  SEM).

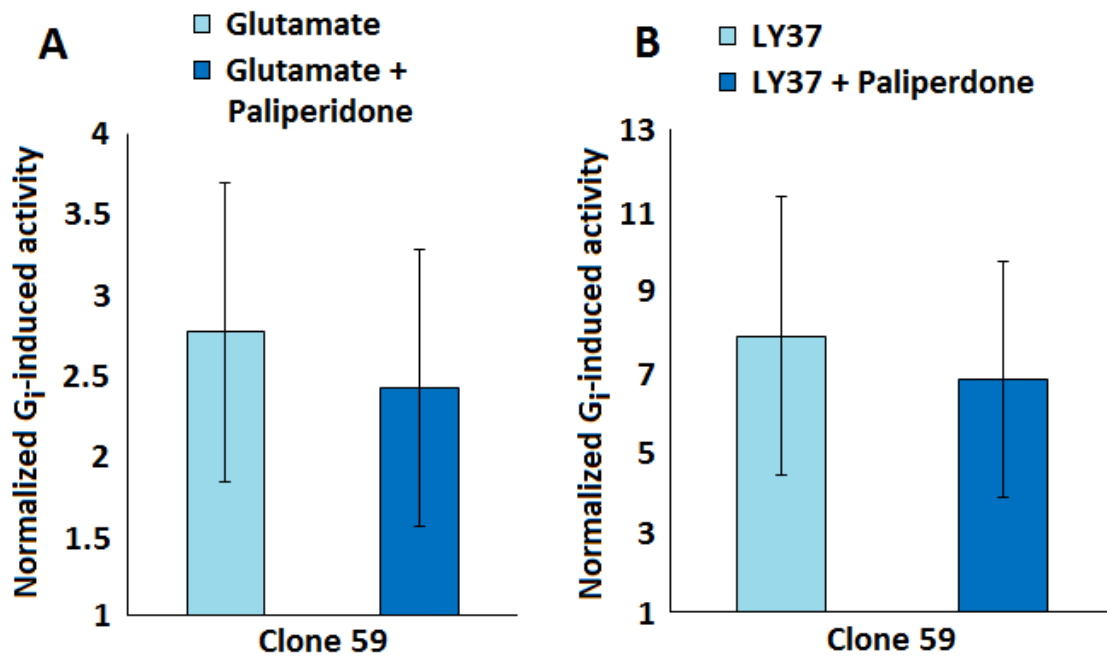


**Figure A1.2. 5HT2AR (2A) mutant G<sub>q</sub> activity.** Summary bar graph of G<sub>q</sub> activity measured in oocytes: The addition of 1μM 5HT increases G<sub>q</sub> activity of the 5HT2AR (2A) mutant to similar levels as compared to the 5HT2AR (N = 8/condition, Dotted line = 1 or 100%, Data are mean ± SEM).

cRNA injections (2ng 5HT2AR or 5HT2AR (2A)): GIRK4\*, PTX, plus 5HT2AR or 5HT2AR (2A).

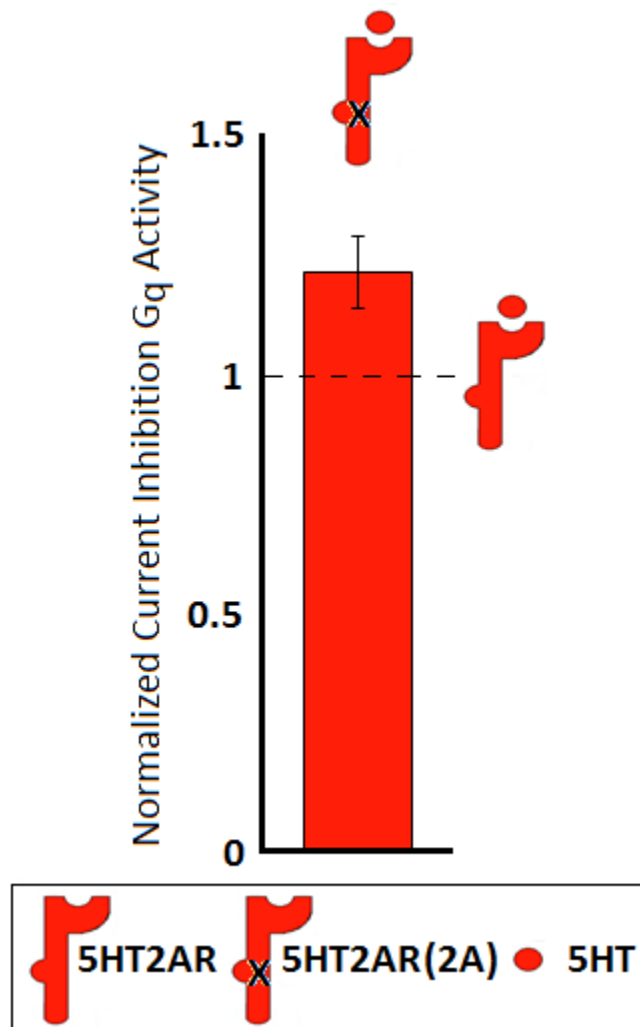


**Figure A1.3. G4\* controls.** Summary bar graph of GIRK4\*activity measured in oocytes: The addition of 1uM dopamine or 5HT, 10uM QP or DOI, 5uM PIMA, 300nM AMIS or AMP, or 100nM PAL does not significantly change K<sup>+</sup> current in oocytes injected with G4\* cRNA only (N = 8-12/condition, Dotted line = 1 or 100%, Data are mean  $\pm$  SEM).  
cRNA injections: GIRK4\*.

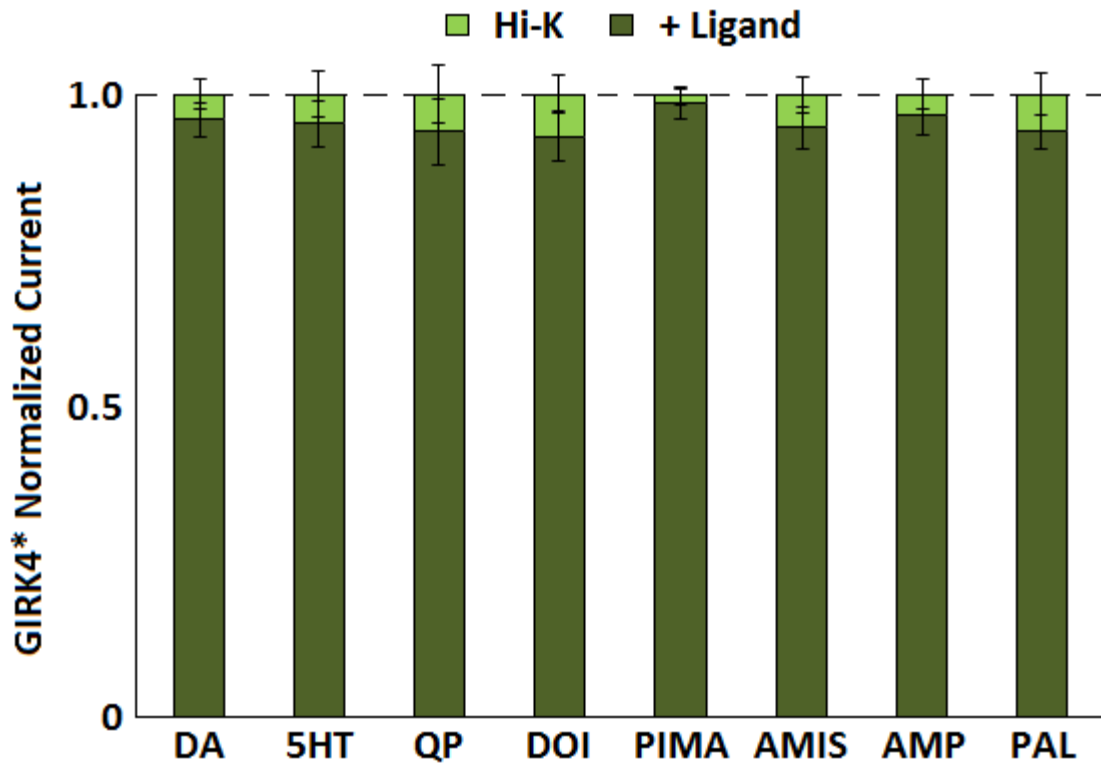
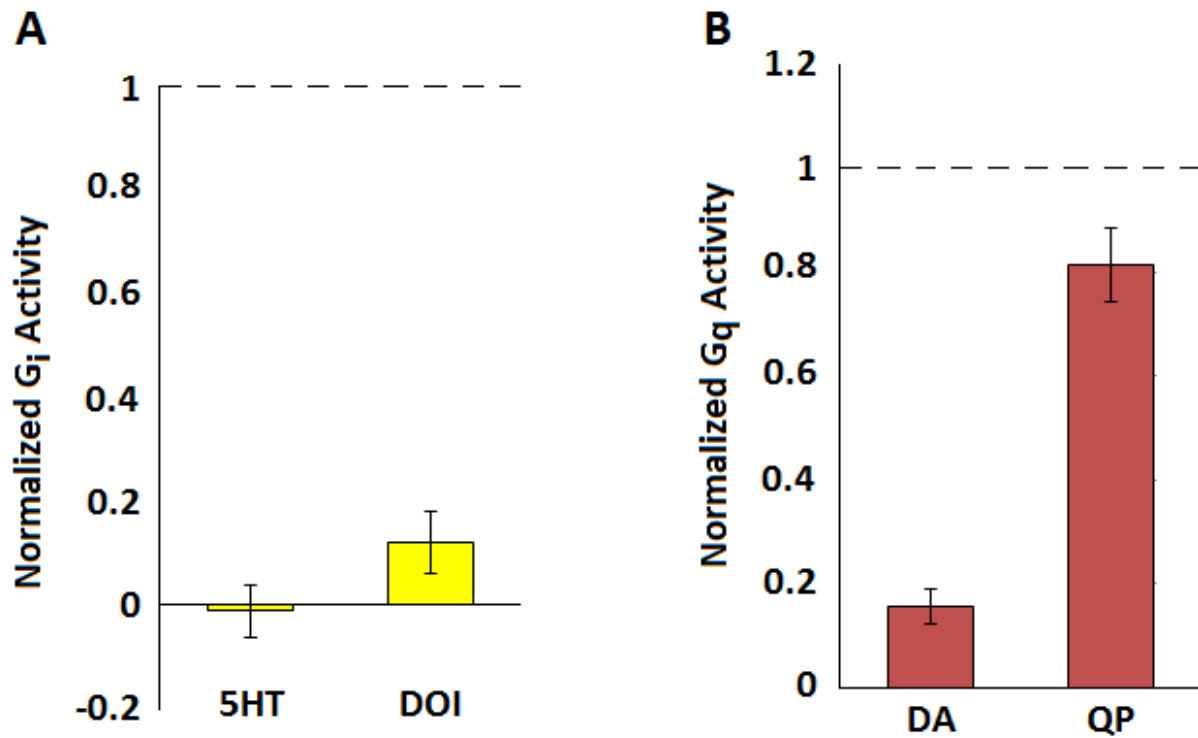


**Figure A1.4. D2R and 5HT2AR controls.** Summary bar graphs of  $G_i$  and  $G_q$  activity measured in oocytes. **(A)** The addition of 1 $\mu$ M 5HT or 10 $\mu$ M DOI does not increase  $G_i$  activity of the D2R as compared to the addition of 1 $\mu$ M DA (N = 8-9/condition, Dotted line = 1 or 100%, Data are mean  $\pm$  SEM). **(B)** The addition of 1 $\mu$ M DA does not increase  $G_q$  activity of the 5HT2AR as compared to the addition of 1 $\mu$ M 5HT, but the addition of 10 $\mu$ M QP increases  $G_q$  activity of the 5HT2AR to similar levels as compared to the addition of 1 $\mu$ M 5HT (N = 8/condition, Dotted line = 1 or 100%, Data are mean  $\pm$  SEM).  
cRNA injections (1ng D2R or 2ng 5HT2AR): GIRK4\*, RGS2 or PTX, plus D2R or 5HT2AR.



## VITA

Jason Wayne Younkin was born on July 13, 1973, in Somerset, Pennsylvania, and is a United States citizen. He graduated from Rockwood Area High School, Rockwood, Pennsylvania in 1991. He served in the United States Navy as a Nuclear Engineer and Operator for nine years before being honorably discharged. He received his Bachelor of Science in Neuroscience from the College of William and Mary, Williamsburg, Virginia, in 2010. He then joined the Neuroscience Ph.D. program at Virginia Commonwealth University in 2010 where he pursued research full-time in the Physiology and Biophysics laboratory of Dr. Diomedes E. Logothetis.